Experimental and Numerical Investigation of Temporal and Spatial Effects induced by Motion and Load in Joint Biomechanics

A Study of Joint Loading *in vivo*, Functional Imaging, and Finite Element Modeling with Focus on Articular Cartilage

by

Xiang Ian Gu

A Dissertation Submitted to the Graduate Faculty in Biomedical Engineering in Partial Fulfillment of the Requirements for the Degree of Doctor of Philosophy

The City University of New York

New York City, U.S.A

2010

This manuscript has been read and accepted for the
Graduate Faculty in Engineering in satisfaction of the
dissertation requirement for the degree of Doctor of Philosophy.

Dr. Luis Cardoso

Date

Chair of Examining Committee

Dr. Mumtaz Kassir

Date

Executive Officer

Dr. Herb B. Sun

Dr. Stephen C. Cowin

Dr. Susannah P. Fritton

Dr. Mitchell B Schaffler

Supervision Committee

THE CITY UNIVERSITY OF NEW YORK

ABSTRACT

EXPERIMENTAL AND NUMERICAL INVESTIGATION OF MOTION-LOAD INDUCED EFFECTS IN JOINT BIOMECHANICS

A STUDY ON JOINT LOADING *IN VIVO*, FUNCTIONAL IMAGING, AND FINITE ELEMENT MODELING IN A FOCUS OF ARTICULAR CARTILAGE

by

Xiang Ian Gu

Adviser: Dr. Luis Cardoso

Joint diseases are a leading cause of disability worldwide, and there is a tremendous concern about how joint motion and weight bearing impact on joint health. It is generally accepted that joint disuse and overuse both cause cartilage degradation, while moderate loading within physiological range help maintain cartilage integrity; however, the mechanism mediating the dichotomy of mechanical factors in improving or damaging cartilage functional capacity remains largely unknown. It is of significant interest from both a basic science and a clinical perspective to elucidate the complex temporal and spatial effects of joint motion and load bearing in joint biomechanics. Furthermore, a prerequisite for research efforts towards this direction is the establishment and analysis of suitable animal models (preferably rodent) that mimic the normal and pathologic motion-load patterns in humans. Although numerous *in vitro* and *in vivo* studies have been performed to date, due to the apparent experimental difficulties such as the small size, little has been achieved for ideal experimental and analytical research methodologies in small animal models. In this dissertation, experimental and numerical approaches were taken in a series of challenging joint biomechanics research projects, and the purpose of the dissertation was to elucidate the clinical relevant temporal and spatial effect of motion-load induced

mechanical loading applied on the joint. We developed and validated a cutting-edge joint motion and loading system that offers precise control of joint motion and compressive impact load to quantitatively study the mechanoresponsiveness in joint tissues. We explored the early response of cartilage to joint immobilization and remobilization. We created the first FE model in rodent model based on a contrast agent enhanced high-resolution micro-CT imaging approach to characterize the local spatial mechanical environment in which chondrocytes sense and respond. The developed joint motion and load system demonstrated remarkable reliability and reproducibility for challenging protocols. The *in vivo* temporal experiments showed that immobilization of joints may cause cartilage degeneration in a short time, while early intervention of moderate motion that produced biomechanical signals to suppress the acute inflammatory effect can reverse this catabolic process, and overloading produced similar results to that observed from immobilization. The low cost micro-CT arthrography approach using a contrast agent to create high-resolution three-dimensional (3D) geometries of soft tissues in rat joints proved practical and efficient. The FE modeling result of rat knee joint loading showed the stress distribution that supports our hypothesis that gene expression of important mediators is a function of stress in that particular region. The knowledge obtained through these studies may provide more insight into the underlying mechanism orchestrating the relationship between motion, loading and the corresponding biological responses in cartilage, and may further help treat Osteoarthritis and other joint disorders by contributing to design effective motion-based therapies.

DEDICATION

谨将此博士论文献给我敬爱的父母, 可爱的两个小侄儿, 以及尊敬的小学班主任何凤英老师.

I dedicate this dissertation to

1) my parents, Ms. YongMei Yu and Mr. XingDuo Gu for their endless understanding, patience, and support in my nine years of graduate study as well as in my whole life; their health condition in the past ten years was a major motivation for my research in life science;

2) my two angel nephews, Xiangxiang and Xixi, who bring happiness and new hope into our family; and

3) Ms. FengYing He (? – 1990), my primary school mentor to whom I was her last favorite student; Taken away too soon from her beloved by disease (two years in hospital after I graduated from her class), she was my earliest inspiration of a Ph.D. degree, and my life-time model of empowering passion, perseverance, and dedication to what we choose to do.

ACKNOWLEDGEMENTS

I am deeply indebted to many people over the last nine years since I came to the United States from China for higher studies. I have benefited both professionally and personally from the numerous experiences that I have had with these people, especially since I moved to New York City in 2005 from Alabama where I finished my Master's study and started my Ph.D. At this time, I would like to acknowledge and thank the many people who have contributed to my experience.

First of all, I would like to express my sincere gratitude to my mentor, Dr. Luis Cardoso, without whom this work would not have been possible. I am always amazed by and consistently benefited from his broad range of knowledge and endless energy devoted to research. Through his own example, he has instilled in me the passion for perfection, the aspiration to deep understanding into science, the perseverance towards achieving a goal, and the positive attitude to approach a difficult research topic. I would specially like to thank him for giving me lot of freedom in conducting my research and also for the countless, intense and motivating discussions that I have had with him; I am indeed thankful to Luis for all that he has done for me. It has been a real pleasure to work with him over the years. To distinguish myself from his many excellent graduate students yet to benefit from him, I am extraordinarily proud to be his first Ph.D. student, and glad I had the exclusive fortune of sharing the space of his first office and gluing the lab tables for our first lab we already moved out. I truly enjoyed the special experience to be a part of his early career as a wonderful professor, I have no doubt he is going to be very famous in the Biomedical Engineering field. I would also like to gratefully thank my co-mentor, Dr. Herb Sun, who not only initiated a great project that consisted a considerable part of my dissertation but also offered me the opportunity to integrate my understanding of engineering

knowledge into the life science to solve the a real-world clinically relevant problem that addresses the major concern of many of my sporty friends who unfortunately suffered a knee surgery like myself. I am particularly thankful to Herb's highly enthusiastic appreciation of my contribution to the project, and I am deeply indebted from his articulate confidence in me that carries on as truly tremendous psychological strength inside me. I cannot thank Herb enough for his kind encouragements, candid suggestions, and thoughtful arrangements generously rendered to me over the years. I would like to thank our crew at Mount Sinai School of Medicine, Mr. Daniel Leong, Dr. Yonghui Li, and Dr. Zhengzhe Li, whose research in the highly collaborative project helped me enormously in my pursuit of exciting scientific findings. Special thanks must go to my close colleague Dan, as a real team player and an excellent researcher Dan has made my smooth collaboration with him truly pleasant and fruitful experience. Also I would like to acknowledge Natalia Maldonado, an expert of Abaqus, and my NIH mentee Edek Williams, one of the most energetic and intellectual students that I have known for their help that saved the critical time for the documentation of this dissertation; Likewise, thanks must also go to Francisco Guzman and Rashal Mahamud for their contribution to my first publication.

I would like to gratefully acknowledge Professor Susannah Fritton, Professor Stephen Cowin, and Professor Mitchell Schaffler for finding time from their busy schedule to offer critical comments and to carefully read this thesis within a very short span of time. I would also like to thank them for their advice and support during the course of this research work. Particularly, I would like to thank Professor Fritton for her many suggestions to my publication preparation and academic writing, and to thank Professor Cowin for offering the distinguished Tissue Mechanics classes that helped me vastly in the modeling part of this work. Throughout my research, Professor Schaffler has been very supportive and his many insightful suggestions

are truly inspiring and helpful. Besides, I would like to acknowledge Dr. Robert Majeska for his contributions of time and effort in reviewing my abstracts and manuscripts as a co-author of my conference and journal publications; in addition, conversations with Mitch and Bob helped me a lot in shaping my view of research as a career and gaining more insight into the research from another perspective. Furthermore, I would be profoundly ungrateful if I did not acknowledge and thank Professor Bingmei Fu and Professor David Rumschitzki as well as their lab for generously assisting with the lab animals and facilities; particularly, I would like to acknowledge Qin Liu, Jie Fan, Bin Cai, Guanglei Li, Wei Yuan, Lingyan Shi, Dr. Ming Zeng, and Yan Xue for supplying the experimental samples used in this work.

Thanks must be rendered to my fellow biomedical engineering students, colleagues, and friends, Yuliya Vengrenyuk, Yilin Wang for informative discussions and for providing me with helpful information. I would specially like to thank my previous and present lab mates Jacek Dmochowski, Oran Kennedy, Damien Laudier, Gaffar Gailani, Mohamed Benalla, Adreanne Kelly, Zeynep Seref, Adrianna Larrier, Paulo Palacio, Jelena Basta-Pljakic, Joanna Dabrowiecka, Dorra Frikha, Pamela Cabahug for setting up a warm and cheerful atmosphere in a wonderful lab; particularly, daily buffet lunch with Jacek eating a lot in the faculty dining room has been a great pleasure to release the stress of graduation, I truly appreciate his company. I need to also acknowledge the efforts of my fellow colleagues, both in City College of New York and at Mount Sinai School of Medicine; in particular I would like to mention Dr. David Fung for his kind assistance for the *in vivo* experiments at Mount Sinai School of Medicine; likewise I would like to specially thank Dr. Chris Fritton and Mr. Phillip Nasser for his suggestions to this dissertation.

I have to thank Joyce Lin, who has been a considerable part of, and has made tremendous

impact to my life during this very unique time of my graduation, for the great comfort she brought to me and the precious efforts she made in helping me to move forward, indeed I am more grateful than I can say to her. Finally, I would like to personally acknowledge and thank the following persons, all of whom, in one way or another, were instrumental in my completion of this work through our discussions, their words of encouragement, and their moral support: my family in China and my aunt's family in New Jersey and Canada; my very good friend, Howard Qin and Ying Xiong; Lina Liang, Dr. Zhiyong Qiu, Danielle Berardi, Danielle Wu, ZD Shi, Dyvia Sharma, Melissa Ramcharan, Lingyan Shi, Lin Zhang, Dr. Jianxin Su, Daniel Zhu, Dr. Vladimir Fast, Dr. Jian Huang, Mrs. Cynthia Y Johnson, Zhengwei Liu, Kaven Kuang, Denis Jiang, Ada He, and Cecilia Ye.

TABLE OF CONTENTS

Page

LIST OF FIGURES

LIST OF FIGURES (Cont'd)

Figure

LIST OF ABBREVIATIONS

CPM	Continuous Passive Motion
MMP	Matrix Metalloproteinase
OA	Osteoarthritis
RA	Rheumatoid Arthritis
GAG	Glycosaminoglycan
COX	Cyclooxygenase
CITED	CBP/p300-Interacting Transactivator with ED-Rich Tail
MEMS	Microelectromechanical Sensor
FEM	Finite Element Modeling

Chapter 1

INTRODUCTION

1.1 Overview of Research

1.1.1 Motivation of Research

The prevalence of joint disorders in the USA. Life is about motion. The major body motions are exclusively carried out by the function of diarthroidal joints. Joint diseases such as arthritis are common chronics that lower people's life quality and cause disability in the USA. Osteoarthritis (OA) and Rheumatoid arthritis (RA) are the most prevalent forms of arthritis. OA is characterized by the deterioration of cartilage often due to wear and tear, while RA is an autoimmune dysfunction that causes the inflammation of a joint's connective tissues that leads to cartilage destruction. Currently, more than 21 million Americans are OA patients, nearly 2.1 million Americans suffer from RA, and a total estimate of more than 43 million Americans suffer from arthritis [1]. In particular, nearly one third of persons 63 to 94 years of age have osteoarthritis of the knee alone. The annual costs for the medical care and lost wages for arthritic patients are about US$65 billion [1]. As the longevity of the aging population increases and the oldest of the baby boomers born between 1946 and 1964 are now older than 60 years, it has been predicted that OA will affect 60 million Americans by the year 2020 [2].

A real international crisis. In a worldwide scope, the disabling joint diseases can become a global health problem that challenges a country's health budget and its gross national productivity [1, 3]. Take OA in Asia-Pacific region as an example, OA of the knees is more prevalent in this region. Through extrapolation, it is inferred that the impacted individuals of OA can be even several orders of magnitude higher compared with USA. It has been predicted that the nations in the Asia-Pacific region are soon becoming a predominantly aged society. The percentage of elderly aged over 60 years in

China was over 10% in 2000 (130 million), and predicted to reach 18.4% by 2025 (280 million), and 25% by 2050 (about 400 million) [4]. In Japan, the proportion of elderly people aged at least 65 years was 19.9% in 2005 and is expected to rise to 26.0% by 2015 [5]. As population aging will cause many challenges during the year 2000-2050, it is foreseeable that OA will impose tremendous social and economic burdens in these densely populated countries.

Un-physiological mechanical loading: a contribution to the etiology of OA? Prevention and control of the joint diseases necessitate an in-depth understanding of the underlying mechanism responsible for the initiation and progression of the joint degeneration, and research efforts are still advancing at the experimental stage towards achieving more insight into the early-stage joint pathology. Determined by multiple factors such as aging, mechanical force, hormones, and genetics, OA has been conceptualized as a joint degenerative disease that significantly correlates to aberrant mechanical loading. Clinical observations and laboratory study results have indicated a causal relationship between the mechanical environment sensed by chondrocytes, the single type of cells in cartilage, and cartilage homeostasis [6], and a hypothesis has been put forth that cartilage degeneration caused by OA is mechanically induced [7]. In spite of the numerous evidences that have shown that either prolonged synovial joint immobilization or excessive mechanical loading applied on the joint may lead to an increased risk of OA, the early events that trigger the pathological process(es) in cartilage have yet to be thoroughly investigated.

Physiological mechanical loading: a benefit? Currently there is no known cure for OA or RA, and the available treatments are limited, including medications, therapies, and

surgical procedures. Physical therapies are being widely used to help maintain joint movement and possibly enhance the healing of arthritic joints. It appears that moderate motions such as those applied in continuous passive motion (CPM) therapy may protect joint tissues from degradation to some degree, and physiological load levels may exert a chondroprotective effect at least under some circumstances. However, there is no consensus on either the protocol design or whether continuous passive motion has long-term clinical value [8, 9]. Key to the debate are the diversity of treatment variables, including the duration, frequency and intensity of motion, and the complex temporal and spatial biomechanical behavior of cartilage associated with the joint articulation and load transferring conditions.

Ultimate question: how do motion and load affect joint health? The dichotomy of biomechanical results of joint loading implicates the regulatory cues of mechanical loading that impacts joint homeostasis in a dose-dependent manner. The temporal and spatial effects of the motion and load on joint tissues has been hypothesized to be generally characterized by a 'U' shape. That is, the intensity of joint movements and the magnitude of the impact load at cartilage contact surface, if maintained within a physiological range, can be beneficial to joint health; however, if otherwise exceeded this moderate scope, can degenerate the joint tissue. To study the exact mechanism underlying the pathogenesis of joint degeneration such as seen in OA, and to understand how motion-based therapies benefit patients with joint diseases including RA, it is critical to take a quantitative approach to associate acute and long-term mechanical loading effects with cartilage health in small animal models. In this approach, 1) the biomechanical stimuli beyond and within physiological loading limits need to be created

for *in vivo* experimental studies; 2) the local biomechanical environment of stresses/strains needs to be characterized by numerically modeling the tissue geometries under defined loading conditions 3) and pro- and anti- inflammatory mediators as well as mechanotransduction pathways involved in the cartilage mechanoresponsive processes *in vivo* need to be investigated from both temporal and spatial perspectives. To date, in spite of the numerous *in vitro* and some *in vivo* studies that focused on some specific biological responses to certain loading conditions, very few studies have been performed systematically *in vivo* in small animal models to address the listed concerns, and the biomechanical results of early timepoints (e.g., a few hours) beyond physiological range have not been fully investigated. Furthermore, few studies extended the research scope to cover all joint, tissue, cellular, and molecular levels for a big picture of the temporal and spatial effects of joint motion and load bearing. Some of the major challenges include the small size of the rodents anatomy, limitation of current imaging modality on cartilage, and lack of available consortium for both experimental and numerical studies at multiple levels, etc.

1.1.2. Goals of Research

The aim of this dissertation was to study the underlying mechanism mediating the biological response in articular cartilage to motion-load induced mechanical stimuli in a small animal model. In this dissertation, biomechanical, structural, and compositional studies were performed to elucidate the temporal and spatial effects of mechanical loading on cartilage *in vivo* using both experimental and numerical approaches. We hypothesized that moderate mechanical loading have a chondroprotective effect, while

un-physiological levels of loading can cause cartilage degeneration; the tissue responds to the influence of external mechanical stimuli in a time- and location- dependent way. Particularly, our hypothesis prospects that early intervention of moderate motion loading in the initial stage of cartilage degeneration can sufficiently reverse the progressing pathological process. The overview of research is illustrated in Figure 1.1.

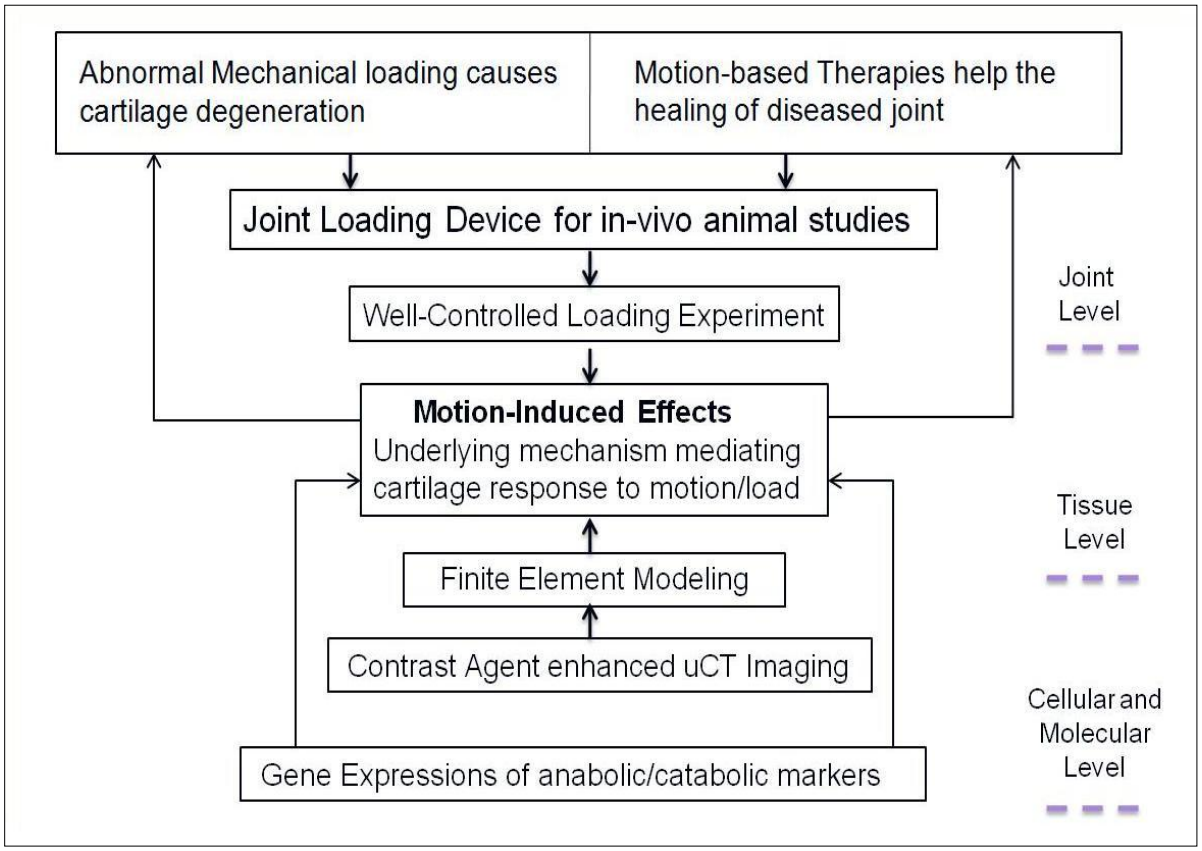

Figure 1.1 Overview of research

The first goal of the dissertation was to develop a joint loading system in a small animal model. An assisted *in vivo* system was proposed to produce effective stimuli applied as continuous passive motion (CPM) that is sufficient for prevention of acute

cartilage degradation in a rodent knee joint. The advancement of the system development led to an upgraded joint motion and loading system (JMLS) which was intended to facilitate both passive motion loading (PML) and compressive motion loading (CML). The JMLS was expected to provide a well-characterized non-invasive joint loading environment where joint loading levels can be controllable not only for the motions from slow to moderate or more intense ranges but also for the magnitude of axial impact load applied on the contact surface; moreover, the specific loading variables were required to be quantitatively monitored.

The second goal was to study the gene expression of pro- and anti- inflammatory markers in cartilage in response to joint immobilization, remobilization, and compressive motion loading condition *in vivo*. By focusing on matrix metalloproteinase (MMP)-1, 3, and 13, the cartilage degradative enzymes that breaks down the extracellular matrix (ECM) constituents, and Collagen II, the most potent protein strength in cartilage, we aimed to examine the effect of immobilization of the joint at different time points, how remobilization applied in CPM may reverse the catabolic response caused by immobilization, and whether overloading condition of twice the body weight integrated with remobilization may exhibit a similar gene expression pattern to immobilization.

The third goal was to create a 3D geometric reconstruction model of hard and soft tissues based on high resolution micro-CT imaging modality. To understand how motion-load induced mechanical loading regulates joint homeostasis, it is important to characterize the local biomechanical environment experienced by joint tissues using numerical analysis performed on tissue geometries in small animal joints, and high resolution imaging modality is essential for this purpose. Traditionally, despite the fact

that micro-CT imaging offers much higher resolution than MR imaging, it has found very limited applications for imaging cartilage due to the low X-ray absorption of soft tissues. We aimed to explore the possibility of a micro-CT arthrography approach that may compensate for the poor radiopacity of cartilage by injection of contrast agent to differentiate soft tissues such as cartilage layers and menisci from bone. We sought to create the 3D geometries of articular cartilage, menisci, as well as bones in a small animal joint model at a high pixel resolution that facilitates advanced computational modeling performed on the joint tissues.

The fourth goal was to develop a finite element model of the rat knee joint for the study of tibio-femoral contact. We aimed to create a finite element model of the small rodent's joint to study the stresses/strains at the contact surfaces between cartilage, bones, and menisci in response to a defined axial load. Moreover, we were seeking to examine the hypothesized correlation between the sites of high stresses and tissue failure, by comparing the biomechanical data obtained from the developed finite element model with our previous findings of the spatial distribution of the pro- and anti- inflammatory gene expressions. Upon completion, the model will provide important numerical information on how mechanical factors influence cartilage homeostasis, and to the best of our knowledge, it would be a pioneering study of finite element analysis developed in a small rodent's joint on both soft and hard tissues.

1.1.3. Overview of Chapters

In the first section, the introduction chapter briefly describes the purpose and scope of the research plan, and three specific goals of the study are proposed. The background

knowledge about the related research is described in the last part of Chapter 1, specifically, the relevance of joint diseases and cartilage, the effect of immobilization on articular cartilage, the effect of overuse/overloading on articular cartilage, animal models of cartilage disease and continuous passive motion, the mechanism of action behind motion therapies, and biomechanical finite element models in cartilage and micro-CT imaging. Thereafter, the detailed design and validation procedure of a novel motion and loading system is presented in Chapter 2, this system is developed to apply well-controlled motion-load environment on the knee joint. Chapter 3 shows the temporal effect of the loading condition on joint homeostasis by presenting the gene expression of pro- and anti- inflammatory markers in cartilage in response to joint loading condition *in vivo*. In Chapter 4, the application of a contrast agent enhanced high-resolution micro-CT imaging modality is described in a small animal model, and the 3D geometric reconstruction of the soft and hard tissues in the rodent knee joint is presented. Chapter 5 shows the finite element analysis performed on the rodent joint to associate the stresses/strains corresponding to the well-defined loading condition with the spatial observations of the biological responses. The conclusion and future study is summarized in Chapter 6 for the research topics in this dissertation.

1.2 Background

1.2.1 The Joint

An articulation (joint) is a contact area between two or more bones. By structural classification, there are three kinds of joints: Fibrous, Cartilaginous, and Synovial. By

functional classification the joints can be divided as Synarthroses (immovable), Amphiarthroses (partially movable), and Diathroses (freely movable).

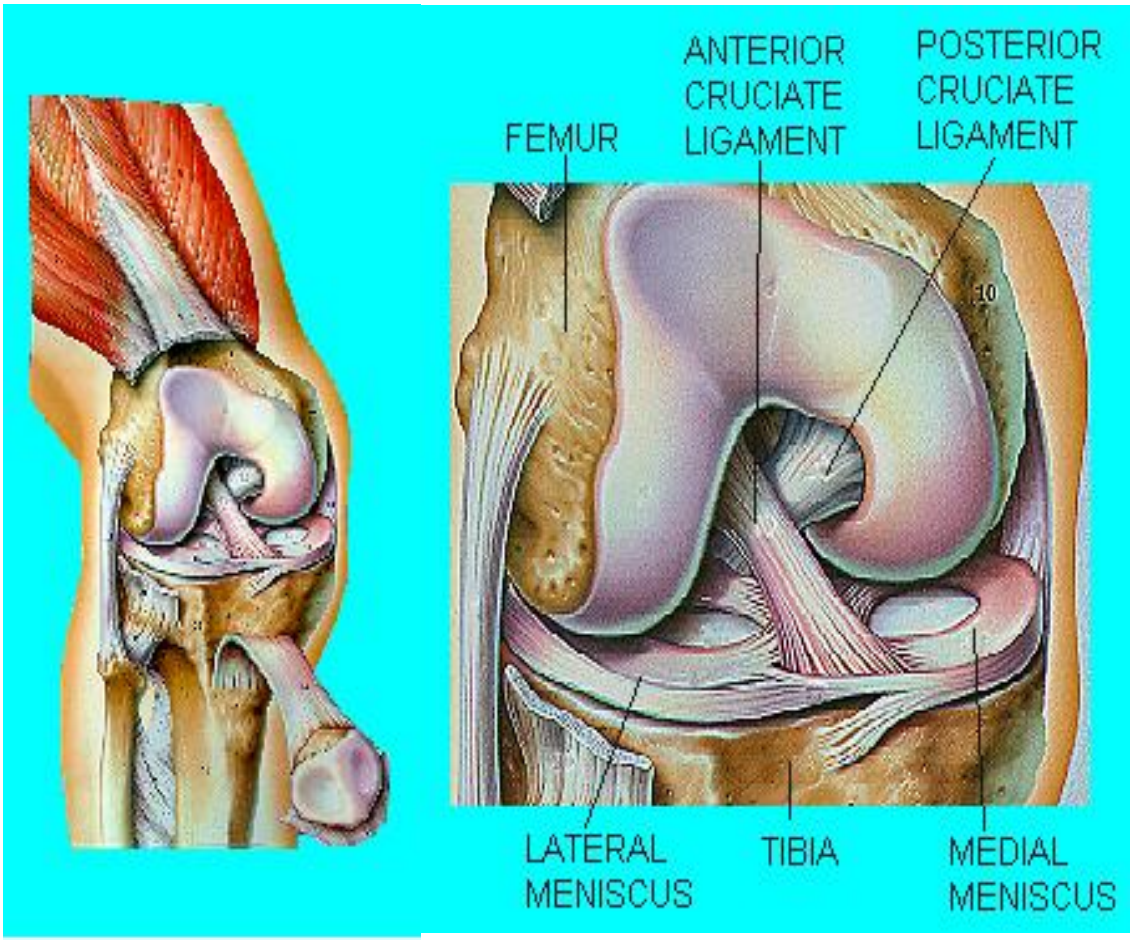

Figure 1.2 Knee joint anatomy [10]

Most joints in the adult body are diarthroses. A knee joint is shown in Figure 1.2 as an example of typical diarthroses. The ends of the opposing bones are covered with hyaline cartilage, the articular cartilage, and they are separated by a space called the joint cavity; the components of the joints are enclosed in a dense fibrous joint capsule. The outer layer of the capsule consists of the ligaments that hold the bones together. The inner

layer is the synovial membrane that secretes synovial fluid into the joint cavity for lubrication. These kinds of joints are sometimes called synovial joints since all of them have a synovial membrane.

1.2.2 Arthritis

Articular cartilage injury and degeneration is frequently found in synovial joints. Osteoarthritis (OA) is characterized by the breakdown of cartilage, a thickening of subchondral bone, and formation of marginal osteophytes. OA is not an autoimmune disease but rather a condition of wear and tear caused by aging or injury. Rheumatoid arthritis (RA) is characterized by inflammation resulting from an over-active immune system that mistakenly attacks the healthy tissue. Joints afflicted by RA may also exhibit progressive destruction of cartilage and subchondral bone [11]; therefore, cartilage degradation is commonly found as a central feature in arthritic joints.

Figure 1.3 shows a normal joint and joints with osteoarthritis (OA) and rheumatoid arthritis (RA). The RA knee joint is most noticeable for the swollen inflamed synovial membrane. In the OA knee joint, the contacting meniscus areas are worn out and the bone ends rub each other without the cushioning effects provided by the cartilage surface and lubrications from the synovial fluids. The typical RA symptoms include joint pain, swelling, tenderness, and redness of the joint. The OA symptoms include joint stiffness, pain, and enlarged joints. RA is associated with symmetrical swelling, while OA is associated with asymmetrical swelling in individual joints that are not part of a pair. RA can affect many different joints and some parts of the body, including the blood, the lungs, and even the heart, and OA commonly affects the joints of the fingers, knees, hips,

and spine, and other less likely joints such as the wrists, elbows, shoulders, and ankles. RA usually causes pain or stiffness that endure 30 minutes in the morning or after long rest or inactivity, while OA stiffness may get worse throughout the day. RA can attack people at all ages but often middle aged and tends to get worse. OA usually occurs as individuals age and in those joints that have become worn down by over use.

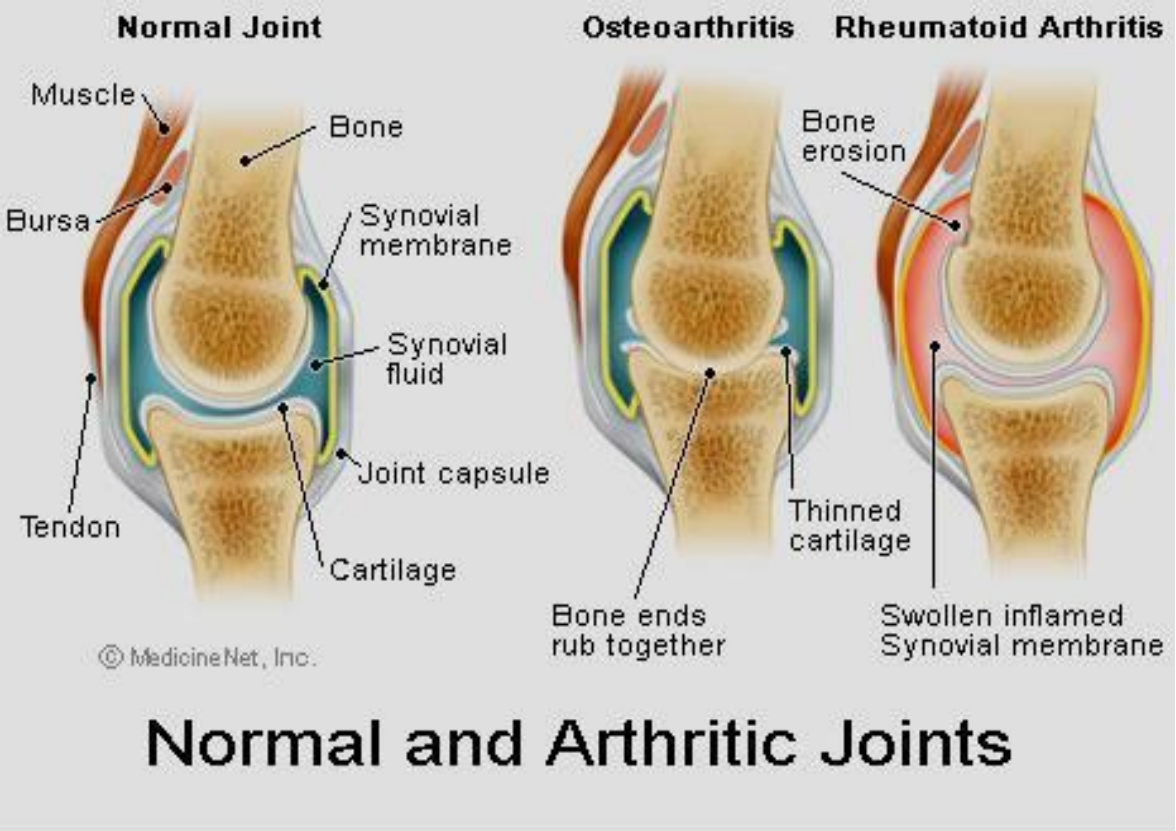

Figure 1.3 Normal and arthritic joints [12]

The treatment of arthritis includes the use of pharmacological therapy, intraarticular therapies, therapeutic ultrasound, arthroscopic or radiation synovectomy, electrical stimulation, magnet therapy, massage therapy, regenerative injection therapy, motion-based therapy, surgical treatment, etc. To date, there are no pharmacological agents

capable of retarding or preventing arthritis, and in terms of the effectiveness versus cost and agony suffered by the patients, current treatments for arthritis is relatively limited and mostly focused on relief of pain, and maintenance of daily life functional independence [13].

1.2.3 Articular Cartilage

Cartilage is a tough, semi-transparent, elastic, flexible connective tissue consisting of cartilage cells (chondrocytes and chondroblasts) scattered through a lipoprotein material supported by collagenous fibers and elastic fibers in a firm gel-like matrix. Matrix is mainly composed of proteoglycans that are large molecules with a protein backbone and glycosaminoglycan (GAG) side chains. [14]. The exterior part of cartilage is covered by dense fibrous membrane called the perichondrium. It should be noted that there are no nerves or blood vessels in cartilage and nutrients are diffused through the matrix. When damaged, cartilage does not heal easily.

There are three kinds of cartilages in the body: hyaline, fibrous, and elastic. Figure 1.4 demonstrates the histological organization in typical hyaline cartilage. This study concerned the structure and mechanical behavior of hyaline cartilage in diarthrodial joints typically called articular cartilage. Articular cartilage is dense, white connective tissue that coats the ends of bones in a diarthrodial joint, it is capable of spreading loads over the joint and allows for movement with minimal friction and wear. The functions of articular cartilage are facilitated by proteoglycans and collagen [15, 16]. The proteoglycan is the structural component of the extracellular matrix of the cartilage, composed of aggrecan, hyaluronan (HA) and link protein (LP). The aggregates provide

cartilage with unique gel-like property and resistance to deformation through water absorption. Thus, proteoglycan gel exhibits much resistance to fluid flow [17] and solute transport [18] in cartilage, and contributes to most of the matrix fixed charge density that may be related to compressive stiffness [19, 20]. As a result, proteoglycans enable the matrix to absorb shocks, whereas collagens provide the rigidity [15].

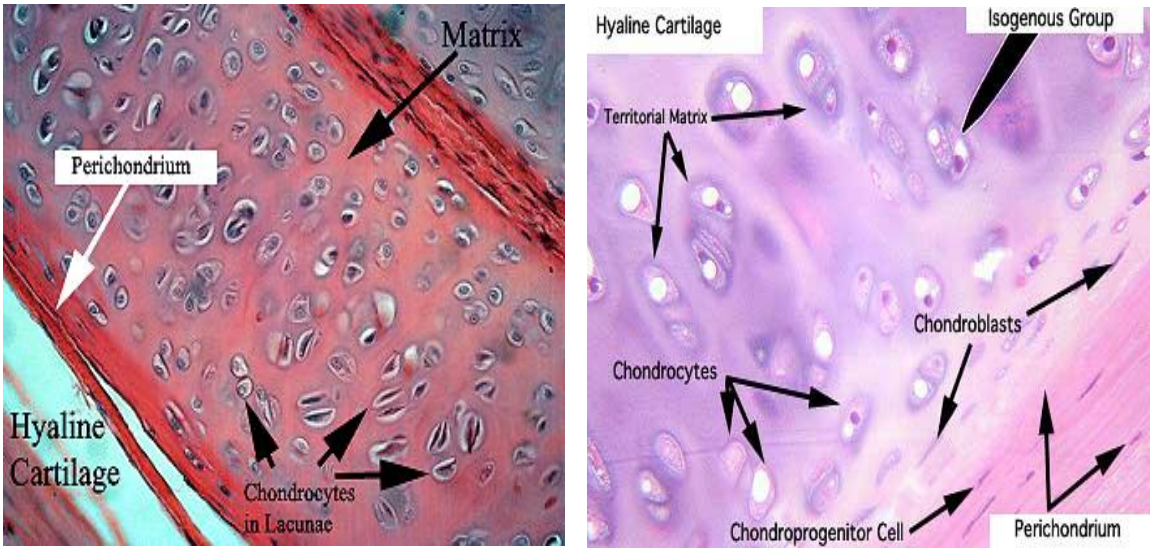

Figure 1.4 Histology of hyaline cartilage [21]

Bone, articular cartilage, ligaments, tendons, muscle, and the joint capsule are the components of the joint and this organ level exists at a scale of greater than 5cm. At a lower scale between 0.1 mm and 1cm, the articular cartilage may be viewed as a solid homogeneous material surrounding the bone ends as a cushion. Further down in the cellular level at a scale between 0.1 μm and 100 μm, the cartilage is found to be highly organized material, with a well-defined microstructure consisting of chondrocytes and collagen type II fibrils.

The articular cartilage layer can be divided into four zones: 1st, the superficial tangential zone (10-20% of the cartilage thickness); 2nd, the middle zone (60% of the cartilage thickness), 3rd, the deep zone (30% of the cartilage thickness), and 4th, the calcified cartilage zone where the cartilage interfaces with the bone. Each of the four zones contains different collagen organization as well as different amounts of proteoglycans and water. The superficial layer consists of chondrocytes and collagen fibrils that line up parallel to the joint surface in order to facilitate the resistance of shear stresses, while in the middle zone the collagen fibrils are more randomly arranged and support vertical units called chondrons containing rows of chondrocytes. In the deep zone the collagen fibrils show a vertical formation and ultimately insert into the underlying subcondral bone in the calcified zone (Figure 1.5).

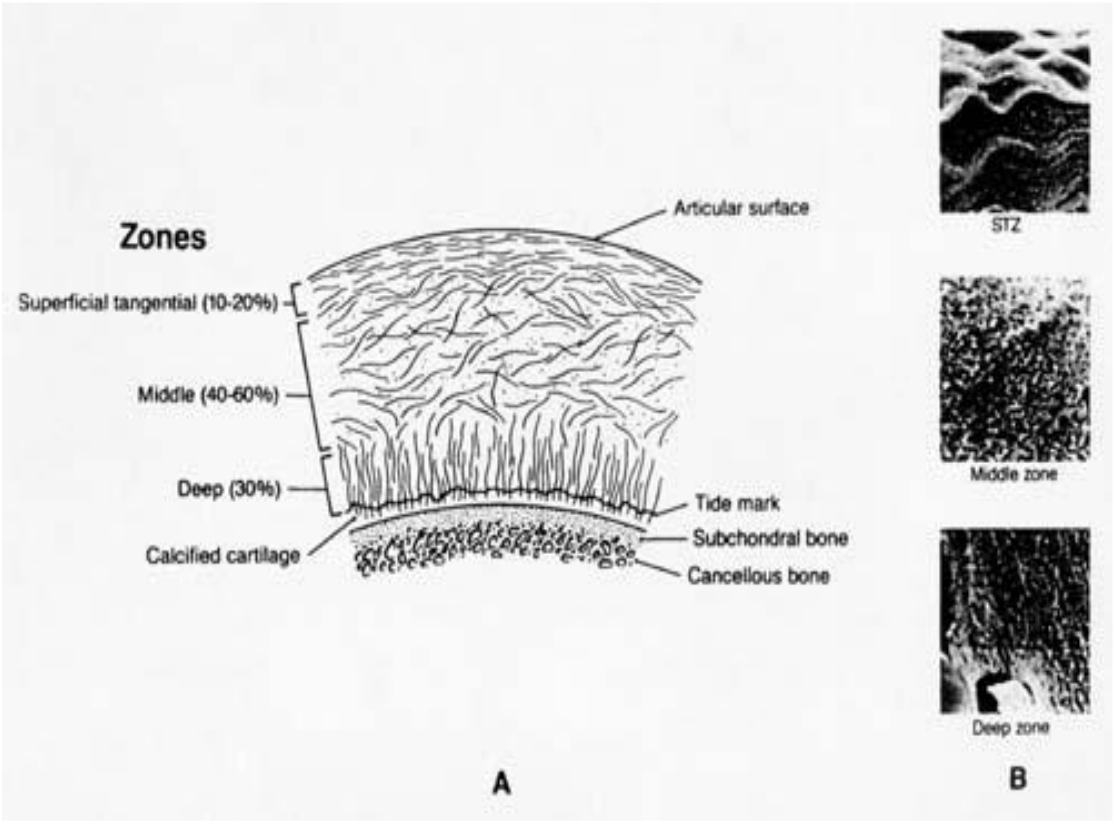

Figure 1.5 Zones in articular cartilage [22]

Articular cartilage is an extremely complex and sophisticatedly structured biological material with a mechanical response that is highly non-linear and both time- and load-dependent [23]. This behavior has shown to be mainly due to the two distinct phases of the cartilaginous tissue in joints: a fluid phase related to the interstitial water and the various inorganic salts dissolved in it, and a solid phase associated with the organic solid matrix comprised of cells, collagen fibrils, proteoglycans, and other glycoproteins. The mechanical properties of the fiber-reinforced composite solid material and the interstitial fluid enable the cartilaginous material to function as a porous, permeable, fiber-reinforced solid matrix swollen with water. The flow of the interstitial water through the matrix generated by the frictional resistance plays an important role in giving rise to the viscoelastic properties displayed by the tissue when deformed [24]. The degenerative variations in progression of arthritis are determined by the biochemical composition and structural arrangement of the extracellular matrix [25].

1.2.4 Cartilage Mechanobiology

Chondrocyte cells are embedded in the lacunae of the cartilage and only represent 1-2% of the total volume in the articular cartilage. They synthesize and maintain the extracellular matrix that represents the majority of the tissue. In contrast, chondroclasts are involved in the resorption of cartilage and synovial cells. They produce a small peptide (catabolin) called IL-1, act to degrade cartilage *in vitro* and play a role in resorption in arthritis. The Transforming Growth Factor-beta (TGFβ) is a family of 25-kDa peptides that enhance chondroblast proliferation and differentiation, enhancing the deposition of cartilaginous and osseous extracellular matrices. The Transforming Growth

Factor β-1 (TGFβ-1) stimulates the chondrocytes to form sheets of cartilage, and chondrogenesis is promoted during cartilage repair by low concentrations of TGFβ-1 in the extracellular matrix [26].

Mechanical load plays an important role in regulating chondrocyte metabolic activity. The alterations of dynamic and static load affect the biological response of chondrocytes. The amplitude or frequency of the load may have a considerable effect on the production of matrix macromolecules and of agents leading to cartilage breakdown. The chondrocytes react to cartilage deformation and to changes in hydrostatic pressure, extracellular ionic composition and streaming potentials induced by the load [27].

Chondrogenesis is the process of cartilage differentiation, and it is initiated by the aggregation of chondroprogenitor mesenchymal cells. Chondrogenesis involves the controlled reentry of quiescent cells into the growth phase of the cell cycle. The growth phase transition is associated with altered cell adhesion characteristics, changed patterns of cell migration, and transiently increased cell proliferation. Chondrogenesis involves the initial development of chondrogenic capacity (i.e., the proto-differentiated state) by primitive undifferentiated mesenchymal cells. This stage involves the production of chondrocyte-specific markers without the ability to produce a typical cartilage ECM. Subsequently, the cells develop the capacity to produce a cartilage-specific ECM as they differentiate into chondrocytes [28].

Cartilage integrity is maintained by metabolic balance that comprises anabolic and catabolic activities. The major anabolic factors are bone morphogenetic proteins (BMPs) and insulin-like growth factor that induce the development of aggrecan, collagen, and link proteins. The major catabolic factors include IL-1 and tumor necrosis factor α

(TNFα) that induce the cartilage-destructive enzymes such as aggrecanases, matrix metalloproteinases (MMPs) and cyclooxygenase (COX). Matrix metalloproteinases (MMPs) are a family of collagen-degrading proteinases that play an important role in tissue remodeling associated with various physiological and pathological processes such as morphogenesis and arthritis; MMP is considered to be tightly related to rheumatoid and osteoarthritis [29]. Cyclooxygenase (COX) is an enzyme that is responsible for formation of prostanoids, and pharmacological inhibition of COX can relieve the symptoms of inflammation and pain. In arthritic joints, the balance between the anabolism and catabolism is broken, catabolic and molecular wear become stronger than the anabolic activities and capacities of the cartilage cells, and as a result, the cartilage matrix degenerates and the joint cartilages erodes [30].

1.2.5 Effect of Mechanical Stimulation on Cartilage: A Multi-Scale Review

Basic and applied research of biomechanics and modeling in mechanobiology is extremely important to elucidate the underlying mechanisms of the mechanobiological response in cartilaginous tissue as a consequence of mechanical loading. The structure-functional characterization of extracellular matrix molecules and mechanotransduction in the cell environment and the dynamic transport processes across the chondrocyte cell membrane is of paramount interest. Ateshian et al. [31] emphasized that a hierarchical approach is critically important for studying cartilaginous tissues under mechanical loading. The papers selected in this study will follow this hierarchical structure that is illustrated by the following schematic diagram:

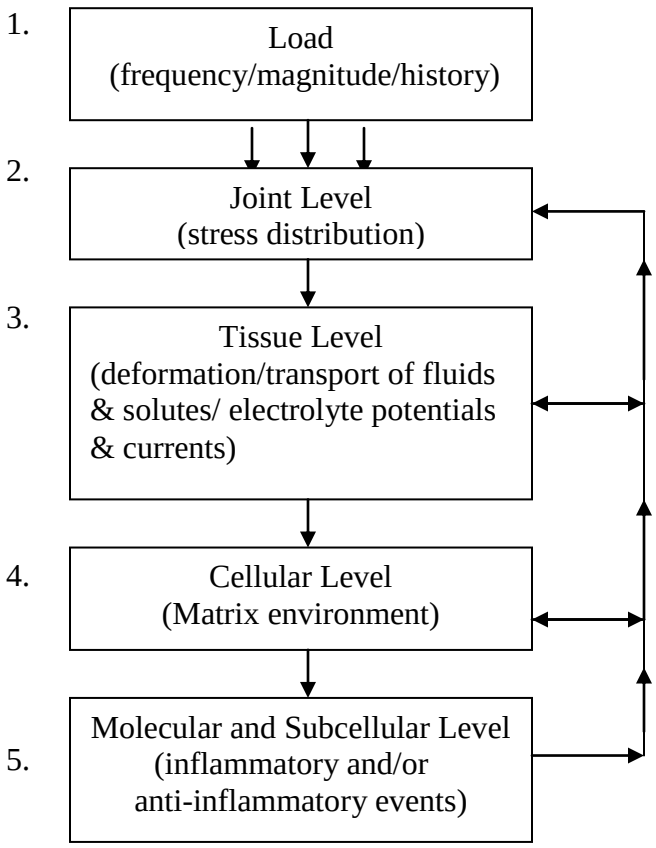

Figure 1.6 Hierarchy of cartilage in response to mechanical stimuli [31]

1. The nature, magnitude, and history of loads applied on the tissue.
2. Joint mechanics in normal and degenerative joints need to be studied by analyzing the stress distribution translated from load and the tissue response.
3. Structure-function relationships, mechanics, and transport phenomena at the tissue level as a result of the applied stresses.
5. How chondrocytes survive in response to physiological, injurious or even deleterious loading conditions is investigated at the cellular level.
6. Mechanotransduction pathways and associated electrical, chemical, and structural changes, along with the molecular mechanisms responsible for the inflammatory and anti-inflammatory events are studied at the subcellular level.

Load

Under normal physiological conditions, articular cartilage is subjected to a wide range of static and dynamic mechanical loads in synovial joints. Normally, articular cartilage can sustain physiological stresses in the range of 2-6 MPa [32, 33], the peak stress amplitudes are between 10-20 MPa during daily activities such as climbing stairs [34]. In clinical practice treating arthritic joints, moderate loading seems to be beneficial for both prevention and treatment, but too high loads imposed on the joint in intensive sports or too low mechanical loads as a result of physical inactivity can increase the risk of osteoarthritis [35].

Salter reviewed the history of rest and motion used for treatment and described the successful applications of CPM in clinical trials and experimental tests [14, 36-38]. For rehabilitation after surgery, he suggested immediate use of continuous non-stop motions for periods ranging from 1 to 4 weeks, with one complete cycle occurring for 45 seconds [39]. Ferretti et al. adopted a procedure of CPM on rabbit knee in which the angle of flexion started by 70^{o} and then followed a cyclic motion ranging from 40^{o} to 110^{o} at a rate of 45 seconds per cycle (0.0222Hz). The results of this experimental study demonstrated the beneficial effects of CPM treatment by showing the inhibition of the pro-inflammatory mediators involved in cartilage destruction and the induction of anti-inflammatory mediator in chondrocyte [40]. Other positive results were obtained by applying CPM 20 hours or only 6 hours a day, but thus far there is no universal protocol that can be applied for motion-based therapies to treat arthritic joints, and it is essentially subjective for the practitioner to decide in what way these load-unload therapies should

be used. Little convincing scientific information exists to enable them to select optimal CPM parameter [41].

Joint Level

Herzog et al. reviewed many aspects of the joint and articular cartilage mechanics, particularly the selected examples of their long-term model of knee osteoarthritis and associated studies of joint degeneration [42]. They observed the development of osteoarthritis as a consequence of the transection of anterior cruciate ligament (ACL) in a cat model. An initial decrease in the ground reaction and knee extensor forces were observed. Moreover, an initial decrease in knee extension in the push-off phase of stance and a loss of muscle control were found after the transection, but these changes can be reversed after 6-12 months. A given amount of force is transmitted across a greater contact area, leading to a reduced peak and averaged contact pressure. They pointed out that increased forces across the knee joint are accommodated primarily with an increase in contact area and little increase in contact pressures. The muscle weakness should be considered as a risk factor for joint degeneration. Other outstanding contributions of this paper include a cell-matrix model and a cell-fiber-matrix model that describe the stress-strain state of articular cartilage and chondrocytes for dynamic loading situations, and a 3-D geometric stress distribution model [42]. To address the link between cartilage degeneration and aberrations of contact areas in patients with osteoarthritis, Anderson et al. presented a contact finite element formulation that provides useful patient-specific quantitative contact stress information for the surgeons to make accurate diagnosis [43]. This was achieved by creating a finite element grid for the ankle joints on which the variations of stress distribution were analyzed versus time.

Tissue Level

The functions of articular cartilage in diarthrodial joints are determined by its morphological and biomechanical properties, and the interactions between the collagen network tensile properties and the proteoglycan gel swelling pressure considerably influence the functional behavior of articular cartilage and its microstructural organization [44, 45]. Quinn et al. provided a theoretical model of collagen network that accounts for changes in microstructural geometry with matrix deformation, based on the accessible microstructural parameters such as collagen fibril density and orientation distributions [46]. This model is more advanced than its previous counterparts in that it is capable of direct scale-up from structural organization and physics at the molecular level to mechanics at the tissue level without case-specific empirical characterization. As a result, it can be applied to matrix from any tissue zone or extracellular location and any mechanical loading conditions. Furthermore, it allows for consecutive small linear deformation steps that can result in nonlinear behavior over large deformations. Thus, this model serves as a bridge between histological data for cartilage structure and theoretical tools for simulating cartilage function, by treating the collagen network as a continuum-like distribution of fibrils instead of a collection of representative spring elements in previous models [46].

Loss of proteoglycans and their associated GAGs is commonly found in joint degeneration [47]. In a study aiming to understand altered mechanical loading secondary to biochemical changes as a potential mechanism in disc degradation, Yerramalli et al. quantified the mechanical consequences of decreased glycosaminoglycans and increased crosslinking in the nucleus pulposus [48]. The load-displacement data were analyzed to

obtain the mechanical properties before and after the degradation of GAGs. The results of the degradation of GAGs showed an increase in compression modulus that resembles a severe degeneration condition, thus proved the hypothesis that GAGs are important to maintain the normal mechanical properties in disc cartilage [48].

Wilson et al. studied the depth-dependent compressive equilibrium properties of articular cartilage and its relationship with the depth-dependent composition [49]. The distribution of the matrix components in articular cartilage is highly depth-dependent, e.g. the fluid fraction is highest in the articular surface and decreases with depth; collagen is highest in the superficial and deep zones and lowest in the middle zone, while proteoglycans are highest in the middle zone and lowest in the superficial zone. Similarly, the structure of articular cartilage is depth-dependent in that the collagen fibers are densely organized parallel to the surface while randomly arranged in the middle zone and exhibit largest diameter in the deep zone. In addition, the distribution of water in articular cartilage is also depth-dependent, leading to a depth-dependent swelling pressure that in turn gives rise to a depth-dependent compressive modulus. In consequence, when strain increases in the superficial zone, the stiffness increases, while in the deep zone the stiffness decreases. The fibril-reinforced poroviscoelastic swelling model in this study included not only the influence of intra- and extra- fibrillar water content but also the influence of the solid fraction on the compressive properties of the tissue. It also proved the hypothesis that depth-dependent compressive equilibrium properties of articular cartilage are inherent consequences of its depth-dependent composition, and not that of any of the individual components [49].

Cellular Level

To evaluate the viability of the chondrocytes in mechanically compressed articular cartilage removed from immature and mature bovine knees, Torzilli et al [44] tested the percentage depth of dead cells that reflects the chondrocyte viability in freshly cut cartilage samples when they were statically loaded in uniaxial confined compression. The measurements were taken in both groups when the load made the sample reach fixed amounts of strain of 10, 20, 30, 40, 50, 60, and 70%. The results suggest immature cartilage presents significantly greater amount of cell death compared to mature cartilage [50].

The extracellular matrix of articular cartilage plays an important role in chondrocyte mechanics and mechanotransduction. This microenvironment consists of pericellular, territorial (mainly proteoglycans), and inter-territorial (mainly collagen) matrices. It has been found that the structure and/or mechanical properties of the chondrocyte and its environment are changed during cartilage degeneration in osteoarthritis as a result of the alteration of the mechanical signals sensed by the chondrocyte [51]. Using a finite element model applied to the chondrocyte and its extracellular environment, Korhonen et al. [46] found that the fluid pressure within the chondrocyte increased nonlinearly as a function of the in-plane Young's modulus of the collagen network, and mechanical characteristics of the collagen network of articular cartilage can modify fluid flow and stresses in chondrocytes, suggesting that the integrity of the collagen network may be an important determinant in cell stimulation and in the control of the matrix maintenance [52]. Ateshian et al. further investigated the water transport between the chondrocyte and its environment matrix and identified the restrictive property of the semi-permeable

membrane of chondrocyte in regulating the water flowing in and out of the cell [53]. Thus, when the external compressive loads exceed or are smaller than the swelling pressure that is determined by the semi-permeable membrane, the cell exhibits either compression or tension, respectively, and the chondrocyte may be compressible or incompressible depending on its extracellular environment [53].

Molecular Level

Ferretti et al. studied the molecular events that account for the beneficial effects of motion-based therapies, e.g. CPM, compared to immobilization in rabbit knees with antigen-induced-arthritis (AIA) [40]. The CPM was provided by a device on which detailed description was not given in the paper. For the knee of the rabbits treated with CPM, the angle of the flexion of the joint was 70 degrees with movement between 40 degrees and 110 degrees at a rate of 45 seconds per cycle, and the knees in the experiment were exposed to CPM or immobilization for 24 to 48 hours. The experiment result of GAGs loss revealed that as compared to the lack of GAGs in 48% of zone A and 26% of the zone B (zone A and zone B are the outer 25% and the inner 75% fibrocartilage, respectively) in the affected knee areas within 24 hours and further lack of GAGs in 37% of the zone A and 26% of the zone B, there is a sustained retain of GAGs in knees treated with CPM in that the exposure of the AIA knee to CPM for the 24 hours resulted in only a 12% lack of GAGs in zone A and 6% in zone B, and further a 8% in zone A and a 3% in zone B after 48 hours of CPM treatment. Examination were performed on the pro-inflammatory mediators such as cyclooxygenase-2 (COX-2), metalloproteinase-1 (MMP-1), and interleukin-1ß (IL-1ß) and the major anti-inflammatory molecules such as interleukin-10, a major anti-inflammatory cytokines

expressed in cells during inflammation, and the results suggest a healing promotion of CPM that inhibits the gene expression of pro-inflammatory mediators and induction of anti-inflammatory mediators compared to immobilization. Meanwhile, in this study CPM was not shown to facilitate increased flow of synovial fluid to the meniscus, but it has been found that CPM does increase the proteoglycan contents [40].

Sun et al. identified *in vitro* the anti-inflammatory effect of gentle mechanical shear at the intensity of a few dyn/ cm^2 in reducing the expression and activities of MMPs, and in a further investigation providing more insight into the mechanism by which chondrocyte's metabolism is altered by shear stress [54] , Yokota et al. correlated the gene expression of MMP in response to mechanical stress with the CITED (CBP/p300-interacting transactivator with ED-rich tail) family, a key transcriptional modulators in embryogenesis, inflammation, and stress responses. In this study, the results showed that flow shear at 5 dyn/ cm^2 increased CITED2 mRNA and down-regulated not only MMP-1 and MMP-13 mRNA but also protein levels and enzyme activities, and there is a link between the CITED2-mediated reduction in MMP expression and TGF-β that associates CITED2 with p300 [55].

To test the hypothesis that mechanical stimuli may act as inductive signals during morphogenic patterning, Henderson et al. investigated the relationship between theoretically predicted patterns of stress and strain generated during the growth of a skeletal condensation and in vivo expression patterns of chondrogenic and osteogenic genes [56]. Two main approaches were pursued in parallel in this study. The first was the calculation of the approximate rate of growth that by combining a finite element model of the cartilage condensation and the surrounding tissue led to the prediction of the

compressive hydrostatic pressure and the tensile strain patterns generated by the growth of the condensation. The other approach was the hybridization analysis of the same embryonic stages by which the spatial and temporal distribution of the gene expression was obtained. The images of Safranin-O-stained transverse tissue sections were used to generate the condensation measurements, and a finite element model was built and analyzed using ABAQUS software, a powerful finite element analysis tool for modeling of complex linear and nonlinear engineering problems. The comparison of the predicted stress and strain patterns and the experimental gene expression patterns exhibits a correlation between the predicted patterns of compressive hydrostatic stress and the expression patterns of chondrogenic genes. Similarly, the predicted patterns of tensile strain correspond to the expression patterns of osteogenic genes [56].

1.2.6 Motion-Load Related Joint Biomechanics

1.2.6.1 Disuse of Joints

Immobilization of the injured or diseased joint has been performed for many centuries in order to avoid worsening the tissue damage or increasing pain. However, systematic studies in animal models at the beginning of the twentieth century started providing evidence on an opposite point of view. It was reported that plaster immobilization of the canine ankle joints resulted in thinning and fibrillation of cartilage [57]. Later, immobilization of the knee joint in rabbits in full extension during 8 days resulted in necrosis of the articular cartilage at the location of contact or compression between the two opposite cartilage surfaces [58, 59]. The necrosis of the articular cartilage was a non-reversible lesion, which was further characterized in a study including both

immobilization and remobilization of adult rat knee joints [60]. This last study reported major changes in cartilage that included matrix fibrosis, fissuring and ulceration; alterations that were considered reversible if the period of immobilization was smaller than 30 days. Complementary to the study by Salter and Fields in 1960, Hall reported in 1963 flattening of the cartilage in the contact areas, degeneration in the non contact areas, and adhesion of the synovial membrane to the peripheral regions of cartilage. This finding was corroborated by Salter's study on prolonged immobilization of the flexed knee joint of the rabbit without compression [61]. Salter found that this type of immobilization obliterated the synovial fluid space, thereby blocking the synovial fluid nutrition from reaching the cartilage, resulting in irreversible degeneration of the cartilage tissue. Studies of healing of full-thickness defects of articular cartilage in the knee joints of monkeys [62] and the rat [63, 64] have shown that immobilization led to adhesions whereas normal active motion stimulate healing. The deleterious effect of immobilization of the animal's knee cartilage was microscopically characterized by loss of affinity to metachromic stains, and abnormality of chondrocytes.

Similar gross and microscopic observations to the reported in animal models have been shown in humans. Patient joints that were immobilized in forced position demonstrated tissue damage associated with continuous compression of the opposed joint surfaces [65]. Furthermore, Salter reported cartilage degeneration, atrophy and even absence of tissue in areas that were not longer in contact with the opposite joint surface for a long period of time [61]. Observation of cartilage degeneration were produced not only at the knee joint, but also at the hip [65], interphalangeal finger joints and metatarsophalangeal joints [61]; posterior intervertebral facet joints following anterior

spinal fusion [66] interphalangeal joints with long-standing flexion deformity [67]; amputated specimens of knee joints that had been immobilized for long periods [68], and many more.

In spite of the adverse effects on joint tissues caused by immobilization, under certain circumstances immobilization of the joint is necessary. It has been reported that limitation of the joint may protect against some types of chemically induced damage to articular cartilage, since the extent of chondrocyte death after intraarticular injection of the metabolic poison sodium iodoacetate was significantly reduced if guinea pigs were immobilized immediately after the injection [69]. Furthermore, Neither osteophytes nor fibrillation of the articular cartilage developed in any of the immobilized animals [70]. Those studies imply resting the joint during a period of severe damage to the chondrocytes may be chondroprotective. In-depth investigations on the effect of immobilization and remobilization are necessary to preserve cartilage integrity and to prevent cartilage damage. Based on our preliminary studies [71], the degrading results of the cartilage is reversible if immobilization time is less than 6 hours on rats, thus, such temporary unloading may permit recovery of the damaged chondrocytes and facilitate subsequent repair of the tissue.

1.2.6.2 Effect of Overuse/Overloading on Articular Cartilage

In contrast to immobilization or underloading conditions of joints, there are more concerns about overuse and overloading conditions associated with the consequential cartilage damage that has a connection with OA.

Cartilage is meant to perform its load bearing function within a physiological range. When the range is exceeded, cartilage can breakdown due to overloading. The damage

begins from the surface down and may be varied throughout the joint because of differential loading capabilities in cartilage layers. Once the cartilage is damaged, the tissue becomes vulnerable to physiological joint forces and the progression can be accelerated with exercise or, in some cases, delayed with immobilization, or improved with passive motion. Cartilage is subjected to both shear and axial longitudinal loading. The shear stress is created by the contact friction [58, 72-75] between cartilage during flexion-extension of the joint and the axial longitudinal loading (Simon et al. 1971, Radin et al. 1973) is produced by the normal forces applied to the cartilage surface due to weight bearing. In a study combining both shear and axial longitudinal loading [76], it was reported the observation of early and progressive damage of the articular cartilage, but not in animals that were subjected to shear loading only. The combination of shear and axial loading also resulted in increased PGE2 and cAMP.

In a recent study, after joint destabilization surgery by anterior cruciate ligament transaction and partial medial menisectomy, Sprague-Dawley rats were subjected to forced mobilization of the joint by walking in a rotating cylinder [77]. Cartilage degeneration was observed 2 weeks after surgery accelerated by the forced mobilization exercise, including proteoglycan loss and chondrocyte hyperthrophy. Several clinical studies have provided evidence that overloading such as intense participation of sports and certain repetitive work-related activity can increase the risk of cartilage degeneration.

1.2.6.3 Effect of Moderate Loading

The most well developed model to reduce the progression of the joint diseases is known as Continuous Passive Motion (CPM). The biological concept of continuous passive motion of synovial joints was created by Salter in 1960 as a possible means of

stimulating healing and regeneration of articular cartilage, as well as preventing or overcoming joint stiffness [65]. CPM got birth by extension of the beneficial effects attributed to intermittent motion of the joints. The premises considered in this type of therapies were that synovial joints are meant to move, that the nutrition of the cartilage is primarily driven by motion of the synovial fluid, and that immobilization is deleterious to the joint tissues.

A motorized motion device was created for the knee joint of the rabbit, and tested for many disorders and injuries of articular cartilage and periarticular tissues. CPM was initiated immediately after the surgical intervention, while the animal was under anesthesia. The motion was performed nonstop for long periods of time (one to four weeks) with a flexion-extension cycle completed every 45 seconds. The effect of CPM was compared against Immobilization and intermittent active motion. In many studies, CPM has been shown superior to immobilization or intermittent active motion to heal articular cartilage and preventing joint stiffness. CPM was well tolerated by the animals despite the duration of the apparently painless therapy. CPM has shown a positive effect not only in cartilage but also in tendons and ligaments, preventing the adhesion of the synovial membrane and the manifestation of joint stiffness. It did not interfere with the normal healing of wounds and the neochondrogenesis is possible under CPM therapy.

For clinical practice, several CPM devices for humans use were created targeting the ankle, ankle-knee-hip, the finger(s), the wrist, the elbow, and the shoulder. Similarly to the previous experience with rabbits, CPM was performed immediately after surgery, and continued nonstop for one week. The device has been used in several operative procedures, including open reduction and rigid internal fixation of displaced intra-

articular fractures, open reduction and rigid internal fixation of displaced metaphyseal and diaphyseal fractures; arthrotomy, capsulotomy, arthrolysis and debriclement for post-traumatic arthritis with persistent limitation of joint motion; surgical release of extra-articular contractures of joints (e.g., quadricepsplasty); arthrotomy and drainage (combined with appropriate antibiotic therapy) for acute septic arthritis; incision and drainage (combined with appropriate antibiotic therapy) for acute tenosynovitis; synovectomy for rheumatoid arthritis and hemophilic arthropathy; biological resurfacing (with a periosteal graft) for a major defect in a joint surface; surgical repair of an acute ligamentous tear; reconstruction of a chronic ligamentous tear using a tendon graft; surgical repair of a complete laceration of a tendon (especially in the hand); rigid internal fixation of a metaphyseal osteotomy (e.g., for arthritis of the knee) and total prosthetic joint replacement.

Noticeable results of CPM included the reduction of pain, maintenance of physiological range of joint flexion and extension; normal wound healing; reduced period of rehabilitation and hospitalization. Salter's studies demonstrated that prolonged immobilization of joints is deleterious and that exercise, continuous passive motion or intermittent motion, is better for joints and their articular cartilage than is immobilization. A metaanalysis on the efficacy of CPM following total knee arthrosplasty analyzed 14 studies (952 patients) and found significant improvements in active knee flexion and analgesic use 2 weeks postoperatively with the use of CPM and physiotherapy (PT) compared to PT alone [9]. The lengths of hospital stay and need for knee manipulations were significantly decreased. In particular, the CPM combined with PT did offer beneficial results for post-TKA patients. This metaanalysis concluded that more research

is necessary to assess the differences in effectiveness with different characteristics of application such as total duration of treatment and intensity of CPM interventions.

The available in vitro loading models provide valuable approaches for investigating a range of biological responses to specific loading protocols on the tissue dissects or explants [78, 79]. Nevertheless, these studies are limited in their ability to address the in vivo joint loading condition, and thus have difficulty interpreting the helpful results further into instructive knowledge in joint level. In the mean time, previous in vivo animal models have presented very useful information regarding the biomechanical properties of the connective tissues and the beneficial effects of CPM [14, 36, 37, 80]; whereas, to date, few experimental devices offer a non-invasive approach to provide precise control of joint loading parameters, or to create the well-quantified physiological loading environment on small animal models such as rats.

1.2.6.4 Mechanism of Motion-based Therapies

The underlying mechanisms mediating the biological response in diseased joints to external mechanical stimuli are not completely elucidated. The rationale behind the development of CPM of synovial joints included the clinical observations of the deleterious effects of prolonged immobilization of synovial joints in patients with persistent stiffness, pain, muscle atrophy, disuse osteoporosis, and late degenerative arthritis. These observations were combined with evidence of the beneficial local effects of early active motion as opposed to continuous immobilization, and the harmful effects of immobilization of joints in a forced position. Contrary to the traditional principle of immobilization of diseased and injured joints as a means to better heal and reduce pain, Salter proposed that CPM should 1) enhance the nutrition and metabolic activity of

articular cartilage, 2) stimulate pluripotential mesenchymal cells to differentiate into cartilage, and 3) to accelerate healing of both articular cartilage and periarticular tissues, such as tendons and ligaments [36]. The nutrition of articular cartilage has been investigated by quantifying the diffusion of radioactive gold through the matrix [81]. It was documented that the intake of radioactive gold by the cartilage was increased by exercise of the joint, concluding that the nutrition of cartilage is improved by articular motion. Osteochondral defects can undergo spontaneous repair mediated by the proliferation and differentiation of mesenchimal stem cells that migrate from the bone marrow [82]. The stem cells differentiate into fibroblasts, chondrocytes and osteoblasts, synthesizing new cartilage in the chondral region of the defect. However, the surface was covered by fibrous tissue that degenerated over time with extensive fissuring and fibrillation. Stimulation of the new tissue formation with CPM may help to reduce the formation of fibrous tissue and a durable functional cartilage layer. It has been proposed that the reduction in pain generated by CPM may be a consequence of the "gate control theory", in which the continuous generation of impulses from the continuously moving joint and their transmission to the spinal cord or brain may "block" the transmission of pain impulses to the brain [83]. Further investigation, both clinical and experimental, is required to test the validity of this hypothesis.

Studies applying hydrostatic pressure and shear stress to chondrocytes in vitro have demonstrated that physiological levels of cyclic hydrostatic pressure (2.8 to 10 MPa) result in an increased expression of aggrecan and type II collagen [84, 85]. Studies applying shear stresses demonstrated upregulated expression of Ihh and type X collagen [86, 87]. Chondrocytes under intermittent tension, or elevated hydrostatic pressure have

shown increased expression of type X collagen when loaded in tension in a magnitude dependent manner [88]. Hydrostatic pressure has a chondroprotective effect [89], while cyclic tension has the opposite effect by increasing the expression of MMP-13, responsible for the cleavage of type II collagen and CTGF. This behavior of cartilage is contrary to other cell types that downregulate MMPs when subjected to tension in vivo [90].

In addition to enhancing the solute transport in cartilage, CPM has been reported to play a role on the production of molecules linked with beneficial effects on cartilage [91]. Animals that developed arthritis induced by an antigen method, underwent one or two days of CPM and compared to immobilized knees. The immobilization of the limb resulted in disease progression in a time dependent manner, cell disorganization, matrix degradation, loss of stratification, and eventual degeneration of the cartilage within 96h. The expression of pro-inflammatory mediators MMP-1, COX-2, and IL-1 was notably increased. However, CPM attenuated the progression of the disease, revealing a rapid and sustained decrease in GAG degradation and the expression of all pro-inflammatory mediators during the entire period of CPM treatment. More importantly, CPM induced synthesis of the anti-inflammatory cytokine IL-10. Therefore, potent anti-inflammatory signals on meniscal fibrochondrocytes were correlated with CPM treatment, providing important insights on the molecular basis of the beneficial effects of CPM, suggesting that CPM somehow suppresses the inflammatory process of arthritis as opposed to immobilization.

In spite of these evidences, there is still controversy surrounding the clinical use of the motion-based therapies, mainly regarding the effectiveness of those therapies in

treating different joint diseases and the validity of the empirical treatment protocols applied to the patients. Moderate loading seems to be beneficial, but the beneficial range of the loading in terms of magnitude, frequency, duration, or the loading rates is often unclear, As a consequence, how moderate is moderate remains one of the most important questions to answer. More insights into the mechanobiological mechanisms in cartilaginous tissues in response to dynamic loading conditions are required. This highlights the need for more elaborated theoretical and experimental research on the role of mechanical stimuli on cartilage remodeling.

Chapter 2
TEMPORAL EFFECT OF MOTION-LOAD ON JOINT BIOMECHANICS (PART I):

DEVELOPMENT AND VALIDATION OF A JOINT MOTION AND LOADING SYSTEM FOR A RAT KNEE JOINT IN VIVO

ABSTRACT

The influence of biomechanical stimuli on modulating joint homeostasis is well recognized; however, the underlying mechanism mediating joint tissue responses to external mechanical loading is not clear, and many aspects of cellular mechanotransduction in cartilage remain unknown. Experimental studies using suitable joint loading device to create highly controlled and well quantified motion and loading environment is critical to advance our insight into joint physiology and to better control joint diseases such as osteoarthritis (OA). We developed a computer-controlled joint motion and loading system (JMLS) to study the biological response of cartilage under well-characterized mechanical loading environments. The JMLS was capable of controlling i) angular displacement, ii) motion frequency, iii) magnitude of the axial compressive load applied to the moving joint, and it featured real-time monitoring. The accuracy and repeatability of angular position measurements, the kinematic misalignment error as well as the repositioning error of the JMLS were evaluated. The JMLS demonstrated remarkable accuracy and reliability for the measurement and kinematics tests. This novel non-invasive system may be useful for joint biomechanics studies that require different treatment conditions of load and motion *in vivo*.

Keywords: Joint Motion and Loading; Articular Cartilage; Axial Compressive Load; Knee joint; Immobilization; *in vivo*; Rat knee.

INTRODUCTION

Articular cartilage in the knee joint provides low friction, prevents wear and tear at contacting joint surfaces, and enables the knee to absorb shocks. Chondrocytes react to mechanical stimuli due to joint motion and compressive loading by modulating both anabolic and catabolic activities, thus preserving or degrading their extracellular matrix, respectively. The degradation of articular cartilage is the central feature of major joint diseases such as osteoarthritis (OA) and involves a complex interaction between mechanical, environmental, anatomical, and biological factors [92-94].

Biomechanical stresses beyond a physiological range may induce cartilage degeneration and alter the ability of cartilage to perform its normal function. On the one hand, prolonged synovial joint immobilization seems to lead to cartilage degradation [57]. necrosis of the articular cartilage at the location of contact or compression between the two opposite cartilage surfaces [65], [58], matrix fibrosis, fissuring and ulceration [60], flattening of the cartilage in the contact areas, degeneration in the non-contact areas, and adhesion of the synovial membrane to the peripheral regions of cartilage [61], cartilage tissue adhesion, [63, 64], persistent joint stiffness, pain, muscle atrophy, disuse osteoporosis, and degenerative arthritis. Cartilage degeneration occurs not only at the knee joint, but the hip [65], interphalangeal finger joints and metatarsophalangeal joints [61]; posterior intervertebral facet joints following anterior spinal fusion [66]; interphalangeal joints with long-standing flexion deformity [67]; etc. On the other hand, if the physiological load-bearing capacity of cartilage is exceeded as a result of overuse or overloading, as seen in intense sports [95-99], repetitive high-impact activity [100, 101]and obesity [102, 103], the tissue is subject to higher risk of breakdown. Under

excessive mechanical loading stimuli, the tissue can breakdown from the surface down and the damage may be varied throughout the joint because of differential loading capabilities in cartilage layers. Once the cartilage is damaged, the tissue may become increasingly vulnerable to further degradation even by physiological-level joint forces, and the progression of tissue breakdown can be accelerated with moderate exercise [77].

Physiological joint motion and loading are considered to have a chondroprotective effect preventing cartilage degradation [96, 104, 105]. After a period of immobilization, motion of the joint can prevent or overcome joint stiffness by enhancing synovial fluid motion, cartilage nutrition, and stimulating the healing and regeneration of articular cartilage [37]. Beneficial results of motion-based physical therapy include the reduction of pain, maintenance of physiological range of joint flexion and extension, and a reduced period of rehabilitation or hospitalization. Meta-analyses have indicated that continuous passive motion or intermittent motion in humans is better for joints and their articular cartilage than is immobilization [9]. Nevertheless, there is no consensus on either the optimal therapeutic protocol or the long-term clinical effectiveness of continuous passive motion [8, 9]. Key to this debate are the diversity of treatment variables (including the frequency, range of motion, etc.,) and the complex biomechanical processes associated with those treatment variables.

The development of in vivo animal models to study the development of joint diseases is critical from both basic scientific research and clinical use perspective. Much more efforts have been concentrated on the development of animal models of osteoarthritis, rheumatoid arthritis and cartilage defects, relatively less attention has been focused on the development of systems and models to reduce and/or to regress the onset of the disease.

There are four types of animal models related to joint disorders: 1) spontaneous or naturally occurring disease models, 2) genetically modified animal models, 3) chemically induced models and 4) mechanically induced models. The mechanical models were developed to provide an accelerated, yet controlled model of osteoarthritis, or in some cases, to demonstrate the contribution of particular mechanical components or structural elements to the development of osteoarthritis. Among the most popular mechanical/surgical induced disease models are the ACL transection, menisectomy, varus and valgus osteotomies and muscle resection. Immobilization is another approach that leads to joint degeneration.

Previous studies have developed useful animal models in non-invasive approaches to evaluate the impact of physical activity on biological changes in cartilage and tendon [77, 106-109]. All of these non-invasive models have provided important insight into the relationship between mechanical stimuli and subsequent structural, compositional and morphological changes in the tissue. Commonly used loading devices such as the treadmill and rotary cylinder systems force the animal to run at a controlled speed for a determined period of time; however, the mechanical stimulus applied to the joint may be different across animals and difficult to standardize. In devices that use electrical stimulation to produce muscle contraction of the animal's limb, a rapid muscle twitch is generated to allow precise control of mean peak load and repetition frequency; nevertheless, a smooth motion of joint flexion may not be easy to obtain and the loads are not identical in this approach. In contrast, assisted motion devices such as continuous passive motion (CPM) systems seem to offer a better alternative in controlling to control the dose of mechanical loading and range of motion provided to the animal joint [14, 65,

71, 109-111]. Unlike treadmills, rotary cylinders or electrical stimulation-based systems, the CPM devices allow uniform cyclic motion of the joint with quantifiable loading that can be applied at very low repetition rates. Some murine joint loading models have been reported in the recent musculoskeletal mechanotransduction studies [112, 113], these novel joint loading devices offer well characterized loads at various waveforms to study the effect of dynamic mechanical loading on bone formation and fracture healing; whereas, the effect of such loading modality on cartilage has not been reported.

In this study, we designed and constructed a computer-controlled joint motion and loading system (JMLS) capable of performing passive motion loading (PML) and compressive motion loading (CML) on the knee joint of a rat. The system was conceived to provide not only motion-induced mechanical loading but also axial compressive force applied normal to the cartilage surface with real-time monitoring of joint motion and loading. Therefore, this JMLS is not directly comparable to continuous passive motion (CPM) devices, and so, to avoid any confusion with CPM clinical devices, we will use different terminology in describing the system. The novel motion and loading system created in the *in vivo* rat model, in combination with an immobilization-based animal model, allowed the study of key catabolic/anti-catabolic proteins involved in tissue degeneration and cartilage maintenance in response to specific motion and loading protocols.

MATERIALS AND METHODS

Joint Motion and Loading System Design

The JMLS was designed to perform passive motion loading and compressive motion loading on the knee joint of a small animal, providing adjustable control of cyclic motion frequency, range of angular displacement, axial compressive force magnitude between the tibia and femur, and permitting real time monitoring of angular motion and compressive load.

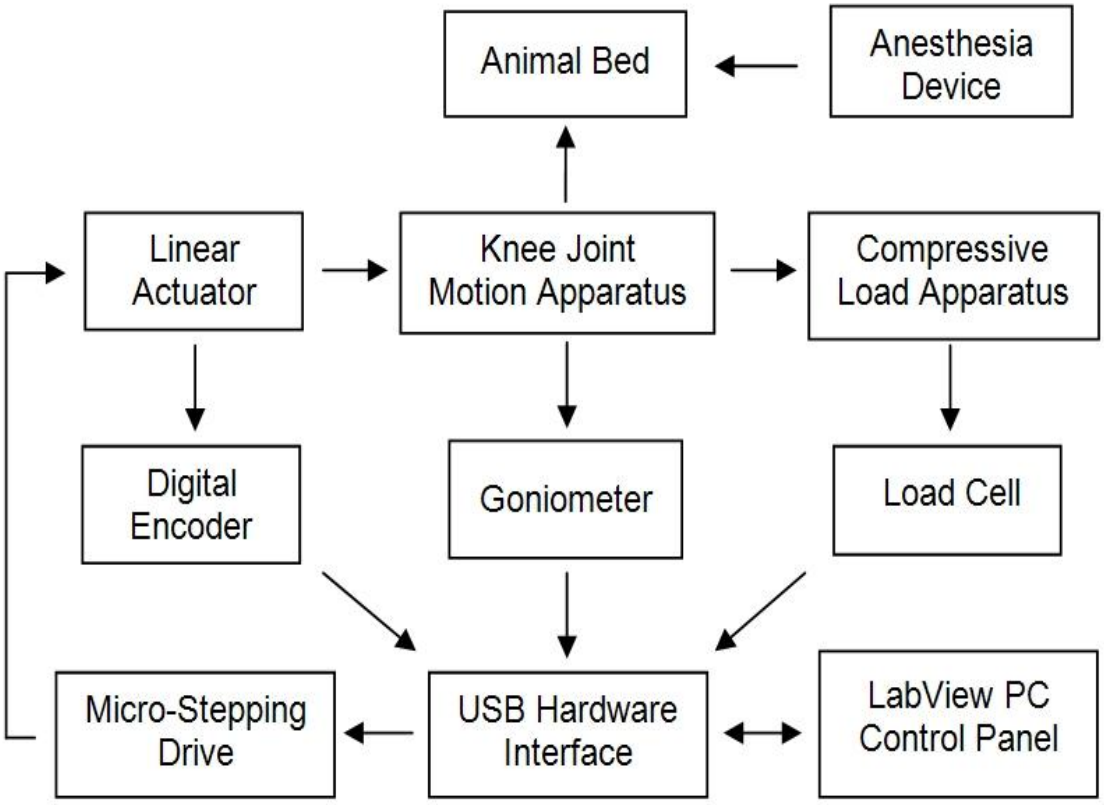

Figure 2.1 Block diagram of the components of the *in vivo* computer-controlled joint motion and loading System (JMLS). The JMLS consisted of an animal bed and the anesthesia device, a knee joint motion apparatus with a monitoring goniometer, a linear actuator with micro-stepping drive and a monitoring encoder, a compressive load apparatus with a monitoring load cell, and the hardware and software interfaces.

The JMLS consisted of an animal bed and an anesthesia machine integrated into a custom-built knee joint motion/load apparatus, a linear actuator with micro-stepping driver and digital encoder, a magnetic goniometer for real-time joint angle readout, a load cell for compressive load monitoring, a USB analog/digital I/O interface module, and LabView control panel (Figure.2.1). The anesthetized animal was placed prone over an acrylic bed, and the hind limbs were introduced through two spaces located at the center of the bed. The right hind limb of the animal was placed in the knee joint apparatus and the animal body was secured to the bed using Velcro straps. Special care was taken during positioning of the limb in the apparatus to align the rotation axes of the knee joint and the structural apparatus. The hip and femur were maintained in a fixed position to minimize lateral displacement or misalignment during the test. Throughout the experiment, the animal was anesthetized using 1-3% isoflurane dissolved in 21% oxygen, while the respiration rate and body temperature were continuously monitored. A gas mask directed the anesthetic to the nose of the animal, and the exhalation gases were circulated toward a carbon-activated filter and exhaust system. The operation of the system did not require any special consideration of the environment (Figure. 2.2).

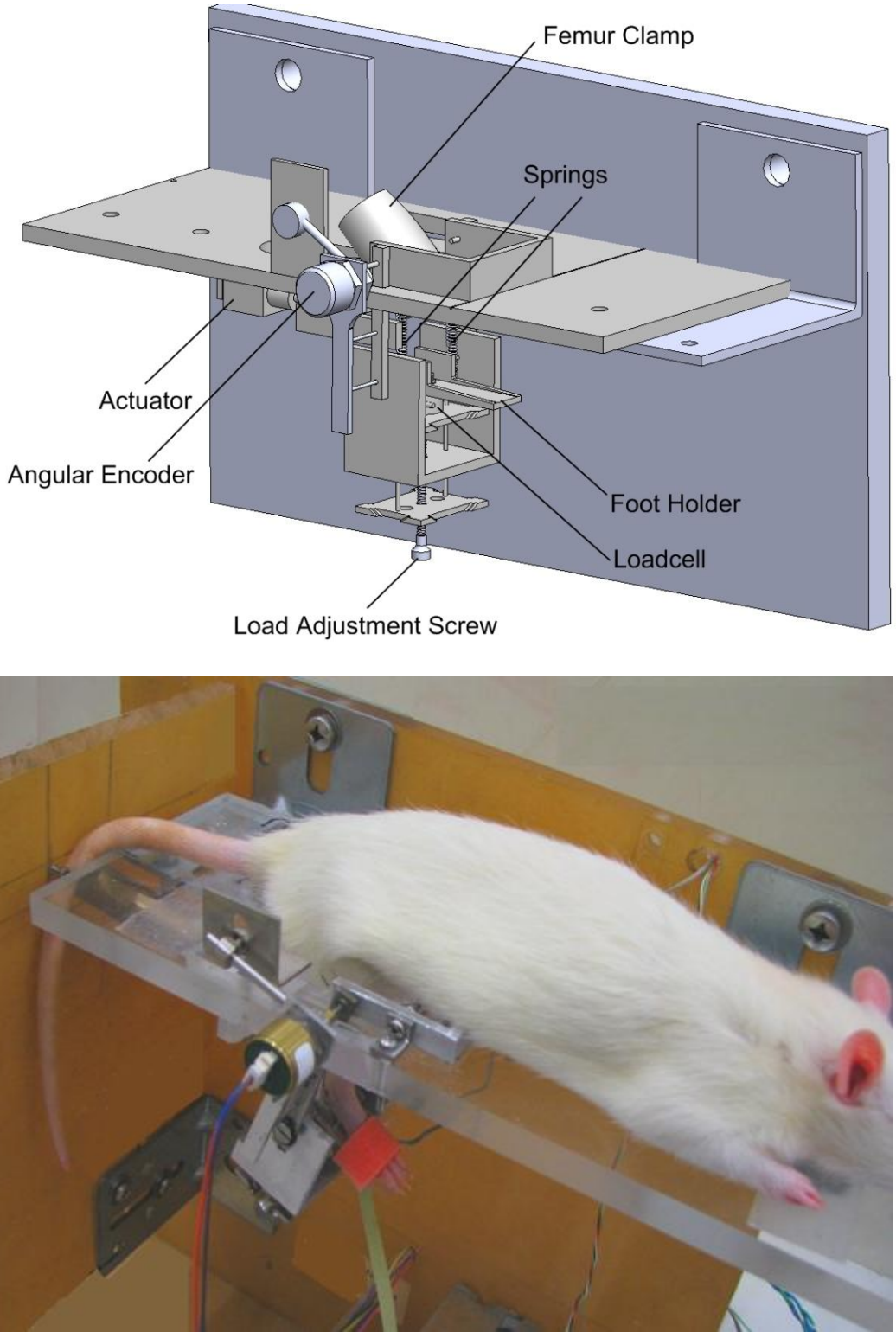

Figure 2.2 (Upper) Schematic diagram of the JMLS design and (Below) Photograph of the experimental setup with an animal undertaking motion and loading experiment.

The knee joint apparatus transformed the linear motion provided by the actuator into angular displacement at the knee joint. Double steel ball bearings were used to minimize the friction during rotation of the structural steel arms of the motion apparatus. The goniometer is a miniature magnetic encoder (US Digital Corp, Vancouver, WA) aligned to the rotation axis of the structural arms that provided a pulse width modulated (PWM) signal proportional to the angular position of the system, the PWM signal was digitized and calibrated using a protractor to exhibit a numerical value within 0~360 ° that represented the angular position. The JMLS had adjustable control of motion frequency and range of angular displacement via a linear actuator with 50 mm travel stroke (bipolar NEMA 13 Hybrid, Haydon Motion, Waterbury, CT) coupled to an incremental rotary encoder (E5S, US Digital Corp, Vancouver, WA). The incremental rotary encoder used an LED and photodetector to identify the angular position, direction and rotation speed of the motor shaft. A micro-stepping motor drive (MD2S-P US Digital Corp, Vancouver, WA) controlled the rate of motion of the actuator, offering a high linear displacement resolution up to 3 micrometers per step. The motion control for the actuator was performed based on the mathematical relationship between angular and linear motion of the apparatus and linear actuator respectively, as shown in the appendix. The linear actuator was able to provide a linear velocity as high as 30 mm/s, which resulted in a maximum cyclic motion frequency of 20 cycles/min for the full range of motion between 65 ° and 135 °.

In addition to PML, the JMLS facilitated a continuous axial force along the tibia and normal to the plantar sole of the animal throughout the cyclic motion. This compressive motion loading capability was integrated into the JMLS to study the role of overloading

on the biological response of the tissue *in vivo*. The anterior aspect of the femur was immobilized at a fixed position, thus, the force applied under the plantar sole was transferred along the major axis of the tibia to the knee joint cartilage surface at any angular position during the flexion-extension procedure. The adjustable load applied to the plantar sole was created by a pair of extended miniature springs attached to the system at the level of the knee joint and a sliding brace under the animal's foot holder. A subminiature load cell (11BL321 Sensotec-Honeywell) situated between the sliding brace and the foot holder produced a continuous measurement of the reaction force under the plantar sole created by the springs. The compressive load can be adjusted by extending or retracting the springs via a vise below the load cell support. This load sensor had a ±25 pound linear range of measurement in tension and compression with infinite resolution and 0.1% full-scale non-repeatability performance. The load cell output was amplified using an instrumentation amplifier (INA 122, Texas Instruments), converted into digital signals using a data acquisition interface (USB-6210, National Instruments) and visualized in real time using LabView (V8.5, National Instruments). The load cell output was calibrated using standard weights (ranging from 2.5 to 500 g) to display the measured force in grams-force (data not shown). Motion and loading protocols were executed via a user interface developed in LabView on which the initial and final angle of the knee joint in degrees of flexion, and frequency of the motion in cycles per minute were defined by the user for the test. This visual interface also displayed and recorded the angular displacement and loading magnitude in real time throughout the motion/load experiment.

Motion Control Algorithm

The control interface developed in LabView was designed in such a way that a user without engineering background or computer program coding experience can perform the operations with ease. According to the designed motion protocol, the user will input the initial and final angles (in deg) as well as the cyclic frequency (in cycles/minute). Given the initial and final angles, the calculation of the mathematic relationship between the sides of the triangle formed by the mobile tibia and fixed femur will provide the linear displacement that the actuator needs to travel for the cyclic motion (Figure 2.3).

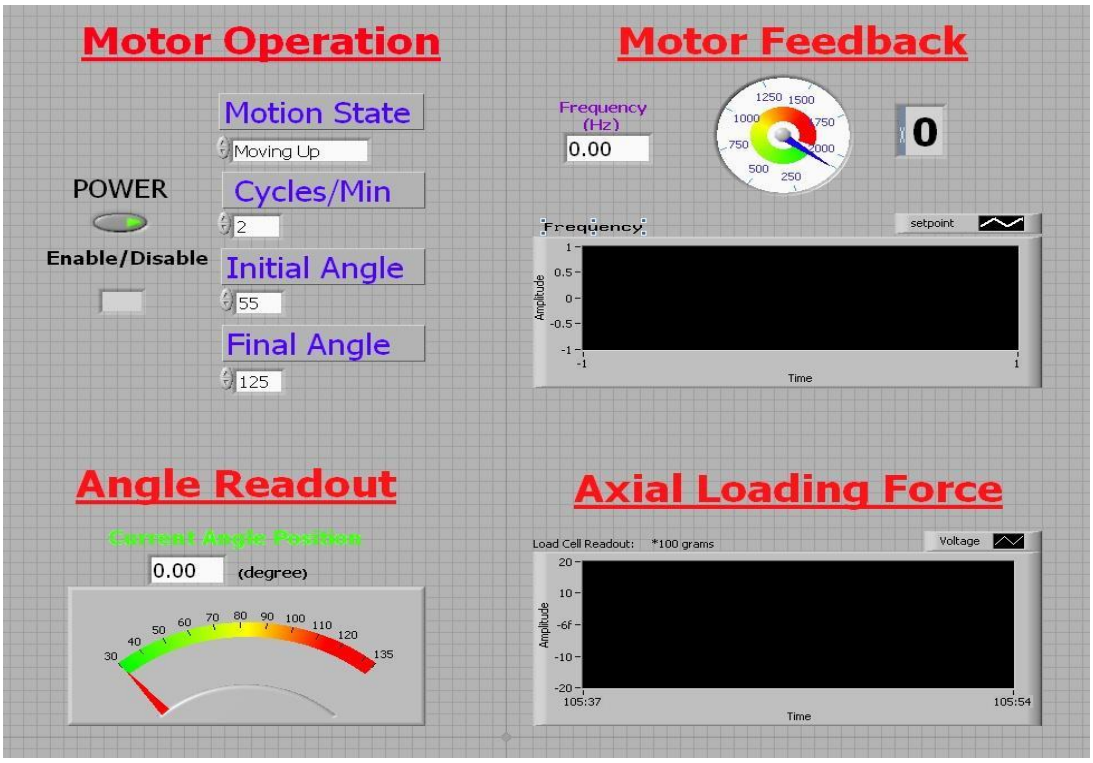

Figure 2.3 Control interface of the joint motion and loading system.

The speed of the linear actuator can thus be obtained by associating this travel length with the cyclic frequency also inputted by the user for the motion control. The linear cyclic motion generated by the computer-controlled linear actuator is transformed by an

adaptor attached on the shaft of the actuator into the repeated angular displacement of the animal's joint between the initial and final angle (Figure 2.4).

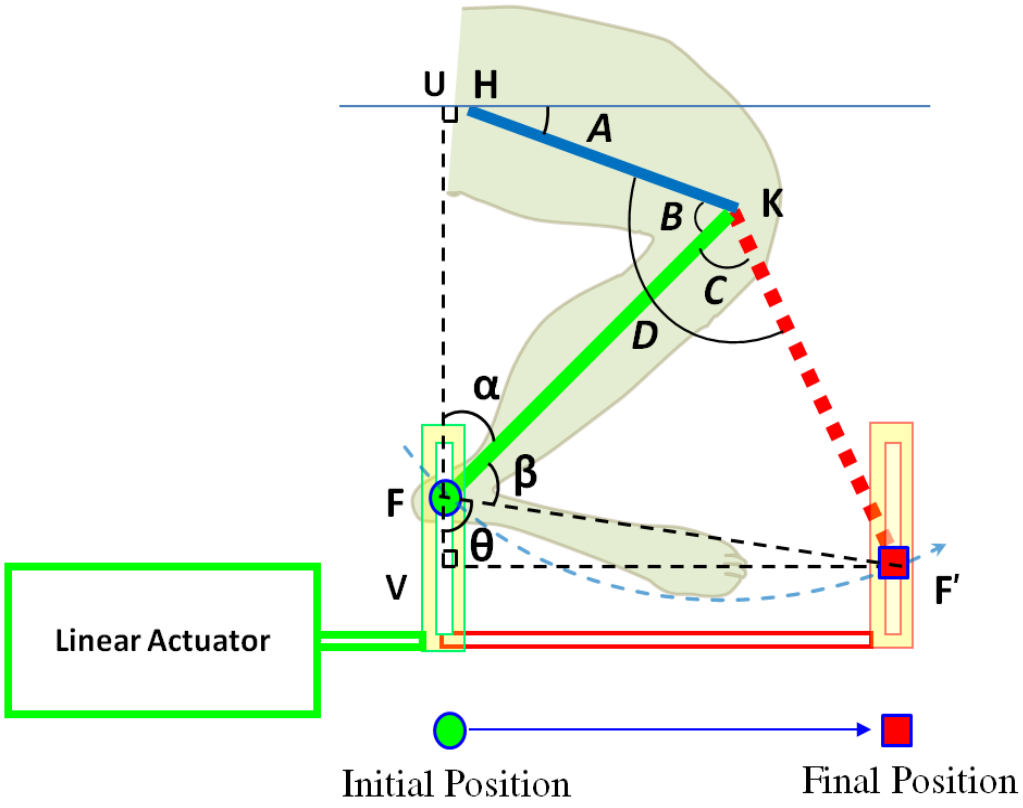

Figure 2.4 Control algorithm of the joint motion and loading system. The animal's femur (HK) is maintained at a fixed position, and the tibia is displaced by the actuator back and forth from KF to KF´that corresponds to the initial angle *B* and final angle *D*. The vertical displacement for the actuator to travel in a half cycle is VF´that corresponds to the angular displacement *C*. Given the parameters (initial angle *B*, final angle *D*, and cyclic frequency N) that the user inputs on the LabView control panel, the software computes the travel length VF´ using FF' and θ that can be described as a function of known variables to obtain the speed for the linear actuator. HK: Length of Femur; KF: Length of Tibia in Initial Position; KF': Length of Tibia in Final Position; VF': Travel Length of Actuator; *A*: Femur Immobilization Angle (*defined by a user)*; *B*: Initial Angle (*inputted by a user*); *C*: Angular Displacement; *D*: Final Angle (*inputted by a user*).

HK: Length of Femur;
KF: Length of Tibia in Initial Position;
KF': Length of Tibia in Final Position;
VF': Travel Length of Linear Actuator;
A: Femur Fixation Angle (*defined by a user*);
B: Initial Angle (*inputted by a user*);

C: Angular Displacement;
D: Final Angle (*inputted by a user*);
N: Cyclic Frequency in cycles/min (*inputted by a user*).

The derivation of the travel length as well as the speed of the actuator for motion control of the system are shown by the equations below:

Given angles α, β, and *C* that can be obtained by *A*, *B* and *D* (to be defined by a user),

$$\because \alpha = 2\pi - \frac{\pi}{2} - (\pi - A) - B$$

$$= \frac{\pi}{2} + A - B; \quad (1)$$

$$\beta = \frac{1}{2}(\pi - C); \quad (2)$$

$$C = D - B; \quad (3)$$

the range of angular displacement is given by:

$$\therefore \theta = \pi - \alpha - \beta$$

$$= \frac{1}{2}(B + D) - A; \quad (4)$$

where the distance FF' is described as a function of the initial and final angles B and D defined by the user,

$$\because FF' = 2 \times FK \times sin[\frac{1}{2}(D - B)]; \quad (5)$$

The linear displacement of the actuator is given by the segment VF' as a function of the angular displacement FF',

$$\therefore VF' = FF' \times \sin\theta$$

$$= 2 \times sin[\frac{1}{2}(D - B)] \times sin\,[\frac{1}{2}(B + D) - A]; \quad (6)$$

Therefore, the speed of the linear actuator (mm/s) is determined upon the required linear displacement to achieve the range of angular motion (characterized by *A*, *B*, and *D*) and cyclic frequency (N) selected by the user:

$$\text{Speed of Actuator}$$

$$= \frac{1}{60}(2\text{N} \times VF')$$

$$= \frac{1}{15}\text{N} \times sin[\frac{1}{2}(D - B)] \times sin\,[\frac{1}{2}(B + D) - A] \quad (7)$$

System Performance Test

The JMLS was designed to produce effective joint kinematic and loading conditions that have been associated with the modulation of joint cartilage biology. The validation test of this new assisted motion/load system included the analysis of the angular positioning error, the repeatability after the animal's hind limb repositioning, and the effectiveness of the JMLS in producing biological responses of cartilage *in vivo*.

- Real-Time Angular Position Monitoring. Direct *in vivo* assessment of the animal's joint angular position would require an invasive intervention to implant a sensor in the tibia of every animal. However, such invasive procedures may induce a systemic inflammatory response that may obscure or alter the levels of regulatory molecules produced as a consequence of the PML and CML treatments. Instead, the JMLS was designed to provide indirect estimates of the angular displacement of the tibia through the measurement of the kinematics of the mobile apparatus frame, avoiding any open injury to the animal's limb. This approach assumed that the limb of the animal remained aligned with the moving apparatus frame during the cyclic motion, thus requiring an experimental validation test. We validated this indirect approach by characterizing the accuracy and repeatability of the magnetic goniometer attached to the mobile frame, and the angular position error between the frame and the tibia.

First, we determined the accuracy and repeatability of the real-time angular position monitoring offered by the magnetic angular encoder. This magnetic goniometer was aligned with the axis of rotation of the apparatus and provided a pulse width modulated signal that is proportional to the angular position of the apparatus frame. This signal was acquired by LabView via digital ports on the DAQ card and then digitized and transformed into equivalent angular position data in arc degrees. Data of five trials of cyclic motion in full flexion/extension from 65 ° to 115 ° at a frequency of 2 cycles/minute for 2.5 minutes each trial were recorded at a sampling rate of 1Hz. The accuracy was assessed by the mean and standard deviation of the error between the recorded measurement data and the set point reference values computed in Matlab 7.2 (The Mathworks) using the mathematical modeling equations shown in the appendix. The repeatability was evaluated by comparing the measurement data from five repeated trials; the first trial was defined as the baseline, and the repetition error was calculated as the absolute difference between the baseline and the second to the fifth repeated trials.

Second, the difference between the angular position of the apparatus frame and the animal's tibia was characterized using three-axis Microelectromechanical (MEMS) accelerometer sensors (MMA 7260QT, Freescale Semiconductors, Arizona). The sensor simultaneously produced three voltages proportional to the orientation of three orthogonal directions of the sensor relative to earth's gravity. The analog measurement of the three voltages was quantified and digitized for the kinematics analysis. A MEMS sensor chip was attached to the tibia midshaft on a five month old male Sprague Dawley rat right after sacrifice. A small incision was created in the skin and muscle at the level of the mid-diaphysis from the medial aspect of the tibia, a small hole was drilled, and a thin

screw was anchored onto the bone. The incision was cleaned free of debris prior to the insertion of the screws and then secured using bone cement. The three-axis MEMS sensor chip was mounted on a small acrylic base attached to the screw head, and the sensor chip was oriented in the same direction as the frame before the cement hardened. A similar sensor chip was installed on the frame of the medial side of the knee joint apparatus frame and aligned with the sensor on the tibia. The voltage output was transformed into equivalent angular position data, and the difference in orientation measured by the two MEMS accelerometers was used to evaluate the alignment between the tibia and the frame during motion. Twenty cycles were recorded from both sensors at a sampling rate of 100Hz, producing voltage signal data points every 10ms. The mean and standard deviation of the difference between the two data series from the frame and the tibia indicate the intrinsic error of our device to indirectly assess the kinematics of the bone using the goniometer that monitored the angular position of the frame.

- **Repositioning Error.** To assess the variability of the measurement results due to the repositioning of the animal's limb, the hind limb of the animal was repositioned five times in the JMLS. Data of the five repeated trials (20 cycles each, 65°~115°, 2 cycles/minute) were recorded at a sampling rate of 100Hz using the same MEMS accelerometer sensors described above for analysis of the repositioning error. In the beginning of each trial, the rat was completely removed from the JMLS before being repositioned by the same operator for the following test. The first trial was defined as baseline, and the repositioning error was defined as the absolute difference between the following four repeated trials (trial 2-5) and baseline.

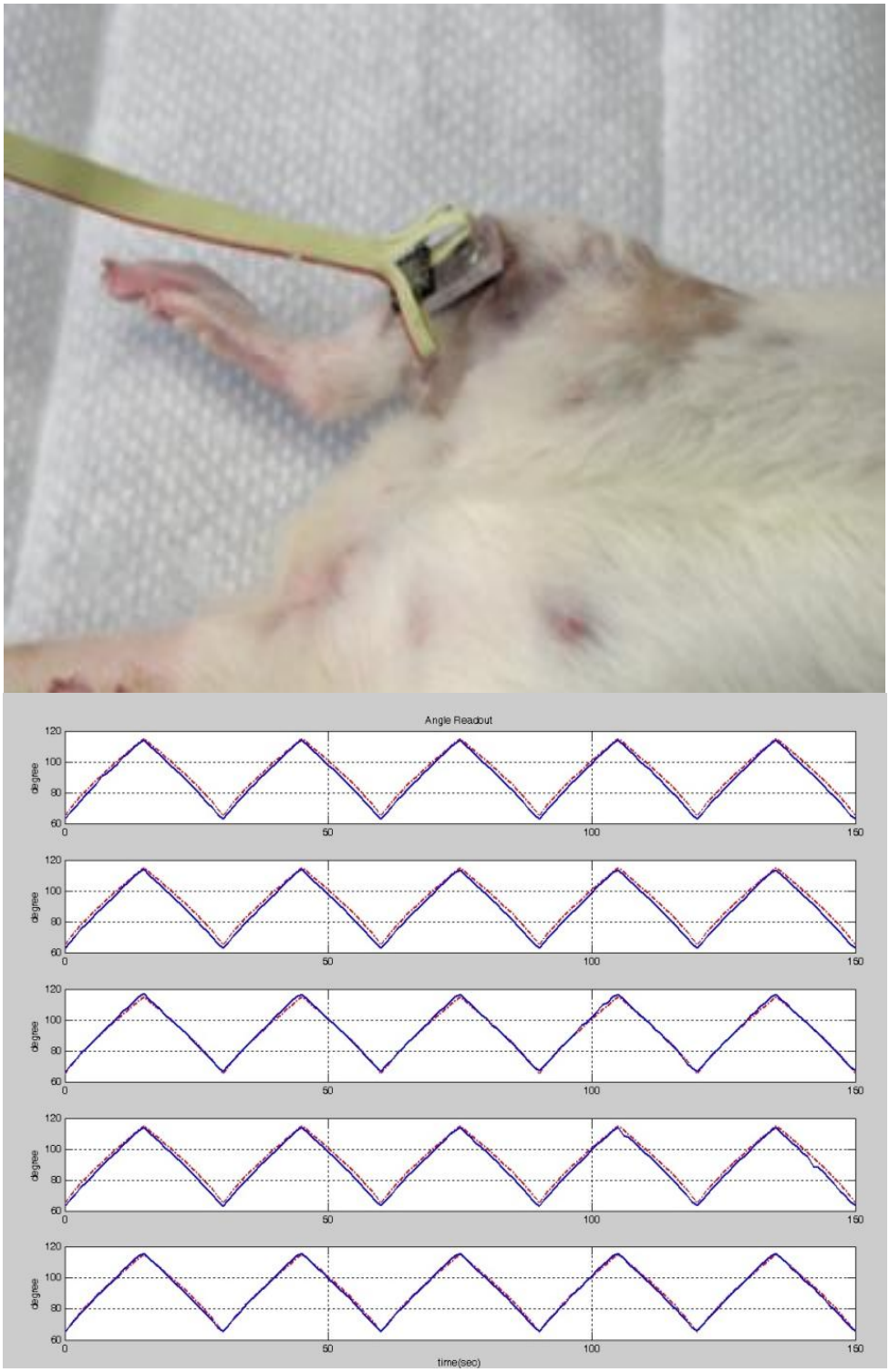

Figure 2.5 (Upper) MEM sensor mounted on the animal limb and (Bottom) Angle measurement acquired by MEMS (Red) plotted against reference values (Blue) Repositioning error is defined as the difference between the four repeated trials and the first trial.

Statistical Analysis

Two-way analysis of variance (ANOVA) was performed on the data testing the real-time angular position measurement by the goniometer and the data testing the kinematics of the apparatus frame and the animal's limb. The correlations among the five-trial measurements were evaluated. ANOVA and the correlation calculations were performed using the Statistic Toolbox of Matlab 7.2. The data were shown as mean ± standard deviation with the percentage denoting the ratio of the computed value relative to the magnitude of the corresponding angular position. ANOVA with Tukey's post-hoc analysis was used to determine statistical significant differences between SHAM, IMM, PML and CML groups versus CTL. A value of $p<0.05$ was considered significant.

RESULTS

Accuracy, Precision & Repeatability of Real Time Angular Position Measurement

The magnetic goniometer was found to produce accurate and precise angular positioning measurements. Comparison of measured data by the goniometer and the set point reference values (Figure 2.6) demonstrated a linear correlation between both quantities (R^2=0.99) with an angular position accuracy of 0.56 °(0.63%) and a precision of ±2.59 °(1.06%).

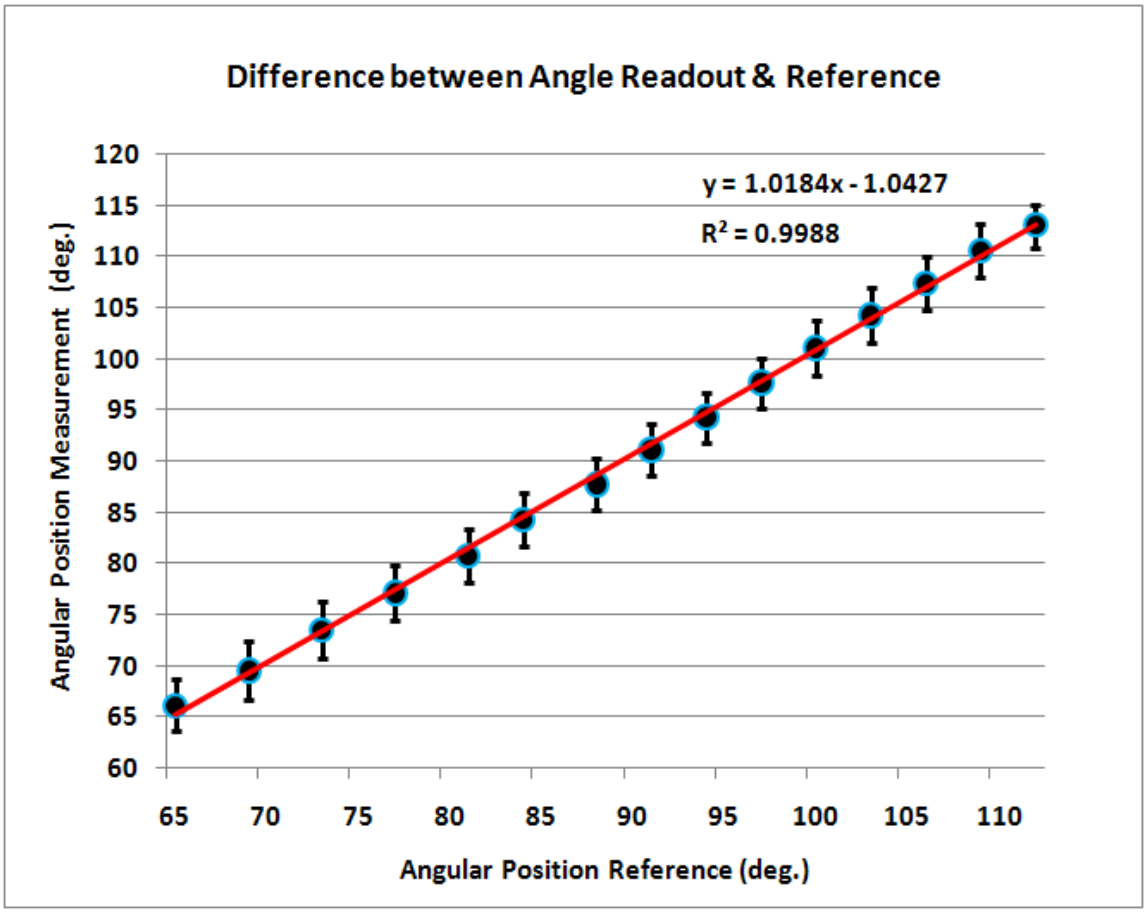

Figure 2.6 Comparison between the angular position measurement from the goniometer and the reference values designated by the control algorithm. There was a linear correlation between the two quantities (R^2=0.99) with an angular position accuracy of 0.56 °(0.63%) and a precision of ±2.59 °(1.06%).

The repeatability test showed that the mean of the repetition errors between trial 2-5 and baseline was 1.21 ° ± 1.55 °(1.40% ± 1.78%) (Figure 2.7). Two-way ANOVA results showed there was no repetition effect or cycle effect ($p >> 0.05$) and there was no interaction between the two effects ($p >> 0.05$), indicating that the five trials of data were essentially the same. This conclusion was further supported by the correlation coefficients between any two of the five trials that were exclusively greater than 0.99 (data not shown), indicating that the five trials of data were essentially the same.

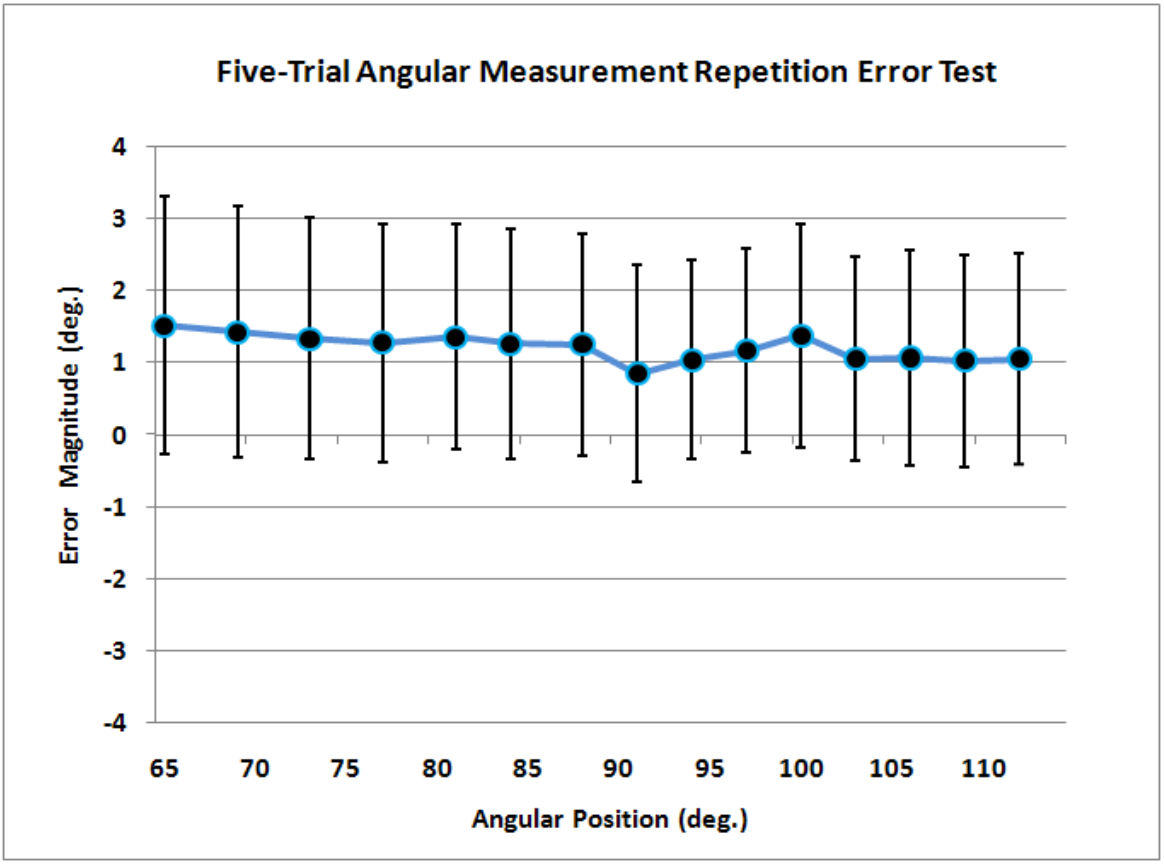

Figure 2.7 Five-trial repetition test result of the angular position measurement offered by the goniometer. Repetition error was defined as the absolute difference between the first trial (baseline trial) and the repeated four trials (trial 2-5). The averaged mean and standard deviation of the errors calculated from trial 2-5 against baseline trial was 1.21 ° ± 1.55 °(1.40% ± 1.78%).

Misalignment between Apparatus Frame and Animal's Tibia during Dynamic Test.

The angular position error between the apparatus frame (or the goniometer) and the animal's tibia measurements indicated a linear correlation between the animal's tibia and the apparatus frame (R=0.99) within the 70 °-110 ° range of motion (Figure 2.8) and an averaged misalignment error of 1.56 ° ± 3.37 °(1.69% ± 3.78%). A slight deviation at the end of the angular motion range was noticed, which may be caused by the natural rotation of the joint during the flexion of the tibia.

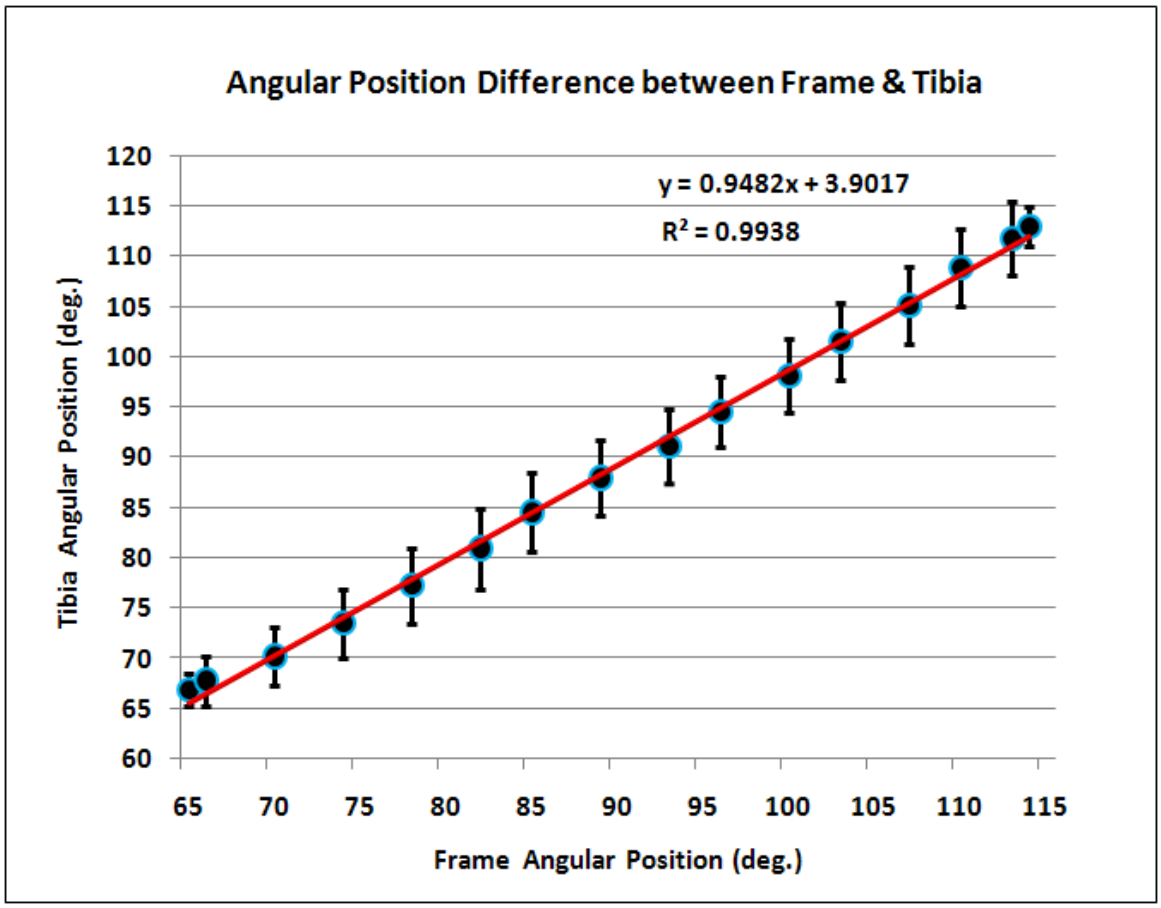

Figure 2.8 Comparison between the angular displacements of apparatus frame and the animal's tibia. The data were measured by the MEMS sensors attached on the frame and the tibia. There was a linear correlation between the two quantities (R2=0.99) and the averaged misalignment error is 1.56 ° ± 3.37 °(1.69% ± 3.78%).

Repositioning Error.

Repositioning of the animal by the same operator in the JMLS produced similar results (<1% difference). Mean and standard deviation of the averaged errors between the measurement trial 2-5 and baseline were plotted out against the corresponding angular position reference values in an increment of 5 ° (Figure 2.9). Repeated-trial data showed that the average mean and standard deviation of the absolute repositioning error from baseline was 0.17 ° ± 0.37 ° (0.18% ± 0.42%) and 0.24 ° ± 0.73 ° (0.27% ± 0.83%) for the frame motion and tibia motion, respectively.

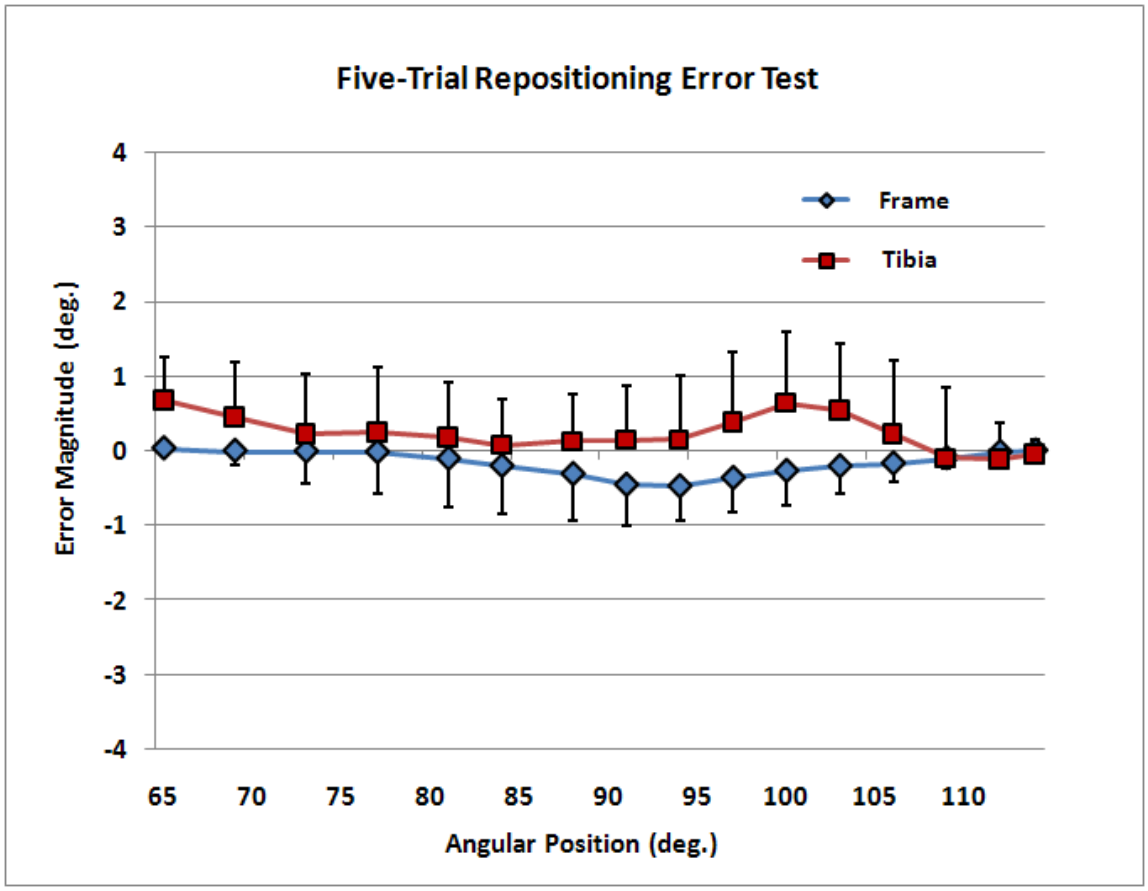

Figure 2.9 Five-trial repositioning test result of the angular displacement of the apparatus frame and the animal's tibia. The data were measured by the MEMS sensors attached on the frame and the tibia. The averaged mean and standard deviation of the repositioning errors calculated from trial 2-5 against baseline was 0.17 °±0.37 ° (0.18% ± 0.42%) for the frame, and 0.24 ° ±0.73 ° (0.27% ± 0.83%) for the tibia.

Two-way ANOVA results performed for repetition effect of the five individual trials showed the p-value was 0.9572 and 0.8169 for the frame and tibia motion measurements, respectively, demonstrating that repetitions of the tested procedure do not significantly vary from one trial to another. The p-value for the repetition effect of 20 cycles within a trial was less than 0.001 for both the frame motion and the tibia motion, indicating that the angular cyclic movement between successive cycles was truly equal to each other over the full flexion range. The correlation coefficients between any two of the five trials were found greater than 0.9970 for the frame measurement and greater than 0.9771 for the tibia measurement, with the p-values < 0.005, demonstrating the high resemblance of the repeated trials.

DISCUSSION

The purpose of this study was to develop a joint motion and loading system in a small animal model that facilitates demanding orthopaedic research requiring well-characterized motion and impact load on the knee joint. The development of such a system can enormously help to study physical activity and weight bearing related joint biomechanics. The JMLS described here provides a reliable, non-invasive way to produce desired angular displacements of a rat knee joint *in vivo.* The angular position generated by the magnetic goniometer was shown to produce accurate, precise and repeatable measurements to monitor in real time the angular displacement of the mobile apparatus. In the accuracy test, the majority of errors between the recorded data and the reference values were < 1% with corresponding standard deviations < 3%, demonstrating profound accuracy and precision of the measurement offered by the goniometer. In the repetition test, the mean (1.40%) and standard deviation (1.78%) of the overall repetition error between the baseline trial and the four subsequent trials indicated the reliability of the goniometer measurement over repeated trials. The repetition error was found to be largely related to the action taken by the operator to position the JMLS to the exact initial angle before starting the motion. Nevertheless, the discrepancy may be considered reasonable for the proposed experiments. In the test for the mobile alignment of the apparatus frame and the animal's tibia during motion, the maximum angular position difference between the frame and the tibia was shown to be smaller than 3 °, exhibiting a high correlation between the displacement of the animal's tibia and the apparatus frame. These results demonstrate that the goniometer measurement of the apparatus angular position can adequately monitor the angular position of the animal's tibia indirectly. This

approach avoids any invasive intervention (i.e. intra-skeletal fixators) that may generate an inflammatory response and obscure the assessment of the biological markers of interest.

Repositioning of the animal in the JMLS resulted in a measurement error < 1%. The absolute difference between the repeated trials 2-5 and the baseline trial was observed to be very small, with the maximum error less than 1 °(0.68% for the tibia measurement and 0.50% for the frame measurement, respectively) and an average close to zero (0.24% for the tibia measurement and 0.18% for the frame measurement, respectively), demonstrating excellent reproducibility in repositioning the animal in the loading apparatus. The standard deviation of measurements in the frame was much smaller than that in the tibia, which was expected since the frame rotates stably on ball bearings, while the tibia has some freedom to move laterally during the rotation of the frame. Nonetheless, the standard deviations can be considered small when compared with the magnitude of the corresponding angular positions. Overall, the motion kinematics of the apparatus and the animal's limb demonstrate remarkable alignment consistency. The performed tests give confidence that the JMLS can facilitate reliable control of the range of flexion/extension and frequency of the cyclic motion applied to the animal's knee joint. Real time monitoring of the angular position, axial loading magnitude, as well as frequency and direction of angular displacement ensured the designed protocols to be accurately implemented.

Altogether, the JMLS differs from the previous *in vivo* loading devices in several respects: 1) It creates a motion and loading environment that is both highly controlled and well quantified. Our intention was not only to provide joint loading levels varying from

slow motion to moderate and more intense ranges, but also to quantify the specific loading variables. 2) The adjustable axial compressive force applied on the joint in motion facilitates the characterization of weight bearing on a moving joint. It has been reported that the weight bearing load on a human joint at certain positions can be as high as 10 times the body weight, which may cause cell death, rupture of the collagen fiber matrix, and increase in tissue water content [114]. Our system can supply a sustained compressive loading condition to examine the detrimental effect of clinically relevant overloading conditions at different magnitudes. 3) It features real-time monitoring for proper implementation of a wide variety of motion and loading protocols. During the testing experiment, the JMLS achieved satisfactory performance visually monitored by three channels of real-time feedback measurements, namely, the actuator encoder, the knee joint angle readout, and the axial compressive force load cell.

In conclusion, this study provided evidence on the effectiveness of a new joint motion and loading system (JMLS) to create the biomechanical environment necessary to induce a clear biological response of cartilage *in vivo* [71]. The flexibility of the JMLS provides a versatile tool for a broad range of biomechanics and mechanotransduction-related experiments on small animals. To our knowledge, this is the first device designed to study the acute response of chondrocytes *in vivo* to mechanical stimuli generated by both motion and loading.

ACKNOWLEDGEMENTS

This work was supported by grants from The City University of New York (Science Fellowship), the National Science Foundation (NSF 0723027 to L.C) and the National

Institutes of Health (NIH AR050968, AR47628, AR52743 to H.B.S, and HL069537-07 R25 Grant for Minority BME Education to S.W & L.C). The authors greatly appreciate the kind assistance from Dr. Bingmei Fu, Dr. Zhiyong Qiu, Qin Liu, Dr. Yonggang Lv, Wei Yuan, Guanglei Li, Dr. Min Zeng, Dr. Yuliya Vengrenyuk, and Dr. Susannah Fritton at City College of New York, and Dr. David Fung, Philip Nasser, Mellissa Ramcharan, Dr. Yilin Wang, and Dr. Chris Fritton at Mount Sinai School of Medicine.

Chapter 3

TEMPORAL EFFECT OF MOTION-LOAD ON JOINT BIOMECHANICS (PART II):

GENE EXPRESSION OF PRO- AND ANTI- INFLAMMATORY MARKERS IN CARTILAGE IN RESPONSE TO IMMOBILIZATION AND REMOBILIZATION OF JOINT IN VIVO

ABSTRACT

In spite of the abundant evidences that indicate a link between aberrant mechanical factors and joint degeneration, the intrinsic mechanism mediating the tissue response to motion and load during the pathological process is poorly understood. In this study, we investigated the temporal response of the cartilage gene expression of MMP-3 and Collagen-II in rat knee joint due to reduced loading and remobilization of rat hindlimbs. Immobilized joints were compared with the joints exposed to 1 hr of passive motion loading (PML: 70 ° flexion, 30 sec/cycle) and those subjected to over-loaded with compressive force at 2x body weight during PML. Furthermore, we compared the effects of immobilization at prolonged periods of 7 and 24 days with PML. The results showed that PML reduced the expression of Matrix Metalloproteinase (MMP-3 and MMP-13) and up-regulated the expression of Collagen II. In contrast, compressive motion loading resulted in catabolic responses (increased MMP, decreased collagen II) similar to those caused by immobilization. Elevated MMP-3 mRNA expression at 6h that was sustained throughout the 21day immobilization period, One hour of daily moderate mechanical loading, applied as passive joint motion, reduced the MMP-3 increases that resulted from immobilization. The current data was consistent with our previous in vitro studies where moderate load had anti-catabolic effects, while underloading or overloading conditions may lead to cartilage degeneration. The data also showed cartilage degeneration may be triggered in a short period of joint immobilization, while intervention of passive motion load of 1 hour can sufficiently reverse the acute catabolic effect. The findings of the temporal study provide future therapeutic guidance to life style related maintenance of joint health and motion-based joint rehabilitation.

INTRODUCTION

The main function of the joint is to facilitate body movement and load transmission throughout normal ranges of motion. Mechanical stimuli induced by motion and load are the most important external factor that influences joint homeostasis. Joint components such as bone, muscle, ligaments, tendons, articular cartilage, and menisci are constantly under pressure and strained as a result of weight bearing and movements. Particularly, articular cartilage plays an important role in maintaining normal joint functions by providing low friction, preventing wear and tear at contacting joint surface, and enabling the joint to absorb shocks. The interaction between chondrocytes, the basic cartilage cells, and mechanical loading induced by motion and weight bearing is critical to joint health.

Chondrocytes react to external mechanical stimuli by modulating both anabolic and catabolic activities, thus preserving or degrading their extracellular matrix, respectively. Biomechanical stresses beyond a physiological range may induce cartilage degeneration and alter the ability of cartilage to perform its normal function, while moderate level mechanical loading seems to be chondroprotective, and possibly necessary for cartilage maintenance. The degradation of articular cartilage is the central feature of major joint diseases such as osteoarthritis (OA) and involves a complex interaction between mechanical, environmental, anatomical, and biological factors [92-94].

Significantly reduced loading such as caused by prolonged synovial joint immobilization seems to lead to cartilage degradation [57]. Major symptoms of immobilization include necrosis of the articular cartilage at the location of contact between the two opposite cartilage surfaces [58, 65], matrix fibrosis, fissuring and

ulceration [60], flattening of the cartilage in the contact areas, degeneration in the non-contact areas, and adhesion of the synovial membrane to the peripheral regions of cartilage [61], cartilage tissue adhesion, persistent joint stiffness, pain, muscle atrophy, disuse osteoporosis, and degenerative arthritis [62-64]. Cartilage degeneration occurs not only at the knee joint, but the hip [65], interphalangeal finger joints and metatarsophalangeal joints [61], posterior intervertebral facet joints following anterior spinal fusion [66], interphalangeal joints with long-standing flexion deformity [67], etc.

On the other hand, if the physiological load-bearing capacity of cartilage is exceeded as a result of overuse or overloading, as seen in intense sports [95-99], repetitive high-impact activity [100, 101] and obesity [102, 103], the tissue is subject to higher risk of breakdown. Under excessive mechanical loading stimuli, the tissue can breakdown from the surface down and the damage may be varied throughout the joint because of differential loading capabilities in cartilage layers. Once the cartilage is damaged, the tissue may become increasingly vulnerable to further degradation even by physiological-level joint forces, and the progression of tissue breakdown can be accelerated with moderate exercise [77].

Normal physiological joint motion loading does not harm cartilage and instead helps to prevent cartilage degradation [96, 104, 105]. Motion can prevent or overcome joint degradation by enhancing synovial fluid and cartilage nutrition, and stimulating the healing and regeneration of articular cartilage [37]. Beneficial results of motion-based physical therapy include the reduction of pain, maintenance of joint flexion and extension, increased mobility, and a reduced period of rehabilitation or hospitalization. Meta-analyses have indicated that continuous passive motion or intermittent motion in humans

is better for joints and their articular cartilage than is immobilization [9]. Nevertheless, there is no consensus on either the optimal therapeutic protocol or the long-term clinical effectiveness of continuous passive motion [8, 9]. Key to this debate are the diversity of treatment variables (including the frequency, range of motion, etc.) and the complex biomechanical processes associated with those treatment variables.

In this study, we examined the gene expression of pro- and anti- inflammatory markers in cartilage in response to joint immobilization, remobilization, and compressive motion loading condition in vivo. MMPs are a family of proteinases that act as the cartilage degradative enzymes to break down the extracellular matrix (ECM) constituents. Collagen II is the most potent protein strength in cartilage. We aimed to study the effect of limb immobilization at different time points in cartilage, how remobilization of the limb applied in CPM may reverse the catabolic response caused by immobilization, and whether overloading condition integrated with remobilization may exhibit a similar gene expression pattern to immobilization.

MATERIALS AND METHODS

- *In vivo* 6-hour Immobilization and Remobilization Experiment on Cartilage: The use of rats for this study was approved by the IACUC committee at Mount Sinai School of Medicine. To assess the effects of reduced, moderate and intense mechanical loading (in the form of immobilization, passive motion loading, and compressive motion loading, respectively) on the acute biological response of cartilage, five month old male Sprague Dawley rats (n=5/group, weighing 580 ± 35g)) were randomly assigned to five testing groups and exposed to different motion and loading conditions Table 1. The first group

of animals maintained normal cage activty as served as a baseline control (CTL). A second group of sham control animals (SHAM) were treated exactly the same way as the following loading groups, except that the device was not activated and the animal's hind limb did not receive any loading. In the immobilization group (IMM), animals were immobilized for six hours using a cast made of cotton and steel mesh which fixed the knee in full flexion (115°) as described previously in the literature [115]. A forth group of animals (PML) was immobilized for 2.5 hours, remobilized using passive motion for one hour, and immobilized again for 2.5 more hours. The relative range of angular flexion was 50° with angular displacement from 65° to 115° at a rate of 2 cycles per minute. The fifth group consisted of animals that were treated similarly to the PML group, except their joints were additionally loaded during the one hour motion treatment by applying an axial compressive load (CML) equivalent to approximately twice their body weight (1150±50g). After each rat's respective experiment endpoint, the lateral and femoral condyles were dissected, rinsed in 1X PBS prepared with DEPC-treated water, and frozen in liquid nitrogen. The tissue samples were then homogenized with a Mikro Dismembrator S (S. Braun Biotech International, Germany) for 90 seconds. Lysis buffer was added to the ground tissue and RNA was extracted with the RNeasy Mini kit following manufacturer's instructions. The RNA was reverse transcribed (RT) using Oligo(dT) as a primer, and the RT products were amplified with real-time PCR, using GAPDH for normalization. The primers used for real-time PCR were: MMP-13-F: acatggaggagcatgaaagg, MMP-13-R: gacaggagctaaggcagaca, Collagen2a1F: cctgtctgcttcttgtaaaac, Collagen2a1R: agcatctgtaggggtcttct, GAPDH-F: aggaccaggttgtctcctg, and GAPDH-R: atgtaggccatgaggtccac.

TABLE 3.1 Protocol for JMLS's Effectiveness Test *in vivo*

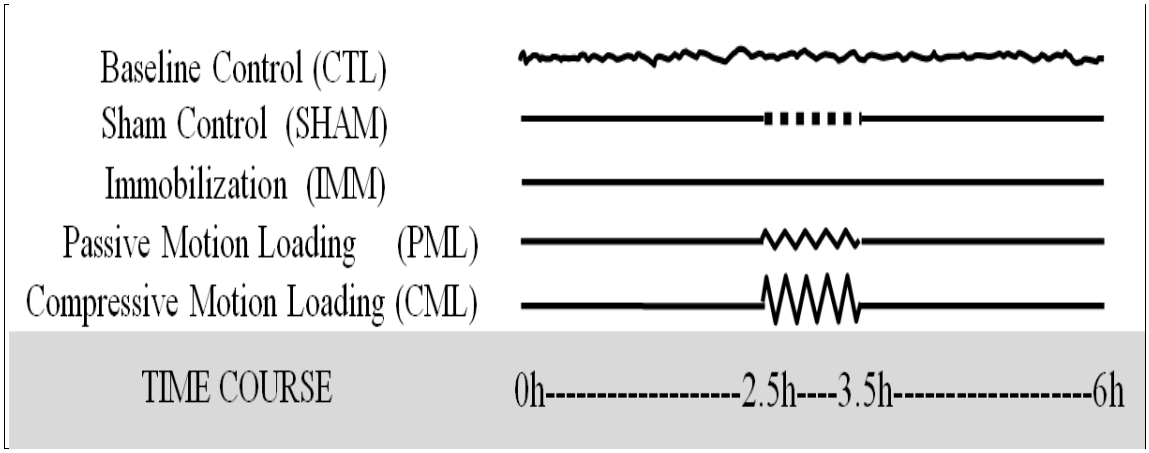

- *In vivo* 6-, 24-hour and 7-, 21-day Immobilization and Remobilization Experiment on Cartilage. The use of rats for this study was approved by the IACUC committee at Mount Sinai School of Medicine. Fifty-four male Sprague-Dawley rats (5-6 months old, weighing 580 ± 35g) were used in this study. Rats were housed in a 12hr light/dark environment and were given free access to food and water. The right limbs of rats 30 rats were immobilized as previously described [115]. The rats were anesthetized with isoflurane and were fitted with a cast made of steel mesh and cotton materials which fixed the knee in full flexion. The rats were immobilized for 6 and 24 hours, and 7 and 21 days. A separate group of 5 rats was used as naïve controls.

Motion loading. Three groups of five rats were subjected to immobilization as described above for 6 or 24 hours, or 7 days. During the middle of each immobilization period (for 6 and 24 hour groups), and daily, 12 hours after the initial application of the casts (for 7 day group), rats were anesthetized, the casts were removed, and the rats were placed on a joint loading system [116] for 1 hour. During that period, these rats were subjected to motion loading at a frequency of two cycles per minute, with a range of motion between 65° and 115°, while a separate group of 5 rats were maintained in the

device without motion, at 115° of knee flexion (sham group). After the experimental period, all rats were either sacrificed or re-cast until the next motion loading session.

Laser capture microdissection. Distal femora were dissected, decalcified with Morse's solution for 2 days at 4ºC, fixed in methacarn for 1 hr at 4ºC [117], embedded in paraffin, cut into 5-7μm thick sections and mounted on Superfrost/Plus slides. After deparaffinization, slides were air-dried and laser capture microdissection (LCM) was performed with the Arcturus Pixcell IIe (Mountain View, CA). Approximately 500 chondrocytes were microdissected from the each of the superficial, middle, and deep zones of the lateral and medial condyles using the following instrument settings: Power – 85mW, Spot size – 7.5μm, Duration – 600μs-2.5ms. Captured cells were collected in microtubes containing lysis buffer (Qiagen, Valencia, CA).

RNA isolation, cDNA synthesis, real-time PCR. Total RNA was extracted using the RNeasy mini kit (Qiagen) with DNase treatment. RNA was quantitated with a Nanodrop spectrophotometer (Thermo Fisher Scientific, Wilmington, DE), then reverse transcribed (RT) using oligo(dT) primers. Two nanograms of total RNA was analyzed by real-time PCR to assess MMP expression, as well as GAPDH and β-actin as controls. PCR primers pairs used were: MMP-3, forward 5'-TCAGCGGATCTTCACAGTTG-3', reverse 5'-ACTTCAGTGCGCCAAGTTTC-3'; MMP-8, forward 5'-AAGGAGTGTCCAAGCCATTG-3', reverse 5'-CTGCTGGAAAACTGCATCAA-3'; MMP-9, forward 5'-CCACCGAGCTATCCACTCAT-3', reverse 5'-CCTGTGAGTGGGTTGGATTC-3'; MMP-13, forward 5'-ACATGGAGGAGCATGAAAGG-3', reverse 5'-GACAGGAGCTAAGGCAGACA-3'; GAPDH, forward 5'-GAGGACCAGGTTGTCTCCTG-3', reverse 5'-

ATGTAGGCCATGAGGTCCAC-3'; β-actin, forward 5'-TTGCTGACAGGATGCAGAAG-3', reverse 5'-ACATCTGCTGGAAGGTGGAC-3'. Real-time PCR with SYBR Green was performed by "hot start" at 95°C for 2 min, followed by 40 cycles of denaturation (95 ℃, 15 sec), annealing (55 ℃, 20 sec) and extension (72 ℃, 30 sec). Expression values of GAPDH and ß-actin for each treatment condition were averaged and used as a denominator to determine the relative gene expression of MMPs 3, 8, 9, and 13. Data were quantified as described previously [118].

MMP activity assay. Tissues were dissected, flash-frozen in liquid nitrogen and stored at -80°C. Frozen tissue samples were pulverized (Dismembrator, B Braun Biotech, Germany) and enzyme activity was quantitated in tissue extracts using fluorogenic substrates specific for individual MMP's as described previously [119]. To measure total MMP levels in the tissue, assays were carried out in the presence of the activator 4-aminophenylmercuric acetate (APMA); endogenous active MMP levels were determined in assays carried out in the absence of APMA.

Statistical Analysis

Two-way analysis of variance (ANOVA) was performed on the data testing the real-time angular position measurement by the goniometer and the data testing the kinematics of the apparatus frame and the animal's limb. The correlations among the five-trial measurements were evaluated. ANOVA and the correlation calculations were performed using the Statistic Toolbox of Matlab 7.2. The data were shown as mean ± standard deviation with the percentage denoting the ratio of the computed value relative to the magnitude of the corresponding angular position. ANOVA with Tukey's post-hoc analysis was used to determine statistical significant differences between SHAM, IMM,

PML and CML groups versus CTL. A value of $p<0.05$ was considered significant. Results were expressed as the mean ± SEM. Statistical analysis was carried out using a one-way ANOVA and Tukey's test for post hoc analysis with significance set at $P < 0.05$.

RESULTS

- In vivo 6-hour Immobilization and Remobilization Experiment.

Motion and loading provided by the JMLS can effectively modulate MMP-13 and Col II expressions in chondrocytes (Figure 3.1). The immobilization of the knee joint for 6 hours resulted in i) increased expression of MMP-13, a protease known to cleave type II collagen, and ii) reduced expression of Col II, the predominant structural protein in cartilage. Compared with immobilized knee joints, cartilage exposed to 1 hr of PML inhibited the synthesis of MMP-13 by 2.7 fold and up-regulated the expression of Collagen II by 2.2 fold. This result demonstrated the ability of the JMLS to produce an effective chondroprotective stimulus via PML that led to suppression of the catabolic effects of immobilization. In contrast, the biological response of the group of animals treated with compressive motion loading was catabolic and exhibited a pattern similar to that observed in the immobilization group.

- *In vivo* 6-, 24-hour and 7-, 21-day Immobilization and Remobilization Experiment on Cartilage.

Reduced joint loading applied by immobilization of the joint induces an early and sustained increase in expression and activity of multiple MMPs. We initially screened mRNA expression of several MMPs implicated in cartilage matrix turnover (3, -8, -9, -13), and found all except MMP-8 to be increased significantly above the levels in non-immobilized limbs at 6 and 24 hours after immobilization (Figure 3.2A). MMP-3, 9 and 13 showed similar expression patterns when enzyme activity was measured; levels of both active and total MMPs were increased above controls at both 6 and 24 hours (Figure 3.2B). Approximately, half of each MMP in the tissue was active in control joints; the

A.

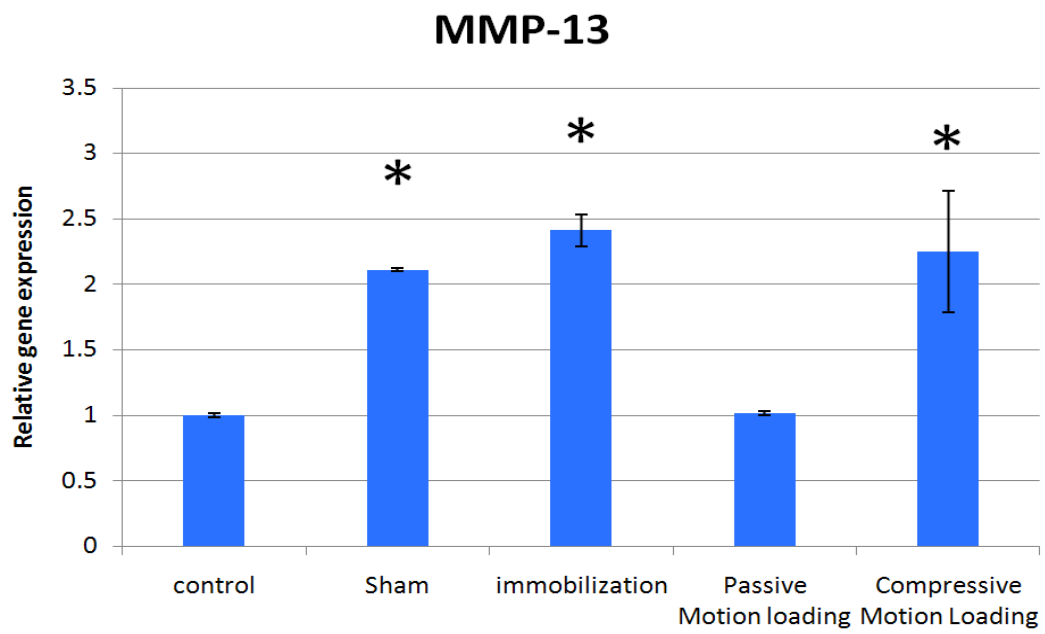

B.

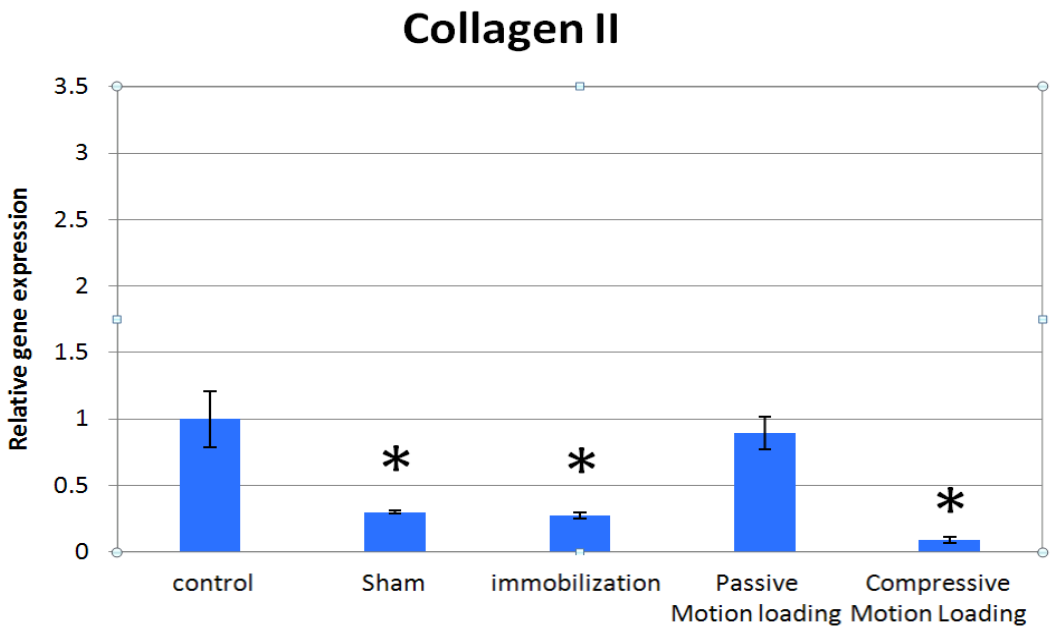

Figure 3.1 Gene expressions of pro-inflammatory effector MMP-13 (Upper) and major structural protein in cartilage Collagen II (Bottom) in response to immobilization (IMM), moderate passive motion loading (PML), and compressive motion loading conditions (CML). IMM and CML groups exhibited an up-regulation of MMP-13 and a down-regulation of Collagen II, while PML reversed the catabolic responses caused by immobilization by showing reduced gene expression of MMP-13 and increased gene expression of Collagen II.

remainder was in latent proenzyme forms, requiring APMA treatment to be detected (Figure 3.2B). Following immobilization, the ratio of active to latent forms of MMPs 3 and 8 remained unchanged over 24 hr; In comparison, the percentages of active MMPs 9 and 13 rose to 80 - 86% of the total MMP activity after 24 hours of immobilization.

Our further study focused on MMP-3 because observed increases in mRNA and enzyme activity following immobilization and its previously demonstrated ability to activate multiple MMPs [120-124] suggested a possible early role of MMP-3 as a mediator of tissue responses to changes in mechanical state. We found that MMP-3 mRNA expression and enzyme activity both increased further between 24 hours and 21 days after immobilization. MMP-3 mRNA expression rose up to 10-fold over control levels (Figure 3.3A) while enzyme activity increased approximately 4.7 times the control level at 21 days (Figure 3.3B).

In the prolonged immobilization and remobilization experiments, immobilized rat hind limbs were subjected to 1 h of passive motion in the middle of 6 or 24 h immobilization periods, or to daily 1 h periods of passive motion during 7 days of immobilization. We found MMP-3 mRNA levels in the immobilized cartilage were elevated; however, these increases were prevented in limbs subjected to passive motion (Figure. 3.4A). Furthermore, passive motion loading also completely blocked the increase in total articular cartilage MMP-3 activity (Figure. 3.4B).

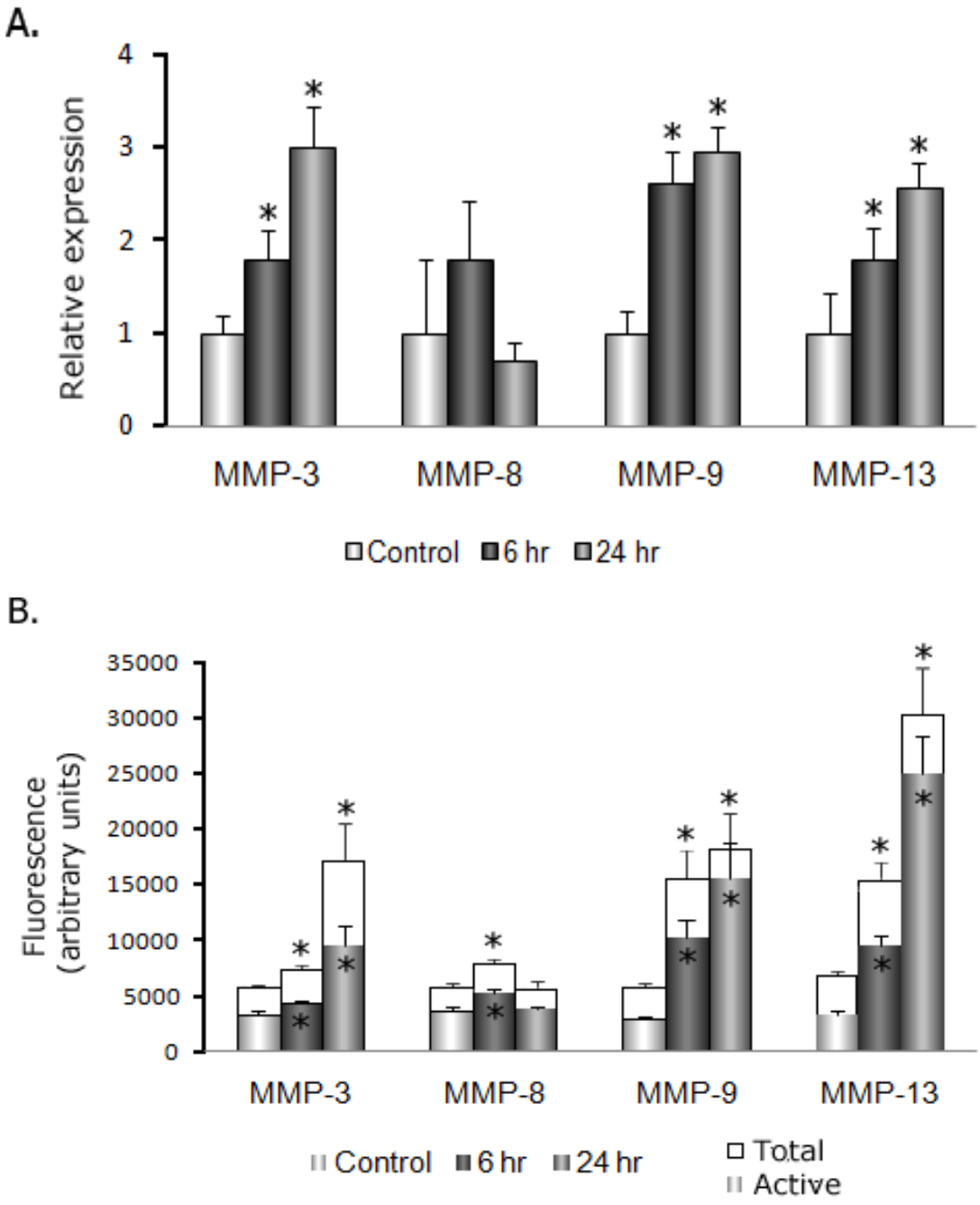

Figure 3.2 Responsive changes in MMP mRNA expression and enzyme activity after immobilization. A) mRNA levels for MMP-3, -8, -9, -13 were quantitated by RT-PCR after 6 and 24 hours of immobilization and expressed relative to levels in unimmobilized controls. B) Levels of active (shaded bars) and total (open bars) MMP activities in total cartilage extracts from immobilized and non-immobilized cartilage following 6 and 24 h of immobilization. Total activities (active + latent) were determined following APMA activation. Data show mean + SEM (n=5). * = $P < 0.05$ versus unimmobilized control. [125]

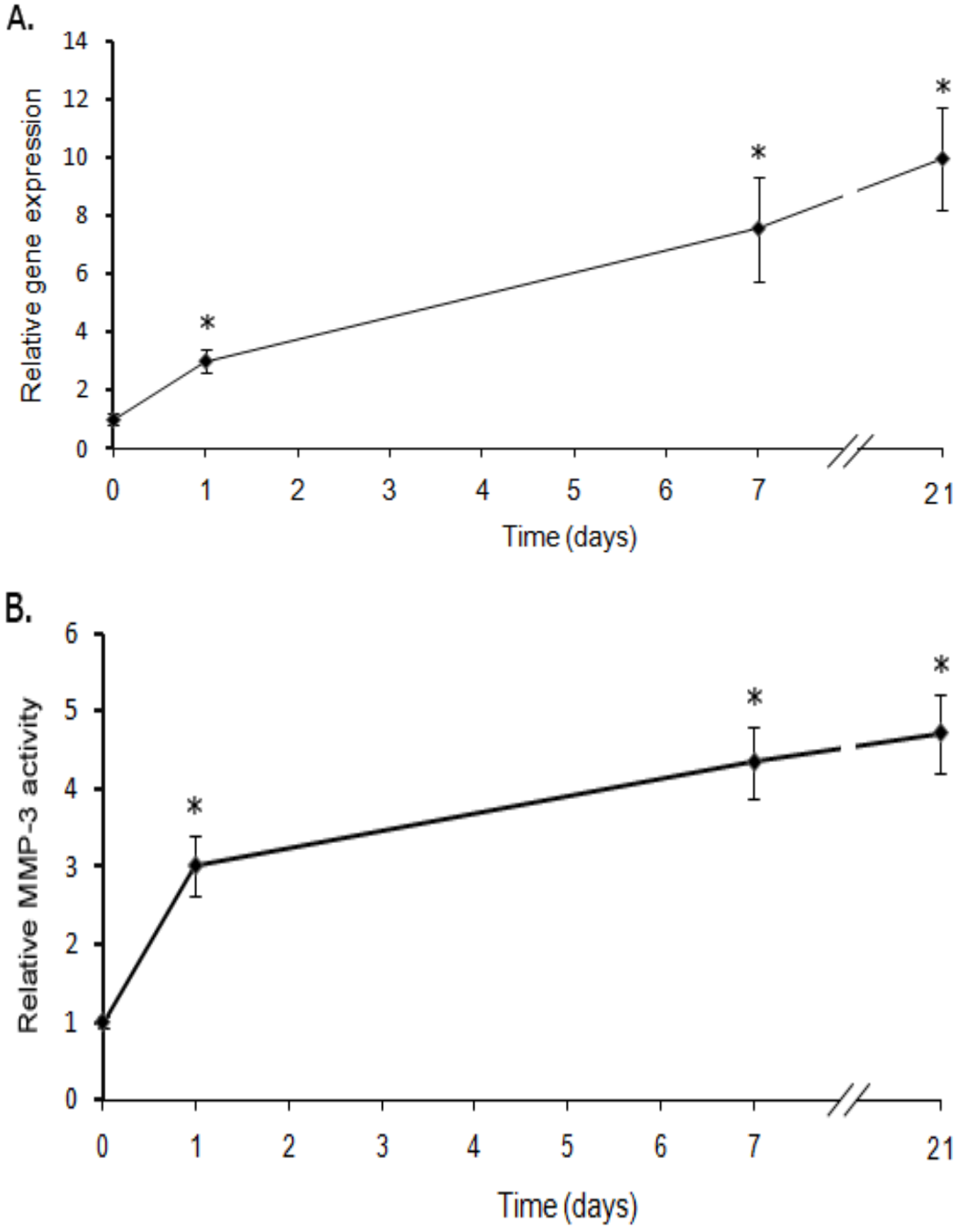

Figure 3.3 Responsive changes of MMP-3 mRNA and activity changes in articular cartilage due to immobilization. A) Levels of MMP-3 mRNA (RT-PCR). B). Total MMP-3 activity expressed relative to levels in unimmobilized controls. Whole condyles, rather than tissue sections, were used as tissue sources for MMP-3 activity assays. Data show mean and SEM of (n=5). * = $P < 0.05$ versus unimmobilized control [125].

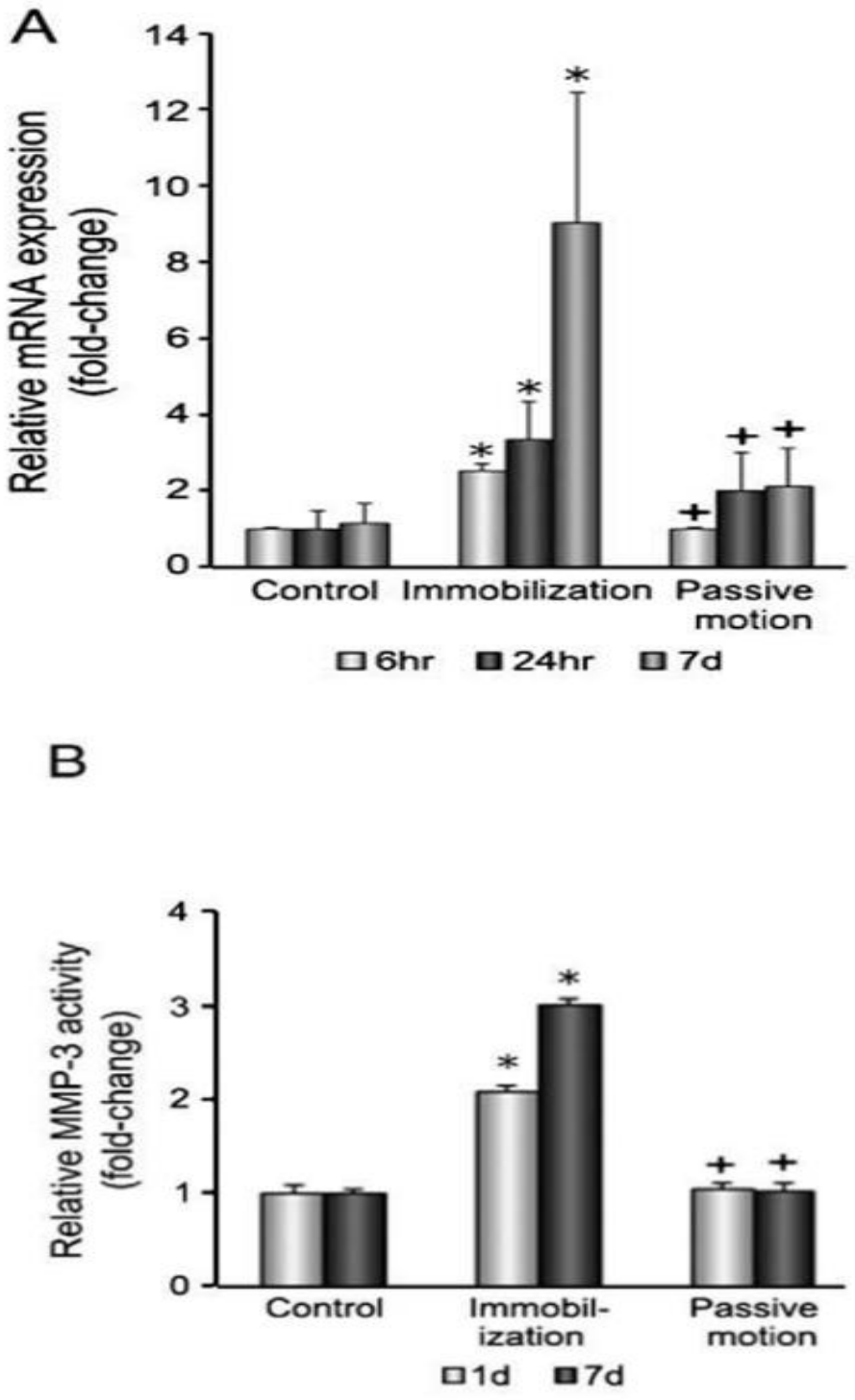

Figure 3.4 Responsive changes in cartilage mRNA and enzyme activity due to immobilization and motion loading. (A) Relative MMP-3 mRNA gene expression after 6 and 24 h, and 7 days after immobilization, with and without motion loading. (B) MMP-3 activity after 7 days immobilization with and without motion loading [125].

DISCUSSION

Associations between motion/loading and the cartilage homeostasis have been extensively investigated; however, the acute biological response in cartilage tissue has only been explored in vitro. In the current study, we used an acute model of cartilage degradation through immobilization of the joint, which have been well-documented in the after-surgery immobilization reports, and seems to share pathologic similarities with cartilage degradation caused by overuse as seen in osteoarthritis. This model showed cartilage destruction may be triggered by a short period of time of immobilization that induces acute catabolic effects in cartilage. To study the temporal effect of well-characterized motion-loading environment, we used the JMLS, an assisted joint motion and loading system to investigate the regulation of pro- and anti-inflammatory proteins in cartilage in response to mechanical stimuli in vivo within a few hours of treatment. The passive loading produced by JMLS was capable of down-regulating MMP-13 as well as up-regulating the expression of Col II. The synthesis of MMP-13 exhibited a U-shaped response as a function of load intensity. MMP-13 was increased in response to reduced load (immobilization), and this increase was suppressed by a moderate level of loaded (passive motion loading) on the background of immobilization. When moderate load was replaced with a high load (compressive motion loading), a decrease in MMP-13 was not observed; levels of MMP-13 due to compressive loading were comparable to levels after immobilization. The opposite behavior was seen for the production of Col II, demonstrating acute mechanosensitivity of both synthetic and degradative processes *in vivo*. These observations were not seen in the joints after releasing from immobilization

alone (sham control), showing passive motion load was solely responsible for the anabolic effect.

These findings were consistent with our previous *in vitro* studies and reported literature where moderate load had a chondro-protective effect, while immobilization or excessive impact load may have a deleterious effect in cartilage [91, 126, 127]. In vitro studies applying shear stress to chondrocytes have demonstrated up regulation of the expression of Ihh and Collagen Type X [86, 87]. Uniaxial compression has also been shown to increase the expression of Collagen Type X in a magnitude dependent manner [88]. Furthermore, hydrostatic pressure has been associated with a chondroprotective role [89], because it results in synthesis of aggrecan and Col II [84, 85]. In vivo, cartilage is continuously subjected to both shear and axial longitudinal loading. The shear stress is created by the contact friction [58, 72-75], between cartilage during flexion-extension of the joint, while the axial compressive loading [128, 129] is produced by normal forces applied on the cartilage surface. Long-term studies have shown that early and progressive damage occurs in cartilage subjected to excessive shear and axial loading, but it is not seen in cartilage subjected to shear loading only [76]. In a recent study by Ferreti et al., immobilization for 24h and 48h in rabbits showed a time-dependent GAG degradation, and increased expression of pro-inflammatory mediators MMP-1, COX-2, and IL-1β, while no GAG degradation and reduced expression of MMP-1, COX-2, and IL-1β was found when animals were treated with continuous passive motion for 24h and 48h, respectively [109]. Our findings were consistent with Ferreti's study, and extended those results to include a shorter treatment time. In our study, we analyzed the effect of the axial compressive loading on a moving joint, and we demonstrated that motion

loading is effective even when applied during a short interval between two periods of immobilization. We speculate that passive motion loading (PML) as provided by the JMLS produces a moderate shear loading at the contact cartilage surfaces of the knee joint, while compressive motion loading (CML) generates both increased shear and compressive loading, and that shear and compressive loading seem to have opposite effects on acute MMP-13 and Col II synthesis *in vivo*.

In our study, MMP-3 gene expression and enzyme activity in articular cartilage were upregulated within 6 hr following immobilization, remained elevated during a 21 day immobilization period, suggesting a catabolic response can be triggered at an early phase after reduced loading conditions. Moreover, changes in MMP-3 expression were markedly suppressed by a moderate motion loading regimen, indicating a brief period of joint mobilization may be able to control cartilage breakdown. Cartilage degeneration, whether a result of normal remodeling or pathologic degeneration, likely involves numerous degradative enzymes, including several MMPs [130]. Our study suggested that reduced joint loading increased the mRNA levels of multiple MMPs, as well the proportion of active enzyme in many instances. Different MMPs have distinct functions. For example, MMP-13 has been considered to play a major role in degrading bulk cartilage matrix due to its high activity against type II collagen [131, 132], while gelatinases like MMP-9, largely inactive against intact collagen, may further degrade the large cleavage products formed as a result of the actions of MMP-13 and other collagenases [133]. In addition to its proteolytic activities against matrix constituents, MMP-3 also cleaves MMP pro-forms at specific sites, rendering them catalytically active [123, 134, 135]. Whether the capacity to activate other MMPs represents the major role

of MMP-3 in immobilization-induced cartilage breakdown remains to be investigated. However, we noted in this study that MMP-3 mRNA levels increase within 6h following the onset of immobilization. Previously, the earliest changes reported after immobilization were an increase of MMP-1 within 24 hours in antigen-induced-arthritis rabbits [109], and a loss of luster on the cartilage surface after 7 days of immobilization in rats [136]. Assessments of MMP-3 activity have shown correlations with cartilage degeneration in several instances [134, 137-139]; moreover 2-year-old MMP-3 knockout mice showed a 67% reduction in cartilage damage associated with spontaneous osteoarthritis (OA), including deep fissures and complete loss of the cartilage layer, when compared to age-matched controls [131]. Importantly, our study implied that a short intervention f joint mobilization per day was able to suppress the upregulation of MMP-3. We observed the duration of loading required to suppress the catabolic effects of immobilization in cartilage to be relatively short, suggesting that shorter periods of loading might be sufficient for chondroprotective effects, and could be necessary for after-surgery immobilized joints.

In conclusion, our current study of temporal effect of mechanical loading showed that prolonged immobilization of the limb can trigger a catabolic gene expression response at an early stage which may lead to cartilage degeneration in a prompter speed than that has been previously reported. More importantly, our study provided evidence that a small early intervention of motion is necessary to induce a clear biological response of cartilage *in vivo* [71] to reverse the catabolic effect of joint immobilization, which can serve as a guidance for people who adopt a sedentary life style or those who need to keep their joint in a fixed position as restrained by profession. To our knowledge, this is the first attempt

to study the acute response of chondrocytes *in vivo* to mechanical stimuli generated by both motion and loading.

ACKNOWLEDGEMENTS

This work was supported by grants from The City University of New York (Science Fellowship), the National Science Foundation (NSF 0723027 to L.C) and the National Institutes of Health (NIH AR050968, AR47628, AR52743 to H.B.S). We greatly appreciate the kind assistance from Dr. Bingmei Fu, Dr. Zhiyong Qiu, Qin Liu, Dr. Yonggang Lv, Wei Yuan, Guanglei Li, Dr. Min Zeng, Dr. Yuliya Vengrenyuk, and Dr. Susannah Fritton at City College of New York, and Dr. David Fung, Philip Nasser, and Dr. Chris Fritton at Mount Sinai School of Medicine.

Chapter 4
SPATIAL EFFECT OF MOTION-LOAD ON JOINT BIOMECHANICS (PART I):

MICRO-CT ARTHROGRAPHY: AN APPROACH TO HIGH RESOLUTION 3D RECONSTRUCTION OF SOFT AND HARD TISSUES IN A RAT KNEE JOINT

ABSTRACT

Studies on joint diseases resulting from changes in composition, biosynthesis and morphometry of joint tissues often rely on effective imaging of the tissue structures in the joint. There also is an imperative need to characterize the local biomechanical environment in small animal joint models using numerical analysis performed on the real anatomic geometries in the joint. Currently, available high-resolution imaging methodologies for small animal soft tissue reconstruction are extremely scarce. In this study, we explored the potential of high resolution micro-CT arthrography for 3D modeling of soft and hard tissues in an intact rat knee joint. We used a silicon based contrast agent to compartmentalize the synovial fluid component from cartilage, menisci and other soft tissues, and image acquisition was performed using a Skyscan 1172 micro-CT scanner with isotropic voxel size of 5.5 or 2.7 microns. 3D reconstruction of soft tissues such as femoral and tibial cartilage, as well as menisci were performed in Mimics imaging processing software. Contrast agent was distributed throughout the whole knee cavity to provide remarkable boundaries based on which soft tissue components can be distinguished and segmented. Geometries of cartilage, and menisci were successfully reconstructed in 3D as well as femur, tibia, and patellar. This approach may be useful for advanced computational analysis of joint biomechanics that plays an important role in the maintenance of joint health. To the best of our knowledge, this is the first 3D geometrical reconstruction model of both hard and soft tissues in a complete rat knee joint using high-resolution micro-CT.

Keywords: micro-CT, Contrast Agent, Soft Tissue, Cartilage, Menisci, High-resolution, Rat Knee Joint.

INTRODUCTION

Mechanical forces are the most prominent external factor to determine joint health. Joint diseases resulting from changes in composition, biosynthesis and morphometry of joint tissues are often known to be caused by aberrant mechanical forces imposed on the tissues through joint motions and weight bearing. To understand how motion-load induced mechanical loading regulates joint homeostasis, and how abnormal loading stimuli causes excess deformations of tissue that lead to tissue degradation, there is an imperative need to characterize the local biomechanical environment in small animal joint models using numerical analysis performed on real geometries in the joint. For this purpose, high-resolution imaging of anatomical structures inside the joint based on which 3D reconstruction of joint geometries can be obtained is of vital importance.

Advances in improved imaging modalities during the last few decades have led to a better understanding of joint biomechanics. The development and analysis of imaging-based geometric reconstruction have broadened our insight into the pathologic progress in joint diseases. Three-dimensional (3D) geometric reconstruction of bone tissue and soft tissues such as cartilage and ligaments have been widely used in human studies of joint biomechanics. These efforts, extensively using Magnetic Resonance Imaging (MR) modality for imaging soft tissues in the joint, have generated tremendously valuable knowledge about the joint contact mechanics by allowing for advanced numerical modeling of the localized tissue responses to mechanical load. Nevertheless, due to the limitation of the pixel resolution, MRI have had very limited applications in 3D reconstruction of joint tissues for small animals such as rats until in some recent studies that reported a resolution of 51 μm [140, 141]. This resolution, although superb for MRI

on soft tissues, may not be geometrically ideal for creating an accurate finite element model of cartilage or menisci in small animal joints.

Micro-Computed Tomography (μCT) is a non-destructive high-resolution imaging modality. Micro-CT has advantages over the 2D destructive approach of histomorphometry [142], and it facilitates high resolution and cost efficiency versus MRI that offers a resolution inadequate for advanced numerical studies in small animal models. Traditionally, micro-CT technology has been extensively applied on imaging hard tissues such as bone; Due to the low X-ray absorption of soft tissues, micro-CT suffers very limited applications for imaging cartilage. Micro-CT arthrography has been explored to compensate for the poor radiopacity of articular cartilage by injection of contrast agent to enhance the detestability of cartilage. A novel contrast-enhanced technique based on quantifying the Equilibrium Partitioning of an Ionic Contrast agent via μCT (EPIC-μCT) was developed [143]. This technique was based on the principle that a charged contrast agent allowed to reach equilibrium will partition nonuniformly within the articular layer depending on the distribution of charged matrix molecules (PGs). In such a way the high resolution, quantitative 3-D data can be obtained for composition and morphology analysis of articular cartilage [144]. Hexabrix 320, a clinically available CT contrast agent was used to determine the GAG content in cartilage [144, 145]. Hexabrix 320 contains ioxaglate, a negatively charged hexaiodinated dimer, a radio-opaque negatively charged ionic iodated dimer with an attenuation-ratio of three. The negatively charged ioxaglate will be locally repulsed by the negative fixed charge density of the cartilage, which results from the local GAG content. This means that ioxaglate penetration into the cartilage results in a concentration that is inversely related to the GAG content. This

approach provides a simple procedure to distinguish healthy and degenerative cartilage, since when GAG is depleted, the distinction proved to be detectable and measurable [145], thus, the EPIC-μCT technology has been proven efficient for imaging of the GAG content inside cartilage. In light of the feasibility of clearly defining the cartilage layers from the synovial fluid or other soft tissues such as ligament, micro-CT arthrography using large molecule compound may be more appropriate as it provide an instant way to indirectly visualize the anatomy of the soft tissues in the joint. In a study, a suspension of oil and barium sulfate was used as contrast material, and it was shown that this technique can be applied to provide the distinct features of the soft tissue structures in the rat knee joint in 2D [142]. However, micro-CT based 3D geometric reconstruction of the soft tissues in a small animal joint has not been reported in literature.

Our goal of the study was to utilize the high-resolution micro-CT images to reconstruct 3D geometries of hard and soft tissues in a small animal knee. The 3D joint tissues model was expected to sufficiently represent the anatomic features of the tissue structures that can support advanced numerical analysis such as finite element modeling for biomechanical characterization. To overcome the limitation of micro-CT which hardly resolves soft tissues (i.e. cartilage) from fluid medium (i.e. synovial fluid), we used a contrast agent approach to explore the potential of micro-CT imaging for 3D reconstruction of a rat knee. We expected the contrast agent injected into an intact knee would facilitate the segmentation of synovial fluid from uncalcified tissues, and we aimed to create the 3D geometrical representation of both soft and hard tissue components in the knee joint of rats.

MATERIALS AND METHODS

Contrast Agent Injection

Silicon based contrast agent (microfil, flowtech inc) was injected into the synovial cavity of a dissected rat knee joint (Sprague Dawley, five month old female) in the left hind limb right after sacrificing the animal. Microfil, a liquid compound conventionally used to fill and opacity the vascular spaces on non-surviving and post mortem tissues by injection, has a similar X-Ray absorption to bone and therefore offers an indirectly approach to image the soft tissues if taking the spaces of synovial fluid. Several injections were made from the anterior, posterior, medial, and lateral side to make the contrast agent fill the synovial cavity. The knee joint was mobilized to homogenize the contrast agent in the synovial cavity. The sample was blotted on gauze to absorb excess fluid, and wrapped in parafilm to prevent dehydration or shrinkage during the scan, and then carefully placed in a tube holder for the micro-CT scan.

Micro-CT Scanning and Reconstruction

Images acquisition was performed using a Skyscan 1172 micro-CT scanner (Skyscan, Belgium) with isotropic voxel size of 2.7 microns (100kVe, 100mA, field of view 11mm), Scan duration was 1 hr 56 mins for each of the 3 scanned sections evenly divided from top to the bottom of the joint. For image acquisition, 900 consecutive x-ray projections were taken. Five exposures by projection were used to produce high contrast low noise images. The raw images were corrected for possible pixel defects in the digital detector using bright and dark fields, and a standard reconstruction algorithm (Feldkamp cone beam) included in the acquisition system were applied to generate 3-D volumes from the planar X-ray projections. Tissue composition and density were calibrated by using a

phantom containing hydroxyapatite (a main component of bone mineralized phase), air, lipid and water, which were included with each scan. Initial reconstruction of the whole volume were carried out at 70-μm voxel resolution. A region of interest corresponding to the cartilage were identified to re-scan that region a higher resolution (3-μm). Multiplanar reconstructions were performed on a desktop computer using NRecon software (V1.6.1.2, SkyScan). 5271 images were reconstructed and compensated for misalignment, ring artifacts and beam hardening. Image reconstruction time was approximately 2.5 hrs.

3D Geometrical Model Generation

Mimics software (Ver. 13.0 Materialise Inc) was used for segmentation of compartments of the knee joint and generation of 3D geometries of hard/soft tissues in the model. For region of interest (ROI) at the cartilage surface contact area, high-resolution reconstruction were performed, while for the whole joint reconstruction images were imported for processing at reduced resolution of 22 μm for computational efficiency. The ossified tissue and contrast material volumes were first reconstructed using thresholding and Boolean operations. A global threshold value was used to segment soft (light) and hard (ossified) tissues plus contrast agent fluid (dark). Using the operations of Edit Mask, Region Growing, and a dynamic image growth algorithm based on 28-voxel connectivity. Ossified tissues (Patellar, Femur, Tibia, Meniscal Ossicles, and Sesamoid bones) were generated in 3D geometries; the chondral surface of the femoral condyles and tibial plateaus was differentiated by visualizing the contrast material coating. The segmentation tool of Boolean Operation was then used to separate the synovial fluid space occupied by the contrast agent fluid from ossified tissues. This step is important to define the boundary between soft tissues and contrast material. The

generated 3D femoral and tibial bone volumes were wrapped to include the cartilage, cartilage layers were cropped out after Boolean operations on wrapped bone volumes to intersect with region mask of soft tissues and to exclude the contrast agent fluid. Menisci were obtained in a similar way as in previous steps followed by slice-by-slice edit and Edit Mask in 3D operation. Morphological and Boolean operations were extensively used to define and separate the soft tissues from calcified components or contrast agent fluid.

RESULTS

Contrast agent was distributed throughout the whole knee cavity and exhibited a similar attenuation to bone in the micro-CT scan images. Soft tissues were regularly visualized as a band or inter-space between the subchondral bone and the contrast material. Femoral and tibial cartilage layer (Figure 4.1A), patellar cartilage layer (Figure 4.1B), anterior/posterior cruciate ligament (Figure 4.1C arrow) and medial/lateral lateral ligament (Figure 4.1C arrowhead), and patellar tendon (Figure 4.1D arrowhead) were indirectly visualized as a region of low attenuation between calcified tissue and intra-articular contrast fluid in the knee cavity. Non-calcified meniscus and calcified meniscal ossicle were also visible in the images (Figure 4.1A).

All images and volumes were obtained based on the same high resolution scan (2.7 μm), image correlation among the different models allows for a multi-scale analysis eliminating images co-registration errors. High-resolution reconstruction of joint tissue structures facilitates a detailed modeling of joint anatomy of the knee (Figure 4.2), while reconstructions at lower resolution of 22 μm allows for the effective 3D volume representation for the all the tissue components in the joint at considerably faster computational speed (Figure 4.3). The geometry of menisci (Figure 4.4A) as well as femoral and tibial cartilage (Figure 4.4B) was successfully reconstructed. Noticeably, the femoral and tibia cartilage on the lateral side are in close contact, but not on the medial side, and the cartilage on the medial side horn is thicker than that on the lateral side horn (Figure 4.4B). The 3D reconstruction of the whole joint is shown in Figure 4.5.

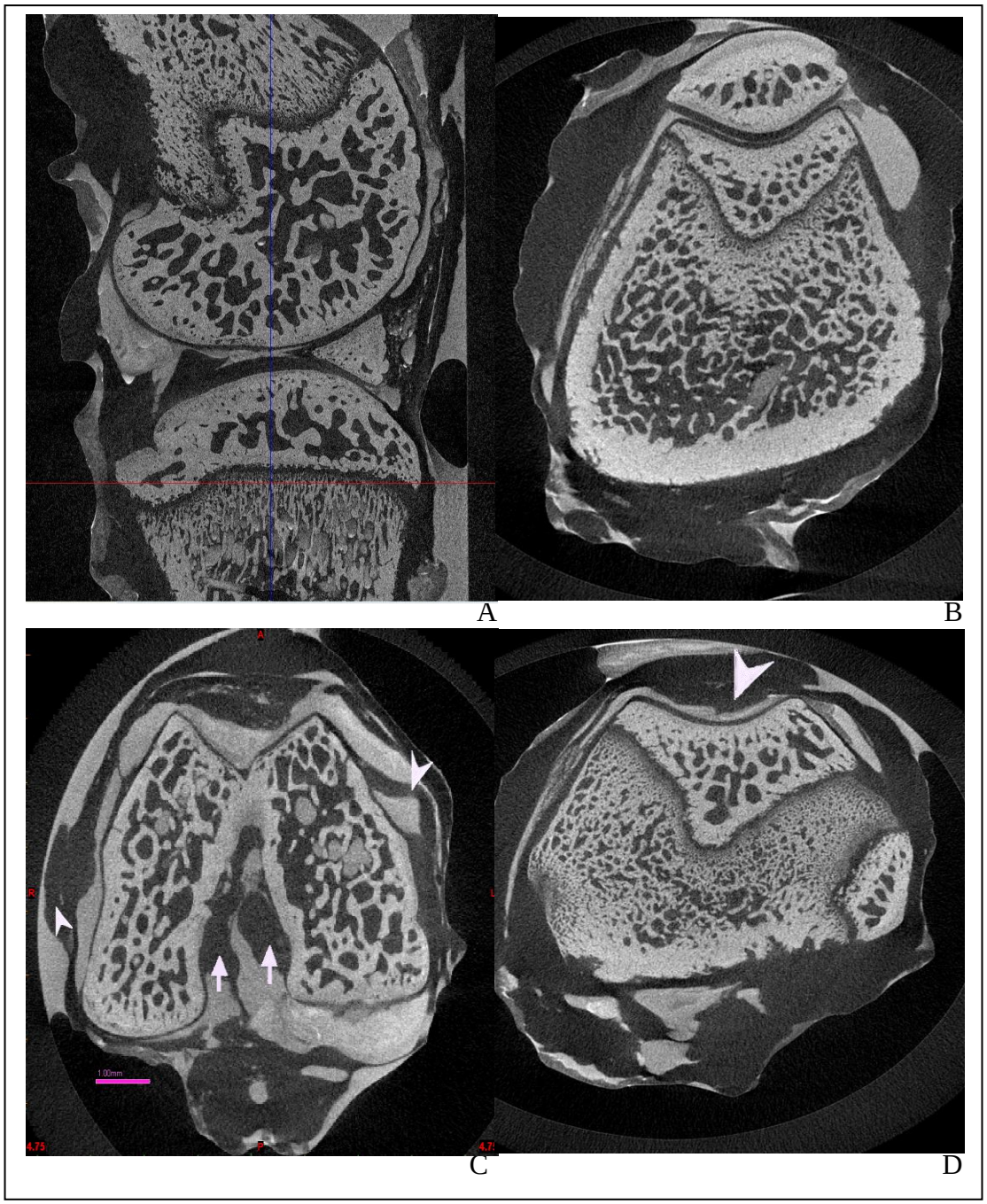

Figure 4.1 Micro-CT scan of a rat knee joint (22 μm resolution) with contrast agent. A) Sagittal view, B) Top view. C) Top view of femoral condyle section, and D) Top view of patellar tendon section. ACL, PCL (arrows) and lateral ligaments (arrow heads), Patellar tendon (arrow head) can be visualized in C and D, respectively

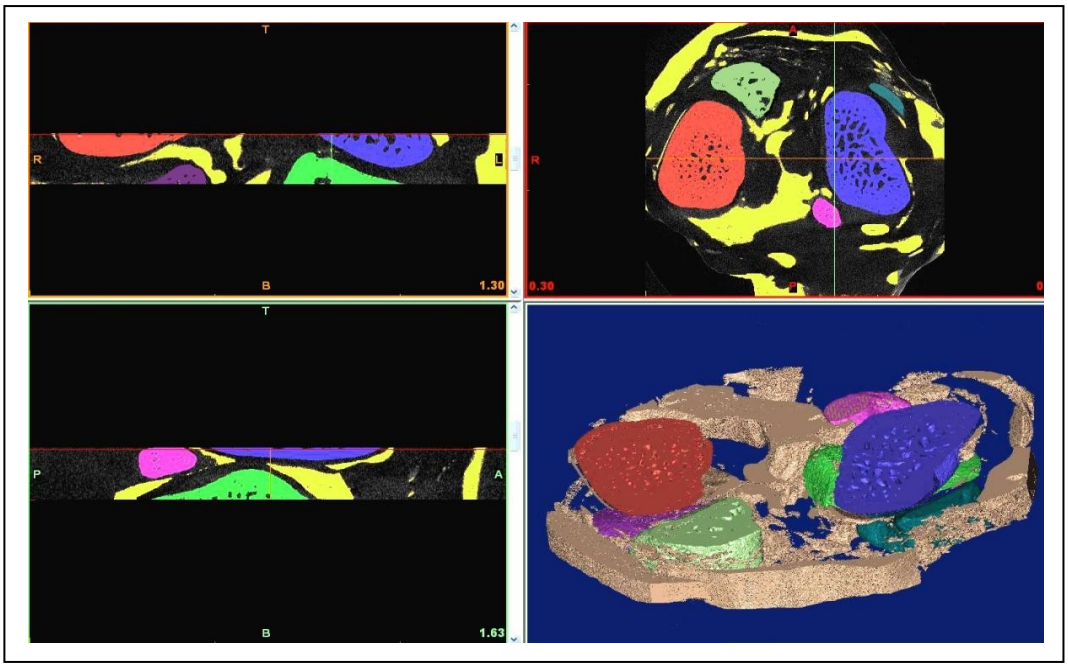

Figure 4.2 High-resolution (2.7μm) views of region of interest (ROI). Selected region was the contact area of the cartilage segments between tibial and femoral condyles (Red and Blue: Femoral condyles; Green and Purple: Tibial condyles; Brown: Contrast agent; Others: Calcified Tissues)

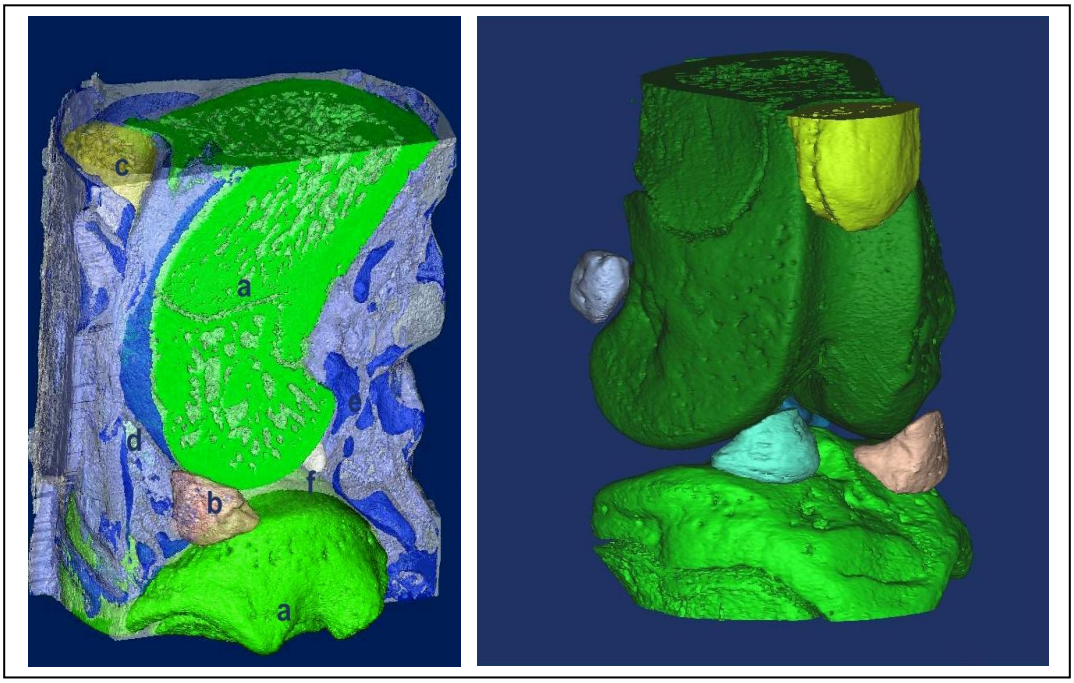

Figure 4.3 Reduced resolution (22μm) views of total joint structures with contrast agent (Left) and calcified tissue structures (Right). (Red and Blue: Femoral condyles; Green and Purple: Tibial condyles; Brown: Contrast agent; Others: Calcified Tissues)

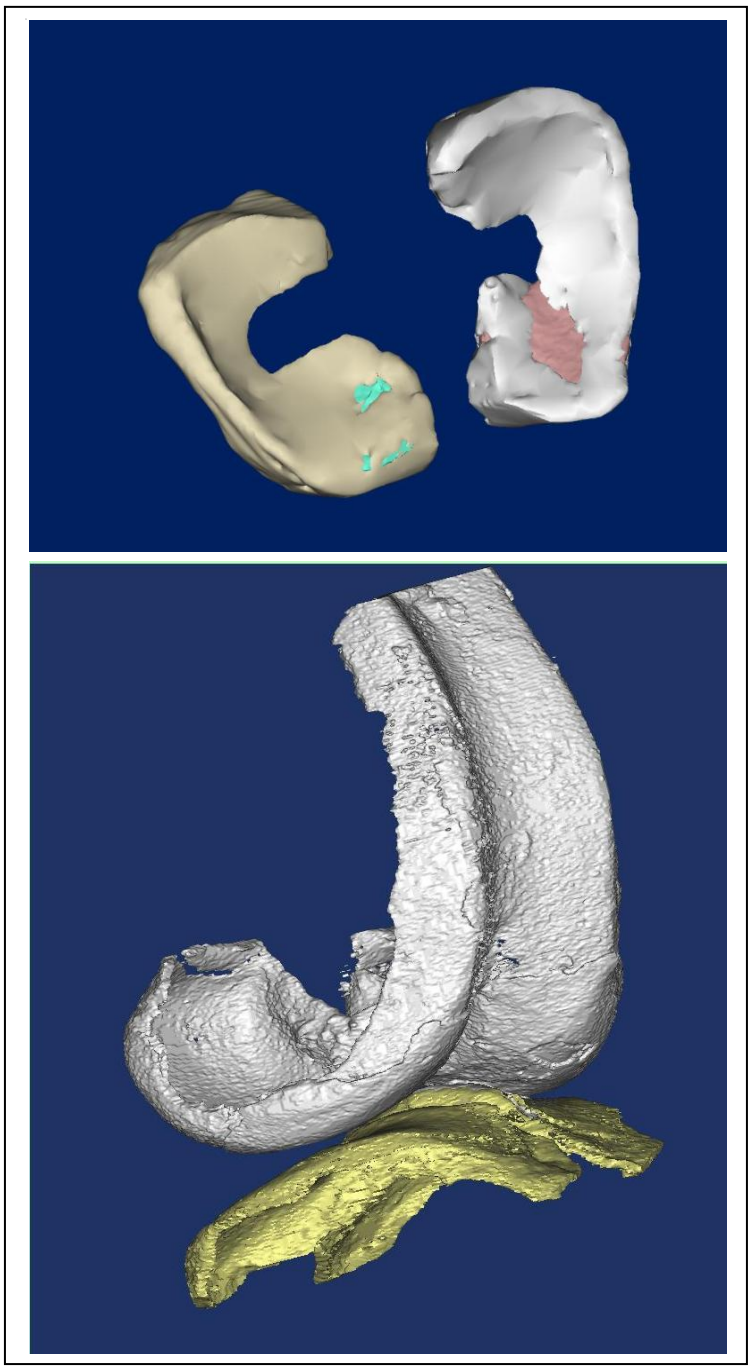

Figure 4.4 Reconstruction of menisci (Upper A) and femoral and tibial articular cartilage (Bottom B)

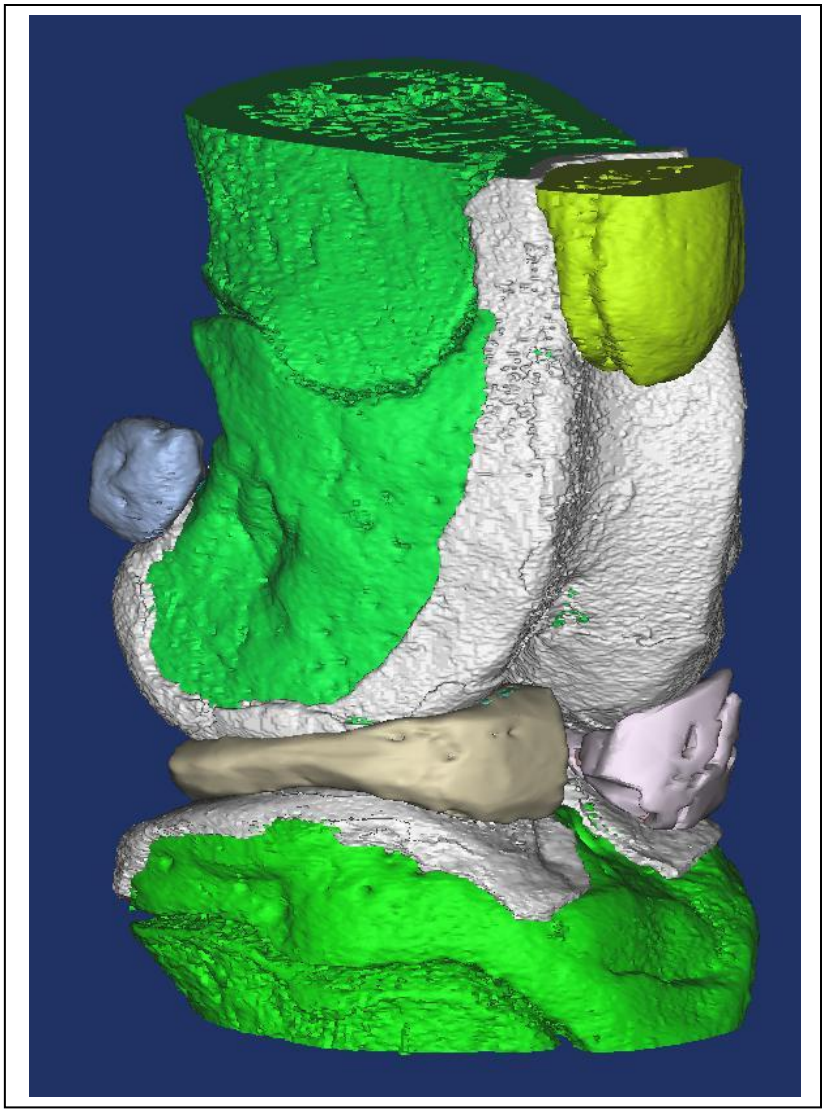

Figure 4.5 Geometric reconstruction of soft and hard tissues in a rat knee joint

DISCUSSION

In the current study, we developed a practical method to reconstruct a small animal joint with its component geometries. The contrast agent approach based on micro-CT imaging modality previously described in literature to visualize the soft tissues in 2D was for the first time adapted successfully for the purpose of high-resolution 3D generation of soft tissues in small joint. The contrast material used in this study had a similar X-Ray absorption to bone and therefore was recognized using the same approach, the silicon based contrast does not penetrate the cartilage, and its X-Ray absorption seems to remain constant over the scan time, which enhanced the distinction of the gray scale attenuations between the hard and soft tissues. The volume for the contrast agent represented the synovial fluid cavity and provided sufficient anatomical details of the soft tissue boundary in the intraarticular space. The soft tissues such as cartilage, menisci, tendon, ligament can be indirectly visualized (Figure 4.1). The interface between the cartilage and the intra-cavital fluid exhibited excellent contrast, as opposed to other studies using ioxaglate based contrast agents [144]. However, ioxaglate based contrast agents are necessary to quantify the proteoglycan density in cartilage, which cannot be obtained with the silicon based contrast agent used in this study.

In our study, the joint sample was scanned at 2.7 μm isotropic voxel size, even after the reduction of spatial resolution for computational speed purpose, the lowered resolution of 22 μm is still higher than the finest reported by the 2D micro-CT (30 μm) or 3D micro-MRI (51μm) studies on imaging rat joint [141, 142, 146]. Low voxel resolution models (e.g. at 22 μm) provide a suitable solution for joint biomechanics studies that require the data in a timely manner in the whole joint including multiple soft

tissues. Whereas intermediate and high voxel resolution models (e.g. at 5.5 or 2.7 μm) make fine analysis of biomechanics possible in different zones inside cartilage, which is most ideal for the cellular level studies that focus on the mechanotransdution mechanism by which chondrocytes detect the mechanically induced strains and respond by adjusting their metabolisms accordingly. In an attempt to generate high-resolution (2.7 μm) 3D model of the joint consisting of ossified tissues and the contrast agent in a defined section, the reconstruction rest result showed we were able to distinguish clearly the femoral condyles, tibia horns, and ossified meniscus from the contrast material (Figure 4.2). The shape of the soft tissues (ACL, PCL, etc) can also be approximately visualized by the empty space between the contrast material and hard tissues in this region. Thus, it can be predicted that, if given more powerful computational capability, high-resolution (2.7μm) reconstruction of the whole joint can be accomplished within a reasonable time frame using the same approach as low-resolution (22 μm) reconstruction.

The 3D geometric model of the whole rat knee with contrast material within the synovial space (Figure 4.3 A) and after the contrast material removal (Figure 4.3 B) can be directly reconstructed at 22 μm pixel resolution, showing that the contrast agent injected into the joint is differentiable from joint tissues in 3D reconstruction. Using the Boolean computational operation, the soft tissues can be further separated from the space defined by the boundaries of ossified tissues and contrast material (Figure 4.4). The cartilage-cartilage contact area was found to be greater at the lateral side rather than the medial side, and the thickness of the tibial cartilage layer on the lateral hone is greater on that on the medial side, which is consistent with the observations reported in the literature [140, 147]. Besides Boolean operation, other key operations to separate, define, and

transform various anatomic components proved essential, and considerable efforts were necessary in the editing process in both 2D and 3D settings to manually characterize the anatomic features of the tissue structures. In the current study, the focus of our research is articular cartilage, as a result we only reconstructed femoral cartilage, tibial cartilage and menisci. If needed, more soft tissues such as tendons and ligaments can be reconstructed using the same methodology. Furthermore, 3D editing manipulations can generate pathological geometries such as seen in arthritic joints or meniscectomy, providing the joint tissue geometries for advanced studies on those diseases.

In summary, we created a 3D geometric model of rat knee that consisted of both soft and hard tissues. This model has the potential of serving as an efficient approach to imaging the progression of diseased joint models inside a small animal joint. The high resolution of micro-CT images can allow for biomechanical research performed at the level of different zones inside cartilage. To the best of our knowledge, this is the first 3D geometrical reconstruction model of both hard and soft tissues in a complete rat knee joint based on high resolution micro-CT imaging modality distinguishing cartilage layers, menisci, and synovial fluid capsule. The implemented approach facilitates advanced numerical modeling on joint stress, strain, hydrostatic pressure, leading to enhanced understanding about how biomechanical factors affect the initiation, progression, and prevention of common joint diseases.

ACKNOWLEDGEMENTS

This work was supported by National Science Foundation (NSF 0723027 to L.C). We are grateful to Dr. Bingmei Fu, Dr. David Rumschitzki and their lab members (esp. Dr. Bin Cai) at the City College of New York for providing the experimental samples.

Chapter 5
SPATIAL EFFECT OF MOTION-LOAD ON JOINT BIOMECHANICS (PART II):

HOW DOES CARTILAGE RESPOND TO STRESSES AND STRAINS?
A FINITE ELEMENT MODEL OF THE RAT KNEE JOINT FOR THE STUDY OF TIBIO-FEMORAL CONTACT

ABSTRACT

Extensive studies have been performed to study mechanotransduction of cartilage in vivo and in vitro. Finite Element Modeling has been proved a useful tool in providing useful information of stresses/strains to characterize the local biomechanical environment in cartilage. However, thus far there have been no reported FE models in a small rodent model. In the current study, a 3D FE model was created from contrast agent enhanced micro-CT images of a rat knee joint to study the effect of axial compressive load on the stress and strain at the menisci and cartilage. The results showed that the maximum stresses and strains occurred on the medial tibial cartilage in response to the axial load from the bottom of the tibia, while a greater percentage change in the contact stresses and strains take place in the lateral cartilage. These results were consistent with the spatial pattern of the MMP3 expression we observed from our in vivo joint loading experiments and partially explained the cartilage degeneration after immobilization, and for the first time characterized the spatial distribution of stresses/strains in a small rodent joint under weight bearing situation. This FE model can be used in an extensive scope to quantitatively investigate the biomechanical effects of pathological conditions created on small animals.

INTRODUCTION

The ability of cartilage to bear the load and to glide with minimal friction is a consequence of changes in tissue morphology, composition, microstructure because of the cellular metabolism of chondrocytes that sense and respond to mechanical loading. Cartilage is continuously subjected to both shear and axial longitudinal loading. The shear stress is created by the contact friction [58, 72-75] between cartilage during flexion-extension of the joint and the axial longitudinal loading [129, 148] is produced by the normal forces applied to the cartilage surface due to weight bearing. Early and progressive damage occurs in cartilage subjected to both shear and axial loading, but it is absent from cartilage subjected to shear loading only [76].

Understanding of how motion-load conditions induce local biomechanical factors that may severely affect cartilage degeneration is the key to the prevention and control of the initiation and progression of OA. Clinical observations and laboratory study results have indicated a causal relationship between the mechanical environment sensed by chondrocytes and the maintenance of joint health [1, 89, 94, 127, 136, 149-151], and hypothesis have been put forth that the degeneration caused by osteoarthritis (OA) is mechanically induced [152]; however, the early-stage events that trigger the pathological process of cartilage degeneration are not clearly elucidated. To have more insight into the initiative phenomena of cartilage degradation, in-depth knowledge of the stress fields within the tissues is urgently required to understand the correlation between the sites of high stresses and tissue failure, either via experimental approaches or using computational simulation methods.

Although several studies have reported the utility of individual transducers, pressure sensitive films and pressure sensitive mats, not all of the stress components can be measured, and not all of the reported tissue damages are at the surface [127]. Furthermore, these sensor techniques can only be used on joints of human cadaver or large animals and therefore have limited application on small animal models, because the space inside a synovial joint is extremely reduced. Due to the small size of the geometry, either direct measurement or computational simulation was extremely difficult to be implemented to provide quantitative temporal and spatial information about tissue biomechanics in small joints. A well-accepted alternative is the use of mathematical models that provide quantitative information about the mechanical environment sensed by chondrocytes. The numerical solution to the computational models not only quantifies the partial contribution of the hydrostatic pressure and the contact stresses on the surfaces, but also predicts the stresses throughout the thickness layers that are not reachable by available measuring means.

The computational Finite Element (FE) modeling has been successfully implemented in the joint biomechanics research for OA [153-160]. These models have provided valuable estimates of the internal forces, stresses and strains in the soft tissues at different joints, and compelling indications of the important role that the local biomechanical factors may play during the pathological process in cartilage. Nevertheless, such FE models have been performed exclusively on human joints, and very few FE models were implemented on small animal subject such as rodents on which vast OA-related cellular and molecular level studies were conducted. Currently, MRI is the major imaging modality for soft tissues in the joint; the relative coarse resolution imposes a constraint of

geometric representation of articular cartilage layers in small thickness, leading to a scarce of the FE method in the small animal models. Thus, there is a difficulty to efficiently incorporate the large body of site-specific findings from enormous in vitro and in vivo animal studies with the human-based FE modeling results.

In this study, a three-dimensional (3D) finite element rat knee model with cartilage and menisci were created using contrast agent enhanced micro-CT images. Finite element analysis was performed for the first time on the small rodent's joint to study the stresses at the contact surfaces between the cartilage, bones, and menisci. We aimed to investigate the high stress areas that correspond to normal body weight condition, and we compared the preliminary result data from the developed finite element rat knee model with our previous findings of the specific sites that showed the catabolic responses after immobilization.

MATERIALS AND METHODS

Three-Dimensional Meshed Geometry

The single left knee joint in the hind limb of a Sprague Dawley rat (five month old, female) right after sacrifice was prepared for micro--CT scanning. In our study, two knees at a flexion of 165 ° and 75 ° were used, respectively. The detailed procedure of contrast agent injection and micro-CT scan were described in the previous chapter. The 3D geometric reconstruction of the rat's joint components were remeshed in Mimics using Remeshing operations (e.g., Automesh, Smooth, Reduce). The 4-node tetrahedral surface mesh corresponding to the sample was applied to femoral cartilage, tibial cartilage, menisci, femur, and tibia. A total of 129963 nodes, 676916 elements were used

in the model of 165 ° flexion knee, and slightly more nodes and elements were used for the model of 75 ° flexion knee. The reconstructed femoral cartilage, tibial cartilage, and menisci as well as meshed joint components for 165 ° flexion knee are illustrated in Figure 5.1.

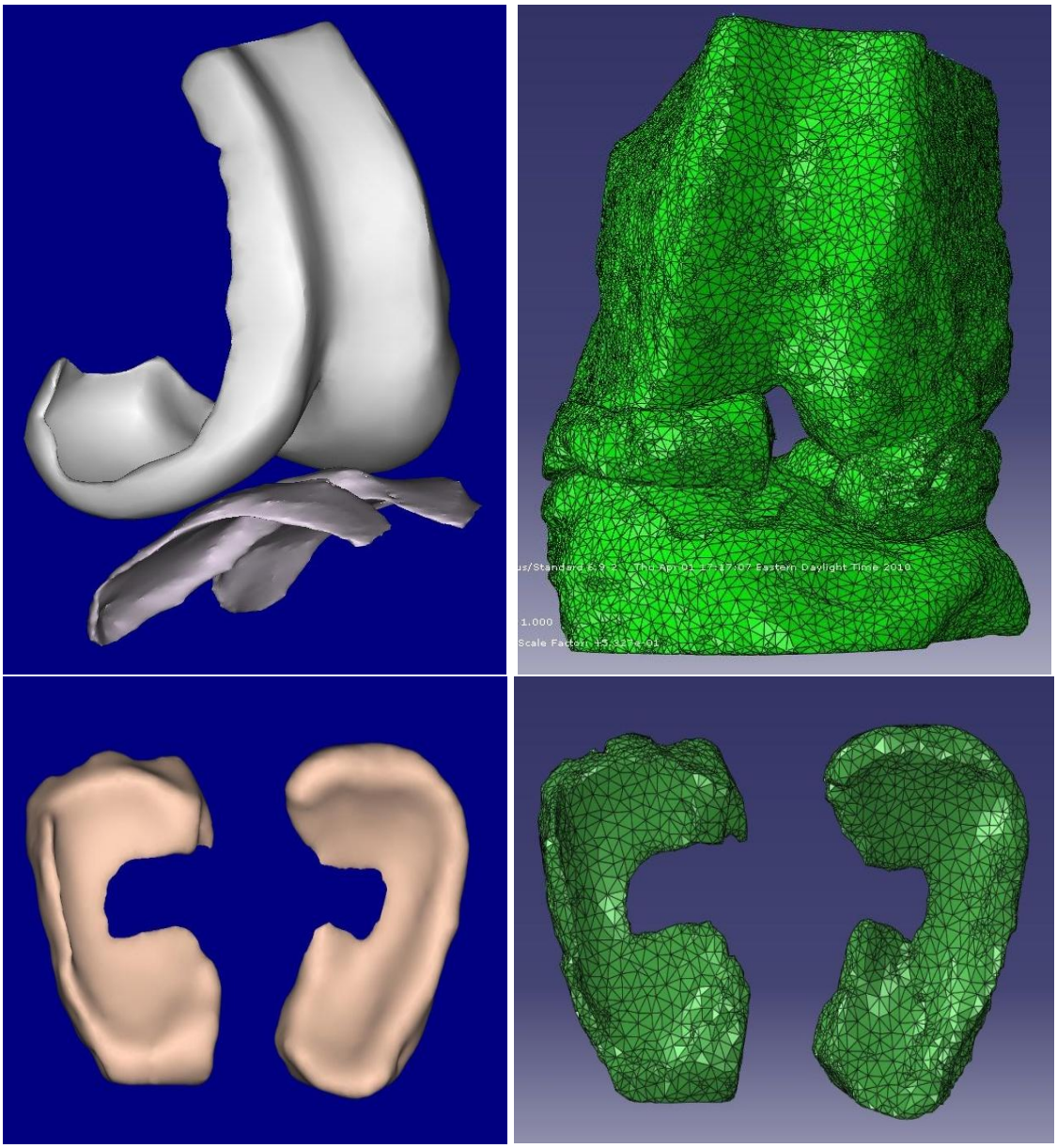

Figure 5.1 Reconstructed and meshed joint geometries.

Finite Element Model of Joint

The 3D meshed geometries were exported to a commercial finite element package ABAQUS (Version 6.7.3 Simulia Inc. RI, USA) and processed to generate mesh type C3D4 using the operation module Remeshing. Adapted from previous FE models [159, 161], the femur, tibia were modeled as rigid material (Young's modulus = 26 Gpa, poisson's ratio = 0.3) as previous work has demonstrated modeling the bones as rigid has no significant differences (<2%) for the contact results but drastically saves computational time [153]. Articular cartilage was modeled as linear elastic, isotropic material (Young's modulus = 15 Mpa, poisson's ratio = 0.45), since the mechanical response of cartilage does not vary considerably with time within a short loading durations [159]. Menisci were modeled as transversely isotropic elastic material (E1=E3=20 Mpa, E2=120 Mpa, v13= 0.2, v12=v23=0.3; G12=G23=57.7Mpa, G13=8.33 Mpa, where E1 and E2 denote Young's modulus in the axial and radial direction, respectively, and E3 denotes Young's modulus in the circumferential direction). In the model, the cartilage was rigidly attached to the bone surface and the menisci were attached to the tibial plateau at the meniscal horns. The material properties used to define the tissues are listed in Table 2.

Table 2. Material Properties for FEM simulation

Part	Material Properties
Cartilage	Isotropic elastic E =15Mpa, v = 0.45
Menisci	Transversely isotropic elastic: $E_1 = E_3 = 20Mpa, E_2 = 120Mpa, v_{13} = 0.2, v_{12} = v_{23} = 0.3$ $G_{12} = G_{23}$ = 57.7Mpa, $G_{13} = 8.33Mpa$
Bones	Isotropic elastic E = 15Gpa, v = 0.3

The boundary and loading conditions were applied in such a way that the femur was fixed in the flexion-extension and varus-valgus rotations in order to simulation the full extension position. The tibia was unconstrained in the axial direction with the applied load and all other rotations and translations were permitted. The axial compressive load was applied at the midpoint of the transepicondylar axis to the central point of knee joint capsule. The load was applied as force at a magnitude of 5 N in one second, corresponding to approximately 1X weight of a normal 5 months old female rat at 510 grams. Global frictionless contact was modeled between the femoral and tibial cartilage, between the femoral and meniscal articular surfaces, and between the tibial and meniscal articular surfaces. Peak surface pressure and contact areas in the articular cartilage and menisci were studied.

RESULTS

The simulation results for the 165 ° flexion knee show that for an axial compression of 5N there was contact between femoral and tibial cartilage, and between cartilage and menisci; both medial and lateral meniscus deformed as a result of load bearing. The peak stresses were 2.61 Mpa and the high stresses were located at the anterior center rims of medial meniscus. The maximum principal stresses were around -7.42 Mpa and concentrated on the anterior center rims of medial meniscus and the posterior center rims of lateral meniscus. The maximum strains of 0.2 mm also took place in those two regions (Figure 5.2 A). For femoral cartilage, the peak contact stresses were around 1.16 Mpa for the applied load (Figure 5.2 B), and located on the contralateral sides of the condyles; there was no significant difference of the stress magnitude between the medial and lateral condyles. For tibial cartilage, the peak contact stresses were around 1.81 Mpa for the applied load, and the lateral side exhibited a more isolated distribution compared with the medial side; there was no significant difference of the stress magnitude or contact areas between the medial and lateral plateaus (Figure 5.2 C). The high stress areas of femoral and tibial cartilage are in the contact regions (Figure 5.3 A), while the maximum displacement occurred on the medial femoral condyle contralateral to the contact area of femoral and tibial cartilage (Figure 5.3B).

The simulation results for the 75 ° flexion knee also demonstrate for an axial compression of 5N there was contact between femoral and tibial cartilages as well as between cartilages and menisci. The higher stress areas expand to the contact edges with the femoral condyles (Figure 5.4 A). In response to the load, the stress pattern on the medial femoral condyle show a belt that covered greater area compared with the lateral

femoral condyle. The peak stresses was found in the posterior center of the femoral condyle (Figure 5.4 B). The peak stresses were on the posterior medial side of the tibial cartilage surface, corresponding to the cartilage-cartilage contact with the femoral cartilage, and the stress distributions are isolated for both medial and lateral tibial plateaus (Figure 5.4C).

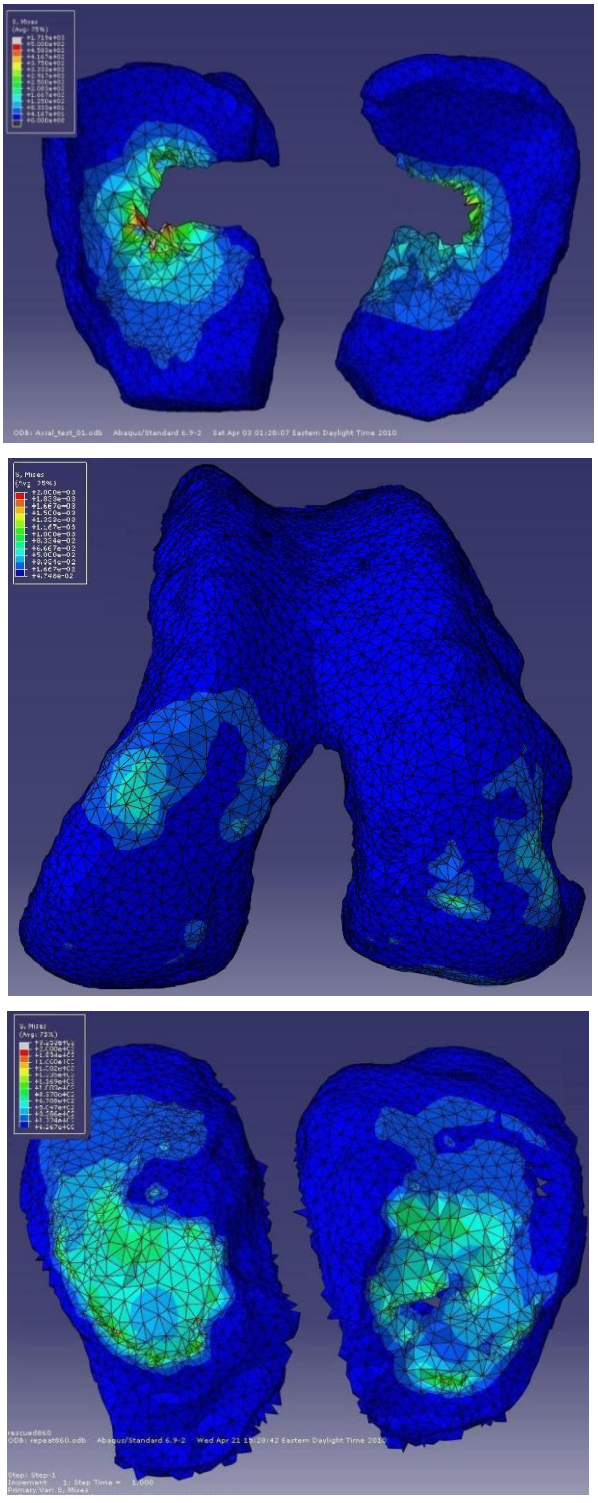

Figure 5.2 FEM results of peak stress in response to an axial compressive load applied from the tibia with the femur fixed at 165 °flexion.

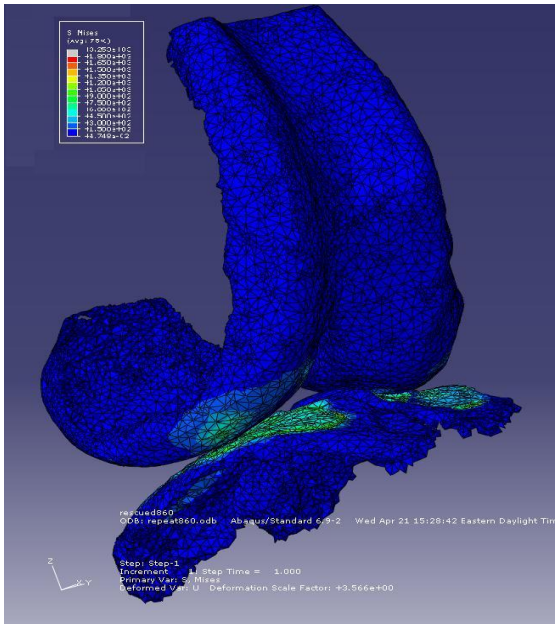

A

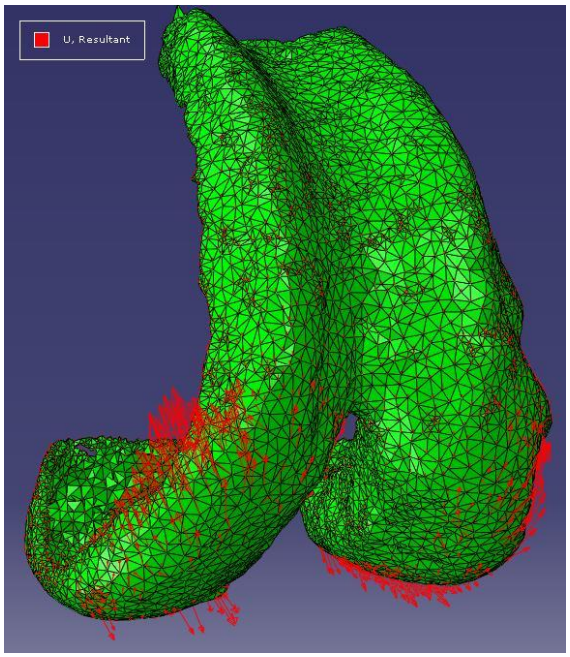

B

Figure 5.3 FEM results of cartilage contact and femoral cartilage displacement in response to an axial compressive load applied from the tibia with the femur fixed at 165 °flexion.

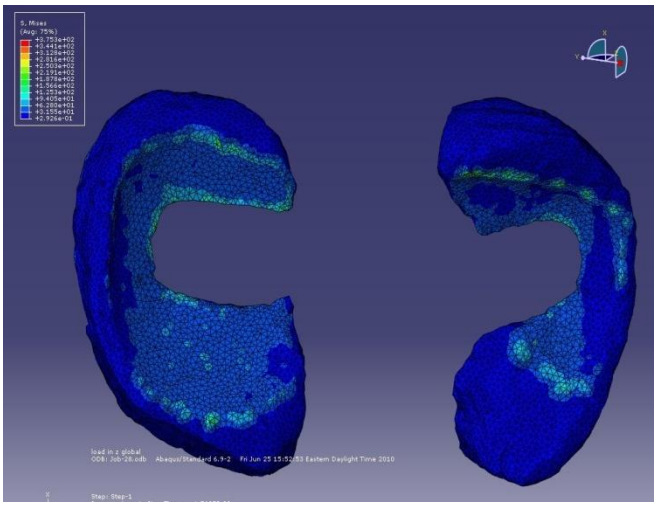

A

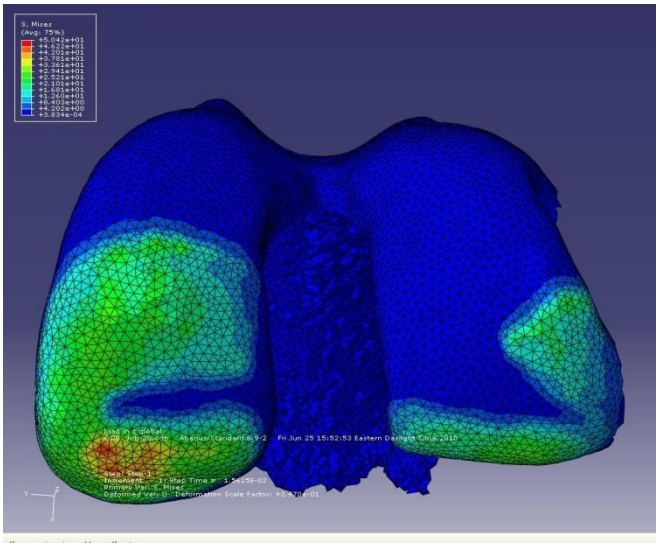

B

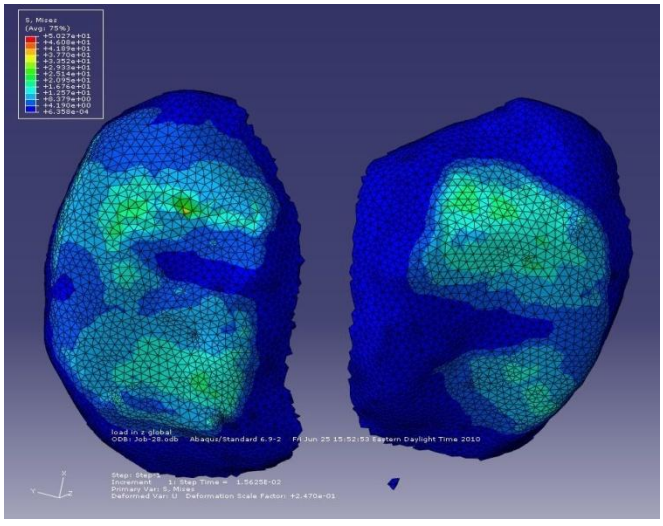

C

Figure 5.4 FEM results of peak stress in response to an axial compressive load applied from the tibia with the femur fixed at 75 °flexion.

DISCUSSION

We developed the first numerical analysis model in an intact small animal joint to analyze the stresses and strains corresponding to physiologically relevant joint loading conditions such as weight bearing. In the current study, we studied the high stress locations in the contact region due to axial compressive load applied from the tibia, and we examined the correlation between the regions of contact stresses and the gene expression and activity of degradative enzymes such as MMP-3. We aimed to clarify the long-term hypothesis that biomechanical factors affect joint tissue homeostasis (particularly, the speculation that excessive loading causes cartilage degradation starting from cartilage surface). Before this study, due to challenges such as the small size of the geometry, it was extremely difficult to obtain quantitative information about tissue biomechanics in small joints. The developed finite element modeling created a venue to numerical analysis of temporal and spatial effect of mechanical stimuli formerly not possible in small animal models.

In our study, two joints were scanned, reconstructed, and modeled. In response to the axial load, the peak contact stress were found to be at the anterior center rims of medial meniscus for the flexion 165 ° joint, indicating the medial meniscus transfers more load compared with the lateral side meniscus. Significant difference between the stresses in the cartilage-cartilage between the medial and lateral side were not observed in the flexion 165 ° joint that was scanned and modeled at an unphysiological flexion; however, greater strains were found at the contralateral femoral cartilage on the medial condyle, which may cause more deformations associated with elevated wear on the medial condyle.

For the flexion 75° joint, a greater stress area as well as a higher peak stress were observed on the femoral condyle compared with the tibial condyle.

The results of the finite element analysis were generally consistent with the previous experimental observations and computational simulation results in human studies. In an earlier work we have demonstrated that following the immobilization, MMP-3 mRNA and activity increased significantly above controls in both femoral condyles; however, levels in the medial condyle were approximately 60% higher than in the lateral condyle after 21 days [125]. There also evidence showing cartilage degenerations are more commonly found in the medical femoral condyle than the lateral condyle [162], and full-thickness lesions are found in approximately 20% of knee arthroscopies and are located most commonly in the medial femoral condyle [163-166]. We have speculated that differences in contact forces or pressures [94, 167], and differential contact with the menisci between the lateral and medial femoral condyles [168] may be a major causal factor for condyle-dependent susceptibility to cartilage degradation. In the current study in the same rat model, for the first time in a small animal model proved that the medial compartment carries greater load than the lateral side in an intact joint when it is in a physiological angle. We also studied the spatial patterns of morphological changes in gene expression of degradative markers in cartilage due to different loading conditions. We clearly show that the load distribution in the joint is indeed transmitted through the medial compartment during weight-bearing activity as reported by previous study [169], and we confirm that in reduced loading conditions, the medial compartment sees a greater percent decrease in stress, resulting in the greater rate of degradation that we observed from MMP-3 expressions and activities [125].

While contact stresses can be critical for wear and tear at the cartilage surface, the subsurface stresses may be more essential for cell metabolism in deeper layers. Chondrocytes are denser in the deep zone and they are highly sensitive to mechanical loading that may be responsible for cell death when exceeding a certain range. A prerequisite for characterization of mechanical environment surrounding chondrocytes is an adequate imaging resolution within cartilage layers, and our geometric reconstruction approach based on high-resolution micro-CT imaging modality may be the only method known to facilitate numerical modeling within the limited thickness of articular cartilage in small animal joint. Although we focused on the surface contact in the current study, our established finite element model can facilitate the the numerical analysis of the subsurface stresses for the sake of high-resolution micro-CT technology.

A limitation of the developed finite element model is the model did not include ligaments or tendons. Currently, we are mainly interested in the cartilage and menisci, the most important parts in the joint, and we aimed to first establish the breakthrough finite element model for numerical analysis of small animal joint biomechanics before making it more comprehensive to include other soft tissues. In the study, we have shown in the 2D scan images that the boundaries between ligaments/tendons and contrast fluid are highly distinguishable; if necessary, the similar methodology for the reconstruction of cartilage and menisci can be applied to generate the geometries of ligaments or tendons.

ACKNOWLEDGEMENTS

This work was supported by the National Science Foundation (NSF 0723027 to L.C). The authors greatly appreciate the kind assistance from Dr. Bingmei Fu, Qin Liu, Wei

Yuan, Guanglei Li, Dr. Min Zeng, Zeynep Seref, Dr. Peter Ganatos at City College of New York for proving joint samples or technical support for ABAQUS.

Chapter 5

GENERAL CONCLUSIONS AND FUTURE DIRECTIONS

General Conclusions

The goal of this dissertation was to understand the pivotal role that motion and load play in the regulation of joint homeostasis, especially on articular cartilage. In this dissertation, experimental and numerical methods were developed and implemented in the challenging small-size animal joint model, and the specific goals were successfully accomplished to contribute our insights into the temporal and spatial effects in cartilage corresponding to mechanical stimuli induced by physical activity and body weight bearing.

The first objective of this dissertation was to create a non-invasive in vivo Joint Motion and Loading System (JMLS) in a small animal model. We have designed, programmed, fabricated, tested, and validated a novel assisted motion and loading system that offers real time monitoring, user-friendly interface, portability, repeatability, and capability of working continuously to carry out extensive loading tests on small animals. Since the onset of osteoarthritis appears to depend on the frequency, intensity and duration of physical activity as well as weight-bearing situation, the JMLS offers reliable duplication of well-controlled mechanical environment comparable to normal and pathological joint loading conditions. In our study, the effectiveness of the joint loading system was validated by analyzing the mechano-response of gene expression due to motion-induced loading in articular cartilage. Experimental results from this loading system will provide important quantitative information in terms of specific beneficial and harmful motion patterns/dosage, and this information may potentially serve as useful scientific guidelines for motion-based therapy design as well as people's involvement of physical activity and sports engagement.

The second goal was to study the gene expression of pro- and anti- inflammatory markers in cartilage in response to joint immobilization, remobilization, and compressive motion loading condition in vivo. The effect of immobilization and remobilization of the rat's joint on articular cartilage in vivo was evaluated by gene expression assays and histological analysis. A significant finding in this study is that the acute catabolic effects can occur in cartilage in a short time of immobilization of the joint, while a low-dose intervention of joint motion can reverse this degradative process. The result suggests that disuse of the joint, even not in a prolonged situation, may cause cartilage degradation; short period but regular joint motion is highly recommended for people who adopt a sedentary life style. The results also confirmed the previous in vitro evidence that immobilization or overloading may result in upregulation of proinflammatory gene production, and signals generated by mechanical forces of low magnitude considered to be within physiological range inhibit the synthesis of catabolic genes such as MMPs [126]. Our study results also support the previous findings that the dynamic motion (frequency dependent) alleviates the pain during arthritis and possibly produces cartilage repair. These low magnitude mechanical stimuli seem to upregulate the synthesis of extracellular matrix, GAGs and Collagen II. Furthermore, while nonsteroidal anti-inflammatory drugs have shown to suppress the inflammatory response in cartilage, there is no evidence of cartilage repair or regeneration. In contrast, the evidence shown in our study suggests that appropriate biomechanical motion may have an effect in both suppressing the pro-inflammatory signals and producing new collagen type II, which implies motion-based therapy may have a superior effects than use of anti-inflammatory drugs.

In chapter 3, we fulfilled the third goal of implementing a novel approach to generate high resolution 3D reconstruction of joint tissues in a rat knee joint. The contrast material injected into the synovial joint created highly distinguishable boundary to define the soft tissues in micro-CT images. We were able to successfully generate the femoral and tibial cartilage as well as menisci at a pixel size of 22 μm, a higher resolution than previously reported 2D micro-CT imaging results and 3D MR reconstruction of rat knee. We also showed we are able to explore even higher resolution given more computational capability. The novel low-cost while high-resolution 3D reconstruction approach to generate small animal joint tissue components can allow for numerical analysis on small joint biomechanics which will improve our insight into the spatial impact of the mechanical stimuli induced from daily motion and weight bearing in both normal and pathological environments.

The achievement of the fourth goal of a finite element model (FEM) in the small joint model was illustrated in Chapter 4. In spite of the prevalence of finite element modeling in nowadays joint biomechanics research studies, the FEM developed here may be the first to be applied in small animal's joint with hard tissues and soft tissues (e.g., cartilage and menisci). The numerical analysis of stresses and strains based on contrast agent enhanced micro-CT imaging technique has generated remarkable information regarding the spatial distribution of tissue responses to physiological loading. The current data confirmed our hypothesis that the gene expression of the key pro-inflammatory mediators is a function of the mechanical loading in a particular region, which leads to significant insight into the biomechanical effects associated with joint motion and load. The numerical approach introduced in this dissertation is a powerful tool to quantitatively

study the onset and development of various joint diseases such as arthritis and meniscectomy that are believed to be predominantly affected by mechanical factors.

In summary, this dissertation dealt with a fundamental question in joint biomechanics research: how does motion and load affect joint health? We elaborated the temporal and spatial effects of mechanical stimuli taking place in articular cartilage in a series of experimental and analytical studies. We explored the early response of cartilage due to joint immobilization and remobilization. We created a pioneering FE model in rodent model based on a contrast agent enhanced high-resolution micro-CT imaging approach to characterize the local spatial mechanical environment in which chondrocytes sense and respond. And we developed a novel joint motion and load system which demonstrated remarkable reliability and reproducibility for challenging protocols in biomechanics research. The in vivo temporal experiments showed that immobilization of joint may cause cartilage degeneration in a short time, while early intervention of moderate motion that produced biomechanical signals to suppress the acute inflammatory effect can reverse this catabolic process, and overloading produced similar results to that observed from immobilization. The low cost micro-CT arthrography approach using contrast agent to create high-resolution three-dimensional (3D) geometries of soft tissues in rat joint proved practical and efficient. The FE modeling result of rat knee joint loading showed the stress distribution that supports our hypothesis that gene expression of important mediators is a function of stress in that particular region. The knowledge gained through these studies may provide more insight into the underlying mechanism orchestrating the relationship between motion, loading and the corresponding biological responses in

cartilage, and may further help treat Osteoarthritis and other joint disorders by contributing to design effective motion-based therapies.

Future Directions

The current dissertation has laid down solid ground for a broad range of future joint biomechanics research projects. The established experimental and theoretical methodologies provide considerable potentials for exploring much more beyond the insight that has been revealed in this dissertation. In a large scope, our research helps the on-going studies to move forward in the following aspects:

1) The invention of the Joint Motion and Load System (JMLS) facilitates wide variety of clinical relevant experiments aiming at studying motion-load effects in small animal models. Inspired by the JMLS in rat model that has been published, we have fabricated a miniature device for mice, and we tested a prototype device for tendon stretch for rats. The device development and its extensions will significantly aid in the important joint loading experiments that were not possible before.

2) The establishment of the 3D rendering methodology for soft tissue geometries in rodents leads to a new venue for the joint biomechanics research studies. Visualization and 3D generation of the tissue structures in both normal and pathological context are foreseeable to be appreciated by future studies that may take advantage of the high-resolution yet relatively inexpensive micro-CT in imaging small animal joint.

3) The development of the finite element model in the rat joint model opens the door to future computational analysis on physiological (walking, squat, etc.) and pathological

(OA, obesity, meniscectomy, etc.) joint loading conditions of clinical relevance in the small animal model.

Characterization of the temporal and spatial effects of motion and load at different levels in the joint is necessary, particularly, how physical regimes may prevent or reverse the degenerative processes is of great interest to patients and motion-based therapists. The development of the in vivo loading system with the ability to apply well-controlled load in a non-invasive approach with close monitoring allowed testing of the intensity level of the motion and load. Cyclic motion frequency in the assisted motion therapy is a common parameter to be controlled to affect the outcome of the therapy, our design of the experiment will test this hypothesis and assess the beneficial range of the moving frequency for a fixed range of cyclic motion. Furthermore, obesity has been shown to be one of the leading risk factors to cause arthritis, suggesting that weight bearing condition can be a critical loading parameter to affect cartilage homeostasis. The developed loading system offers adjustable axial compressive loading on the rat's knee joint, and enables researchers to look into the significance of the weight bearing when in motion in determining the biological responses in joint tissues. Considering the major function of the knee as a hinge to rotate bearing body weight, the loading system adopts a "natural" non-invasive way to apply overloading that may cause cartilage degradation at contact surface, as opposed to other invasive approaches such as surgical intervention of ACL to introduce early OA symptoms, or injection of chemicals to initiate a strong immune reaction in the knee.

As an immediate follow-up study based on the device to further elucidate the temporal effect of motion and load, we will investigate the parameters associated with

mobilization of the knee joint that play a critical role on the homeostasis of the articular cartilage. The developed computer controlled device will be used to investigate the role of frequency, angular range of motion, stimuli duration, and loading amplitude on the biological response of cartilage in both normal and surgically-induced OA models. Then, the effectiveness of the motion therapy in regulating pro-inflammatory and anti-inflammatory mediators triggering/controlling the initiation of cartilage degeneration as MMP-3, MMP-13 and Collagen Type II will be quantified using laser capture and RT-PCR. In the proposed study, we expect to determine the impact of different combination of loading parameters on cartilage in search of an optimal motion protocol to maintain the cartilage homeostasis, the result of the study may help lead to control the progression of cartilage degeneration and to promote the healing of degenerated joint tissues. Similar experiments can be designed to characterize the range of physiological range of mechanical loading imposed on the joint, e.g., the threshold in terms of timepoint, loading parameter, and weight bearing conditions that trigger the gene expression of catabolic mediators such as MMPs in cartilage. The proposed experiments can be performed on knockout mice to study the role of certain key genes whose expression may function to regulate the anabolic/catabolic metabolisms in a magnitude-dependent manner during the well-controlled joint motion and loading environment.

The 3D geometries of cartilage and menisci in the rat joint have been successfully reconstructed using contrast agent enhanced micro-CT imaging approach in the current study. Using the same approach, the future work can expand to include ACL, PCL, MCL, PCL, and patellar tendon, since ligament and tendon provide stability to the joint and therefore also play an important role in joint biomechanics. Thus, by adopting the

developed low-cost while highly efficient, methodology, small animal joint (rats and mice) model consisting of comprehensive soft connective tissue structures, can be established to facilitate the needs of the studies that require increased joint complexities.

The developed finite element model on the small joint biomechanics can be extended to simulate a wide range of physiological or pathological joint conditions. For instance, even though the axial compressive load that was simulated in the current study is believed to play an important role in regulating cartilage homeostasis, shear and tensile stresses that appear as a result of the regular movement of the joint also contribute to the complex processes surrounding cartilage mechanoresponsiveness. Considering the joint that functions as a hinge, simulation of the rotational motion can be created in the FE model to estimate the stress/strains in response to the daily motions of the animal. Furthermore, cartilage pathologies caused by meniscectomy or ACL tear are widely accepted to be caused by mechanical factors, with the established methods for manipulation of geometrical reconstruction to produce the pathological anatomical feature, an understanding the joint contact mechanics can be obtained by modeling the localized tissue deformation in pathogenesis.

REFERENCES

1. Ghosh, P. and M. Smith, *Osteoarthritis, genetic and molecular mechanisms.* Biogerontology, 2002. **3**(1-2): p. 85-8.

2. Lawrence, R.C., et al., *Estimates of the prevalence of arthritis and selected musculoskeletal disorders in the United States.* Arthritis Rheum, 1998. **41**(5): p. 778-99.

3. Reginster, J.Y., *The prevalence and burden of arthritis.* Rheumatology (Oxford), 2002. **41 Supp 1**: p. 3-6.

4. Peng, P., *Causes and consequences of fertility decline in China.* China Popul Today, 1998. **15**(3): p. 5-6, 10.

5. Yamamura, S., et al., *Current state of community pharmacy in Japan: practice, research, and future opportunities or challenges.* Ann Pharmacother, 2006. **40**(11): p. 2008-14.

6. Andriacchi, T.P., et al., *Methods for evaluating the progression of osteoarthritis.* J Rehabil Res Dev, 2000. **37**(2): p. 163-70.

7. Moskowitz, R.W. and V.M. Goldberg, *Osteophyte evolution: studies in an experimental partial meniscectomy model.* J Rheumatol, 1987. **14 Spec No**: p. 116-8.

8. Dorr, L.D., *Continuous passive motion offers no benefit to the patient.* Orthopedics, 1999. **22**(4): p. 393.

9. Brosseau, L., et al., *Efficacy of continuous passive motion following total knee arthroplasty: a metaanalysis.* J Rheumatol, 2004. **31**(11): p. 2251-64.

10. "KNEE JOINT - ANATOMY & FUNCTION" http://www.arthroscopy.com/sp05001.htm.

11. Agarwal S, L.P., Gassner R, et al, *Cyclic tensile strain suppresses catabolic effects of interleukin-1beta in fibrochondrocytes from the temporomandibular joint.* Arthritis Reheum, 2001. **44**(3): p. 608-617.

12. "ARTHRITIS" http://www.medicinenet.com/arthritis/page2.htm.

13. "OSTEOARTHRITIS TREAMENT" http://www.hopkins-arthritis.org/osteo/osteo_treat.html.

14. Salter, R.B., *The physiologic basis of continuous passive motion for articular cartilage healing and regeneration.* Hand Clin, 1994. **10**(2): p. 211-9.

15. Ehrlich S, W.N., Schneiderman R, et al, *The osmotic pressure of chondroitin sulphate solutions: experimental measurements and theoretical analysis.* Biorheology, 1998. **35**(6): p. 383-397.

16. Fithian DC, K.M., Mow VC, *Material properties and structure-function relationships in the menisci.* Clin Orthop, 1990: p. 19-31.

17. Zamparo O, C.W., *Hydraulic conductivity of chondrotin sulfate proteoglycan solutions.* Arch. Biochem. Biophys. , 1989. **274**(1): p. 259-269.

18. Torzilli PA, A.T., Mis RJ, *Transient solute diffusion in articular cartilage.* Journal of Biomech, 1987. **20**: p. 203-214.

19. Frank EH, G.A., *Electrokinetic transduction and the effects of electrolyte pH and ionic strength.* Journal of Biomechanics, 1987. **20**: p. 615-627.

20. Torzilli PA, G.R., Borelli J, Helfet DL, *Effect of impact load on articular cartilage: cell metabolism and viability, and matrix water content.* Journal of Biomech. Eng., 1999. **121**: p. 433-441.

21. "HISTOLOGY OF HYALINE CARTILAGE " http://faculty.une.edu/com/abell/histo.

22. "CARTILAGE STRUCTURE AND FUNCTION" http://www.engin.umich.edu/class/bme456/cartilage/cart.htm.

23. Graindorge S, F.W., Jin ZM, Ingham E, Grant C, Twigg P, Fisher J, *Biphasic surface amorphous layer lubrication of articular cartilage.* Medical Engineering and Physisc, 2005. **27**: p. 836-844.

24. Zeytin S, K.B., Ipek M, Bindal C, Ucisik AH, *An evaluation of human articular cartilage on femoral head.* Material Science and Engineering, 2002. **C**(20): p. 219-222.

25. Knecht S, V.B., Stussi E, *A review on the mechcnical quality of articular cartilage - Implications for the diagnosis of osteoarthritis.* Clinical Biomechanics, 2006. **21**(10): p. 999-1012.

26. Hall BK, *Bone and Cartilage: Developmental and Evoluionary Skeletal Biology*. 2005: Elsevier Academic Press.

27. Urban JP, *The chondrocyte: a cell under pressure.* Br J Rheumatol., 1994. **33**(10): p. 901-908.

28. Langille RM, *Chondrogenic differentiation in cultures of embryonic rat mesenchyme.* Microscopy Research and Technique, 2005. **28**(6): p. 455-469.

29. "MATRIX METALLOPROTEINASES" http://www.encyclopedia.com.

30. Aigner T, S.S., Haag J, *IL-1B and BMPs-Interactive players of cartilage matrix degradation and regeneration.* Equropean Cells and Materials 2006. **12**: p. 49-56.

31. Ateshian GA, *Special Issue on Cartilage (Part II).* Biomechanics and Modeling in Mechanobiology, 2007. **6**: p. 1-3.

32. Ahmed AM, B.D., *In-Vitro measurement of static pressure distribution in synovial joints - Part I: Tibial surface of the knee.* ASME J. of Biomech. Eng., 1983. **105**: p. 216-225.

33. Huberti HH, H.W., *Patellofemoral contact pressures. The influence of Q-angle and tendofemoral contact.* J. Bone Jt. Surg., Am., 1984. **66A**: p. 715-724.

34. Hodge WA, F.R., Carlson KL, Burgess RG, Harris WH, Mann RW, *Contact pressures in the human hip joint measured in vivo.* Proc. Natl. Acad. Sci. USA, 1986. **83**(2879-2883).

35. Roos EM, D.L., *Physical activity as medication against arthrosis--training has a positive effect on the cartilage.* Lakatidningen, 2004. **101**(25): p. 2178-2181.

36. Salter, R.B., *The biologic concept of continuous passive motion of synovial joints. The first 18 years of basic research and its clinical application.* Clin Orthop Relat Res, 1989(242): p. 12-25.

37. Salter, R.B., *History of rest and motion and the scientific basis for early continuous passive motion.* Hand Clin, 1996. **12**(1): p. 1-11.

38. Salter, R.B., *Continuous passive motion: from origination to research to clinical applications.* J Rheumatol, 2004. **31**(11): p. 2104-5.

39. Salter RB, *History of rest and motion and the scientific basis for early continuous passive motion.* Hand Clinics, 1996. **12**(1): p. 1-11.

40. Ferretti M, S.A., Deschner J, Gassner R, Baliko F, Piesco N, Salter R, Agarwal S, *Anti-inflammatory effects of continuous passive motion on meniscal fibrocartilage.* Journal of Orthopaedic Research 2005. **23**: p. 1165-1171.

41. Brosseau L, M.S., Wells G, Tugwell P, Robinson V, Casimiro L, Pelland L, Noel MJ, Davis J, Drouin H, *Efficacy of continuous passive motion following total knee arthroplasty: a metaanalysis.* J. Rheumatol, 2004. **31**: p. 2251-2264.

42. Herzog W, F.S., *Consideration on joint and articular cartilage mechanics.* Biomechanics and Modeling in Mechanobiology, 2006. **5**: p. 64-81.

43. Anderson DD, G.J., Shivanna K, Grosland NM, Redersen DR, Thomas TP, Tochigi Y, Marsh JL, Brown TD, *Intra-articular contact stress distributions at the ankle throughout stance phase-patient-specific finite element analysis as a metric of degeneration propensity.* Biomechanics and Modeling in Mechanobiology, 2006. **5**: p. 82-89.

44. A., M., *Balance between swelling pressure and collagen tension in normal and degenative cartilage.* Nature, 1976. **260**: p. 808-809.

45. Williams JM, U.D., Thonar EJ, Kocsis K, Modis L, *Alteration and recovery of the spatial orientation of the collagen network of articular cartilage in adolescent rabbits following intra-articular chymopapain injection.* Coonect Tissue Res, 1996. **34**(2): p. 105-117.

46. Quinn TM, M.V., *Microstructural modelling of collagen network mechanics and interactions with the proteoglycan gel in articular cartilage.* Biomechanics and Modeling in Mechanobiology, 2006. **6**: p. 73-82.

47. Buckwalter JA, M.J., Mankin HJ, *Synovial joint degeneration and the syndrome of osteoarthritis.* Instr Course Lect, 2000. **49**: p. 481-489.

48. Yerramalli CS, C.A., Miller GJ, Nicoll SB, Chin KR, Elliott DM, *The effect of nucleus pulposus crosslinking and glycosaminoglycan degradation on disc mechnaical function.* Biomechanics and Modeling in Mechanobiology, 2006. **6**: p. 13-20.

49. Wilson W, H.J., van Donkelaar CC, *Depth-dependent compressive equilibrium properties of articular cartilage explained by its composition.* Biomechanics and Modeling in Mechanobiology, 2006. **6**: p. 43-53.

50. Torzilli PA, D.X.-H., Ramcharan M, *Effect of compressive strain on cell viability in statically loaded articular cartilage.* Biomechanics and Modeling in Mechanobiology, 2006. **5**: p. 123-132.

51. Alexopoulos LG, H.M., Vail TP, Guilak F, *Alterations in the mechanical properties of the human chondrocyte pericellular matrix with osteoarthritis.* J. Biomech. Eng., 2003. **125**(3): p. 323-333.

52. Korhonen RK, J.P., Rieppo J, Lappalainen R, Konttinen YT, Juvelin JS, Biomechanics and Modeling in Mechanobiology, 2006(5): p. 150-159.

53. Ateshian GA, C.K., Huang CT, *A theoretical analysis of water trasport through chondrocytes.* Biomechanics and Modeling in Mechanobiology, 2006. **6**: p. 91-101.

54. Sun HB, Y.H., *Messenger RNA expression of matrix metalloproteinase, tissue inhibitors of metalloproteinases, and transcription factors in rheumatic synovial cells under mechanical stimuli.* Bone, 2001. **28**: p. 303-309.

55. Yokota H, G.M., Sun HB, *CITED2-mediated regulation of MMP-1 and MMP-13 in human chondrocytes under flow shear.* Journal of Biological Chemistry, 2003. **278**(21): p. 47275-47280.

56. Henderson JH, F.L., Romero D, Colnot CI, Huang S, Carter DR, Helms JA, *Rapid growth of cartilage rudiments may generate perichondral structures by mechanical induction.* Biomechanics and Modeling in Mechanobiology, 2006. **6**: p. 127-137.

57. Ely, L.W. and M.C. Mensor, *Studies on the immobilization of normal joints.* Surg Gynecol Obstet, 1933(57): p. 212.

58. Trias, A., *Effect of persistent pressure on the aricular cartilage. An experimental study.* . J. Bone Joint Surg, 1961. **43**(2): p. 11.

59. Salter, R.B., R.S. Bell, and F.W. Keeley, *The protective effect of continuous passive motion in living articular cartilage in acute septic arthritis: an experimental investigation in the rabbit.* Clin Orthop Relat Res, 1981(159): p. 223-47.

60. Evans, E.B., et al., *Experimental Immobilization and Remobilization of Rat Knee Joints.* J Bone Joint Surg Am, 1960. **42**(5): p. 737-758.

61. Salter, R.B., D.R. McNeill, and R. Carbin. *The pathological changes in articular cartilage associated with persistent joint deformity. And experimental investigation.* in *Third Canadian Conference on the Rheumatic Diseases* 1965. Toronto.

62. Hohl, M. and J.V. Luck, *Fractures of the tibial condyle; a clinical and experimental study.* J Bone Joint Surg Am, 1956. **38-A**(5): p. 1001-18.

63. Kettunen, K., *Effect of Articular Function on the Repair of a Full-Thickness Defect of the Joint Cartilage. An Experimental Study of Mature Rats.* Ann Chir Gynaecol Fenn, 1963. **52**: p. 627-42.

64. Kettunen, K. and P. Rokkanen, *The repair of a full-thickness articular defect. An experimental study on growing rats.* Ann Chir Gynaecol Fenn, 1973. **62**(3): p. 166-8.

65. Salter, R.B. and P. Field, *The Effects of Continuous Compression on Living Articular Cartilage: An Experimental Investigation.* J Bone Joint Surg Am, 1960(42).

66. Baker Wde, C., T.G. Thomas, and W.H. Kirkaldy-Willis, *Changes in the cartilage of the posterior intervertebral joints after anterior fusion.* J Bone Joint Surg Br, 1969. **51**(4): p. 736-46.

67. Field, P.L. and J.T. Hueston, *Articular cartilage loss in long-standing flexion deformity of the proximal interphalangeal joints.* Aust N Z J Surg, 1970. **40**(1): p. 70-4.

68. Enneking, W.F. and M. Horowitz, *The intra-articular effects of immobilization on the human knee.* J Bone Joint Surg Am, 1972. **54**(5): p. 973-85.

69. Brandt, K.D., *Response of joint structures to inactivity and to reloading after immobilization.* Arthritis Rheum, 2003. **49**(2): p. 267-71.

70. Williams, J.M. and K.D. Brandt, *Immobilization ameliorates chemically-induced articular cartilage damage.* Arthritis Rheum, 1984. **27**(2): p. 208-16.

71. Gu, X.I., et al. *Computer-Controlled Joint Loading System For Biomechanics Research In A Rat Model*. in *Annual Meeting of Biomedical Engineering Society*. 2007. Los Angeles.

72. Bennett, G.A. and W. Bauer, *JOINT CHANGES RESULTING FROM PATELLAR DISPLACEMENT AND THEIR RELATION TO DEGENERATIVE JOINT DISEASE.* Journal of Bone and Joint Surgery, 1937. **19**(3): p. 667-682.

73. Crelin, E.S. and W.O. Southwick, *Changes Induced by Sustained Pressure in the Knee Joint Articular Cartilage of Adult Rabbits.* Anat Rec, 1964. **149**: p. 113-33.

74. Hulth, A., L. Lindberg, and H. Telhag, *Experimental osteoarthritis in rabbits. Preliminary report.* Acta Orthop Scand, 1970. **41**(5): p. 522-30.

75. Murray, D.G., *Experimentally Induced Arthritis Using Intra-Articular Papain.* Arthritis Rheum, 1964. **7**: p. 211-9.

76. Dekel, S. and S.L. Weissman, *Joint changes after overuse and peak overloading of rabbit knees in vivo.* Acta Orthop Scand, 1978. **49**(6): p. 519-28.

77. Appleton, C.T., et al., *Forced mobilization accelerates pathogenesis: characterization of a preclinical surgical model of osteoarthritis.* Arthritis Res Ther, 2007. **9**(1): p. R13.

78. Asundi, K.R., et al., *In vitro system for applying cyclic loads to connective tissues under displacement or force control.* Ann Biomed Eng, 2007. **35**(7): p. 1188-95.

79. Jung, Y., et al., *Cartilaginous tissue formation using a mechano-active scaffold and dynamic compressive stimulation.* J Biomater Sci Polym Ed, 2008. **19**(1): p. 61-74.

80. Lawrence, B.R., *The dose effect of continuous passive motion in postoperative rehabilitation of the first metatarsophalangeal joint.* J Foot Ankle Surg, 1996. **35**(2): p. 155-61; discussion 190-1.

81. Ekholm, R., *[The effect of brief functional activity upon articular cartilage and synovia.]*. Nord Med, 1951. **45**(1): p. 23-4.

82. Shapiro, F., S. Koide, and M.J. Glimcher, *Cell origin and differentiation in the repair of full-thickness defects of articular cartilage.* J Bone Joint Surg Am, 1993. **75**(4): p. 532-53.

83. Wall, P.D. and R. Melzack, *Textbook of Pain*. 1984: Edinburgh, Scotland: Churchill Livingstone.

84. Mizuno, S., et al., *Hydrostatic fluid pressure enhances matrix synthesis and accumulation by bovine chondrocytes in three-dimensional culture.* J Cell Physiol, 2002. **193**(3): p. 319-27.

85. Smith, R.L., et al., *In vitro stimulation of articular chondrocyte mRNA and extracellular matrix synthesis by hydrostatic pressure.* J Orthop Res, 1996. **14**(1): p. 53-60.

86. Wu, Q.Q. and Q. Chen, *Mechanoregulation of chondrocyte proliferation, maturation, and hypertrophy: ion-channel dependent transduction of matrix deformation signals.* Exp Cell Res, 2000. **256**(2): p. 383-91.

87. Wu, M., H. Fang, and S.T. Hwang, *Cutting edge: CCR4 mediates antigen-primed T cell binding to activated dendritic cells.* J Immunol, 2001. **167**(9): p. 4791-5.

88. Wong, D.L., L.J. Anderson, and T.C. Tai, *Cholinergic and peptidergic regulation of phenylethanolamine N-methyltransferase gene expression.* Ann N Y Acad Sci, 2002. **971**: p. 19-26.

89. Smith, R.L., et al., *Time-dependent effects of intermittent hydrostatic pressure on articular chondrocyte type II collagen and aggrecan mRNA expression.* J Rehabil Res Dev, 2000. **37**(2): p. 153-61.

90. Sun, H.B. and H. Yokota, *Messenger-RNA expression of matrix metalloproteinases, tissue inhibitors of metalloproteinases, and transcription*

factors in rheumatic synovial cells under mechanical stimuli. Bone, 2001. **28**(3): p. 303-309.

91. Ferretti, M., et al., *Biomechanical signals suppress proinflammatory responses in cartilage: early events in experimental antigen-induced arthritis.* J Immunol, 2006. **177**(12): p. 8757-66.

92. Badley, E.M., *The effect of osteoarthritis on disability and health care use in Canada.* J Rheumatol Suppl, 1995. **43**: p. 19-22.

93. Sangha, O., *Epidemiology of rheumatic diseases.* Rheumatology (Oxford), 2000. **39 Suppl 2**: p. 3-12.

94. Andriacchi, T.P., et al., *A framework for the in vivo pathomechanics of osteoarthritis at the knee.* Ann Biomed Eng, 2004. **32**(3): p. 447-57.

95. Lequesne, M.G., N. Dang, and N.E. Lane, *Sport practice and osteoarthritis of the limbs.* Osteoarthritis Cartilage, 1997. **5**(2): p. 75-86.

96. Baker, P., et al., *Knee disorders in the general population and their relation to occupation.* Occup Environ Med, 2003. **60**(10): p. 794-7.

97. Chantraine, A., *Knee joint in soccer players: osteoarthritis and axis deviation.* Med Sci Sports Exerc, 1985. **17**(4): p. 434-9.

98. Marti, B., et al., *Is excessive running predictive of degenerative hip disease? Controlled study of former elite athletes.* BMJ, 1989. **299**(6691): p. 91-3.

99. Spector, T.D., et al., *Risk of osteoarthritis associated with long-term weight-bearing sports: a radiologic survey of the hips and knees in female ex-athletes and population controls.* Arthritis Rheum, 1996. **39**(6): p. 988-95.

100. Fontana, L., et al., *Osteoarthritis of the thumb carpometacarpal joint in women and occupational risk factors: a case-control study.* J Hand Surg [Am], 2007. **32**(4): p. 459-65.

101. Cooper, C., et al., *Occupational activity and osteoarthritis of the knee.* Ann Rheum Dis, 1994. **53**(2): p. 90-3.

102. Messier, S.P., *Osteoarthritis of the knee and associated factors of age and obesity: effects on gait.* Med Sci Sports Exerc, 1994. **26**(12): p. 1446-52.

103. Cooper, C., et al., *Risk factors for the incidence and progression of radiographic knee osteoarthritis.* Arthritis Rheum, 2000. **43**(5): p. 995-1000.

104. Deyle, G.D., et al., *Effectiveness of manual physical therapy and exercise in osteoarthritis of the knee. A randomized, controlled trial.* Ann Intern Med, 2000. **132**(3): p. 173-81.

105. Deyle, G.D., et al., *Physical therapy treatment effectiveness for osteoarthritis of the knee: a randomized comparison of supervised clinical exercise and manual therapy procedures versus a home exercise program.* Phys Ther, 2005. **85**(12): p. 1301-17.

106. Huang, T.F., S.M. Perry, and L.J. Soslowsky, *The effect of overuse activity on Achilles tendon in an animal model: a biomechanical study.* Ann Biomed Eng, 2004. **32**(3): p. 336-41.

107. King, K.B., C.F. Opel, and D.M. Rempel, *Cyclical articular joint loading leads to cartilage thinning and osteopontin production in a novel in vivo rabbit model of repetitive finger flexion.* Osteoarthritis Cartilage, 2005. **13**(11): p. 971-8.

108. Thomopoulos, S., G.R. Williams, and L.J. Soslowsky, *Tendon to bone healing: differences in biomechanical, structural, and compositional properties due to a range of activity levels.* J Biomech Eng, 2003. **125**(1): p. 106-13.

109. Ferretti, M., et al., *Anti-inflammatory effects of continuous passive motion on meniscal fibrocartilage.* J Orthop Res, 2005. **23**(5): p. 1165-71.

110. Gu, X.I., et al. *In vivo Mechanical Loading System for Biomechanics Research in Cartilage*. in *Annual Meeting of Biomedical Engineering Society*. 2008. Saint Louis.

111. Gebhard, J.S., J.M. Kabo, and R.A. Meals, *Passive motion: the dose effects on joint stiffness, muscle mass, bone density, and regional swelling. A study in an experimental model following intra-articular injury.* J Bone Joint Surg Am, 1993. **75**(11): p. 1636-47.

112. Zhang, P., G.M. Malacinski, and H. Yokota, *Joint loading modality: its application to bone formation and fracture healing.* Br J Sports Med, 2008. **42**(7): p. 556-60.

113. Zhang, P., et al., *Knee loading dynamically alters intramedullary pressure in mouse femora.* Bone, 2007. **40**(2): p. 538-43.

114. Cohen, Z.A., et al., *Patellofemoral stresses during open and closed kinetic chain exercises. An analysis using computer simulation.* Am J Sports Med, 2001. **29**(4): p. 480-7.

115. Coutinho, E.L., et al., *A new model for the immobilization of the rat hind limb.* Braz J Med Biol Res, 2002. **35**(11): p. 1329-32.

116. Gu X, L.D., Li YH, Shah P, Sun HB, Cardoso L, *Development and validation of a small animal model for joint biomechanics research.* Transactions of the 55th Annual Meeting of the Orthopaedic Research Society, 2009. **34**: p. 1111.

117. Shao, Y.Y., et al., *Analysis of gene expression in mineralized skeletal tissues by laser capture microdissection and RT-PCR.* Lab Invest, 2006. **86**(10): p. 1089-95.

118. Yokota, H., M.B. Goldring, and H.B. Sun, *CITED2-mediated regulation of MMP-1 and MMP-13 in human chondrocytes under flow shear.* J Biol Chem, 2003. **278**(47): p. 47275-80.

119. Lee, J.Y., et al., *Identification of CITED2 as a negative regulator of fracture healing.* Biochem Biophys Res Commun, 2009.

120. Imai, K., et al., *Matrix metalloproteinase 7 (matrilysin) from human rectal carcinoma cells. Activation of the precursor, interaction with other matrix metalloproteinases and enzymic properties.* J Biol Chem, 1995. **270**(12): p. 6691-7.

121. Knauper, V., et al., *Biochemical characterization of human collagenase-3.* J Biol Chem, 1996. **271**(3): p. 1544-50.

122. Knauper, V., et al., *Direct activation of human neutrophil procollagenase by recombinant stromelysin.* Biochem J, 1993. **295 (Pt 2)**: p. 581-6.

123. Murphy, G., et al., *Stromelysin is an activator of procollagenase. A study with natural and recombinant enzymes.* Biochem J, 1987. **248**(1): p. 265-8.

124. Ogata, Y., J.J. Enghild, and H. Nagase, *Matrix metalloproteinase 3 (stromelysin) activates the precursor for the human matrix metalloproteinase 9.* J Biol Chem, 1992. **267**(6): p. 3581-4.

125. Leong, D.J., et al., *Matrix metalloproteinase-3 in articular cartilage is upregulated by joint immobilization and suppressed by passive joint motion.* Matrix Biol.

126. Sun, H.B. and H. Yokota, *Reduction of cytokine-induced expression and activity of MMP-1 and MMP-13 by mechanical strain in MH7A rheumatoid synovial cells.* Matrix Biology, 2002. **21**(3): p. 263-270.

127. Torzilli, P.A., et al., *Effect of impact load on articular cartilage: cell metabolism and viability, and matrix water content.* J Biomech Eng, 1999. **121**(5): p. 433-41.

128. Simon, M.R., *The effect of dynamic loading on the growth of epiphyseal cartilage in the rat.* Acta Anat (Basel), 1978. **102**(2): p. 176-83.

129. Simon, S.R., et al., *The response of joints to impact loading. II. In vivo behavior of subchondral bone.* J Biomech, 1972. **5**(3): p. 267-72.

130. Chakraborti, S., et al., *Regulation of matrix metalloproteinases: an overview.* Mol Cell Biochem, 2003. **253**(1-2): p. 269-85.

131. Blom, A.B., et al., *Crucial role of macrophages in matrix metalloproteinase-mediated cartilage destruction during experimental osteoarthritis: involvement of matrix metalloproteinase 3.* Arthritis Rheum, 2007. **56**(1): p. 147-57.

132. Arokoski, J.P., et al., *Normal and pathological adaptations of articular cartilage to joint loading.* Scand J Med Sci Sports, 2000. **10**(4): p. 186-98.

133. Vanwanseele, B., E. Lucchinetti, and E. Stussi, *The effects of immobilization on the characteristics of articular cartilage: current concepts and future directions.* Osteoarthritis Cartilage, 2002. **10**(5): p. 408-19.

134. Okada, Y., et al., *Localization of matrix metalloproteinase 3 (stromelysin) in osteoarthritic cartilage and synovium.* Lab Invest, 1992. **66**(6): p. 680-90.

135. Wu, J.J., et al., *Sites of stromelysin cleavage in collagen types II, IX, X, and XI of cartilage.* J Biol Chem, 1991. **266**(9): p. 5625-8.

136. Hagiwara, Y., et al., *Changes of articular cartilage after immobilization in a rat knee contracture model.* J Orthop Res, 2009. **27**(2): p. 236-42.

137. Tetlow, L.C., D.J. Adlam, and D.E. Woolley, *Matrix metalloproteinase and proinflammatory cytokine production by chondrocytes of human osteoarthritic cartilage: associations with degenerative changes.* Arthritis Rheum, 2001. **44**(3): p. 585-94.

138. Tetlow, L.C. and D.E. Woolley, *Expression of vitamin D receptors and matrix metalloproteinases in osteoarthritic cartilage and human articular chondrocytes in vitro.* Osteoarthritis Cartilage, 2001. **9**(5): p. 423-31.

139. Walter, H., et al., *Immunohistochemical analysis of several proteolytic enzymes as parameters of cartilage degradation.* Pathol Res Pract, 1998. **194**(2): p. 73-81.

140. Goebel, J.C., et al., *In vivo rat knee cartilage volume measurement using quantitative high resolution MRI (7 T): feasibility and reproducibility.* Biomed Mater Eng, 2008. **18**(4-5): p. 247-52.

141. Rengle, A., et al., *A dedicated two-channel phased-array receiver coil for high-resolution MRI of the rat knee cartilage at 7 T.* IEEE Trans Biomed Eng, 2009. **56**(12): p. 2891-7.

142. Roemer, F.W., et al., *Micro-CT arthrography: a pilot study for the ex vivo visualization of the rat knee joint.* AJR Am J Roentgenol, 2005. **184**(4): p. 1215-9.

143. Xie, L., et al., *Quantitative assessment of articular cartilage morphology via EPIC-microCT.* Osteoarthritis Cartilage, 2009. **17**(3): p. 313-20.

144. Palmer, A.W., R.E. Guldberg, and M.E. Levenston, *Analysis of cartilage matrix fixed charge density and three-dimensional morphology via contrast-enhanced microcomputed tomography.* Proc Natl Acad Sci U S A, 2006. **103**(51): p. 19255-60.

145. Piscaer, T.M., et al., *In vivo imaging of cartilage degeneration using muCT-arthrography.* Osteoarthritis Cartilage, 2008. **16**(9): p. 1011-7.

146. Guermazi, A., et al., *Osteoarthritis: current role of imaging.* Med Clin North Am, 2009. **93**(1): p. 101-26, xi.

147. Li, X., et al., *In vivo 3T spiral imaging based multi-slice T(1rho) mapping of knee cartilage in osteoarthritis.* Magn Reson Med, 2005. **54**(4): p. 929-36.

148. Radin, E.L., et al., *Response of joints to impact loading. 3. Relationship between trabecular microfractures and cartilage degeneration.* J Biomech, 1973. **6**(1): p. 51-7.

149. Carter, D.R. and M. Wong, *Modelling cartilage mechanobiology.* Philos Trans R Soc Lond B Biol Sci, 2003. **358**(1437): p. 1461-71.

150. L'Hermette, M.F., et al., *Articular cartilage, degenerative process, and repair: current progress.* Int J Sports Med, 2006. **27**(9): p. 738-44.

151. Radin, E.L., et al., *Effects of mechanical loading on the tissues of the rabbit knee.* J Orthop Res, 1984. **2**(3): p. 221-34.

152. Moskowitz, R.W., Y. Pun, and T.M. Haqqi, *Genetics and osteoarthritis.* Bull Rheum Dis, 1992. **41**(1): p. 4-6.

153. Donahue, T.L., et al., *A finite element model of the human knee joint for the study of tibio-femoral contact.* J Biomech Eng, 2002. **124**(3): p. 273-80.

154. Papaioannou, G., et al., *Patient-specific knee joint finite element model validation with high-accuracy kinematics from biplane dynamic Roentgen stereogrammetric analysis.* J Biomech, 2008. **41**(12): p. 2633-8.

155. Pena, E., et al., *A three-dimensional finite element analysis of the combined behavior of ligaments and menisci in the healthy human knee joint.* J Biomech, 2006. **39**(9): p. 1686-701.

156. Pena, E., et al., *Finite element analysis of the effect of meniscal tears and meniscectomies on human knee biomechanics.* Clin Biomech (Bristol, Avon), 2005. **20**(5): p. 498-507.

157. Pena, E., et al., *Why lateral meniscectomy is more dangerous than medial meniscectomy. A finite element study.* J Orthop Res, 2006. **24**(5): p. 1001-10.

158. Wilson, W., et al., *The role of computational models in the search for the mechanical behavior and damage mechanisms of articular cartilage.* Med Eng Phys, 2005. **27**(10): p. 810-26.

159. Yang, N., H. Nayeb-Hashemi, and P.K. Canavan, *The combined effect of frontal plane tibiofemoral knee angle and meniscectomy on the cartilage contact stresses and strains.* Ann Biomed Eng, 2009. **37**(11): p. 2360-72.

160. Chizari, M., M. Snow, and B. Wang, *Post-operative analysis of ACL tibial fixation.* Knee Surg Sports Traumatol Arthrosc, 2009. **17**(7): p. 730-6.

161. D, D.D.L., C.C. P, and J. W. Colwell C, *Osteochondral grafting: effect of graft alignment, material properties, and articular geometry.* Open Orthop J, 2009. **3**: p. 61-8.

162. Ledingham, J., et al., *Radiographic patterns and associations of osteoarthritis of the knee in patients referred to hospital.* Ann Rheum Dis, 1993. **52**(7): p. 520-6.

163. Hjelle, K., et al., *Articular cartilage defects in 1,000 knee arthroscopies.* Arthroscopy, 2002. **18**(7): p. 730-4.

164. Curl, W.W., et al., *Cartilage injuries: a review of 31,516 knee arthroscopies.* Arthroscopy, 1997. **13**(4): p. 456-60.

165. Gudas, R., et al., *A prospective randomized clinical study of mosaic osteochondral autologous transplantation versus microfracture for the treatment of osteochondral defects in the knee joint in young athletes.* Arthroscopy, 2005. **21**(9): p. 1066-75.

166. Widuchowski, W., J. Widuchowski, and T. Trzaska, *Articular cartilage defects: study of 25,124 knee arthroscopies.* Knee, 2007. **14**(3): p. 177-82.

167. Bullough, P.G., *The role of joint architecture in the etiology of arthritis.* Osteoarthritis Cartilage, 2004. **12 Suppl A**: p. S2-9.

168. Freeman, M.A. and V. Pinskerova, *The movement of the normal tibio-femoral joint.* J Biomech, 2005. **38**(2): p. 197-208.

169. Thambyah, A., *Contact stresses in both compartments of the tibiofemoral joint are similar even when larger forces are applied to the medial compartment.* Knee, 2007. **14**(4): p. 336-8.